2016

Vegetation community and sediment dynamics at Ukerebagh Island, Tweed Heads

Campbell Young

Vegetation community and sediment dynamics at Ukerebagh Island, Tweed Heads

Abstract

An increasing trend of mangrove expansion into saltmarsh communities has been observed in south-eastern Australia as part of a worldwide trend of woody vegetation encroachment on grasslands (Saintilan & Rogers 2013). Changes in coastal wetland vegetation communities as a result of sea-level rise are likely to alter 'blue carbon' sequestration rates, depending on sediment supply, primary productivity and the inherent ability of vegetation to adjust to regional hydrologic and geomorphic changes. The rate of sediment supply, both mineral and organic, many not meet the requirements to fill 'accommodation space' created by relative sea-level rise (Woodroffe *et al.* 2016). Changes in hydrological and sediment supply characteristics may be influenced by anthropogenic modifications to the estuary, including channel dredging, ocean breakwall construction, and land use change. This study investigated multi-decadal sedimentation rate changes and long-term vegetation community evolution at Ukerebagh Island, a coastal wetland within the sub-tropical Tweed River estuary on the NSW-Queensland border.

$^{210}Pb/^{137}Cs$ analysis indicated that considerable acceleration of sedimentation rates has occurred throughout the latter part of the 20th century, in line with recorded sea level rise. However, any contributing effects of the operation of the Tweed River Sand Bypass, a sand pump assisting longshore drift, cannot be distinguished from sea-level rise related increases in sedimentation. Down-core variation in carbon stable isotope ($\delta^{13}C$) values were used to infer shifts between C_3 (mangrove) and C_4 (saltmarsh – Sporobolus virginicus) communities. Sediments in mangrove communities indicated the continuous influence of mangroves on soil carbon, while saltmarsh sediments displayed a marked shift between C_3 and C_4 signatures, suggesting the former presence of either mangroves or C_3 saltmarsh species. Mixed cores exhibited an intermediate $\delta^{13}C$ signature, indicating the joint contribution of mangrove and saltmarsh to soil organic carbon. Variations in $\delta^{13}C$ correspond to time series analysis of vegetation distribution by Saintilan (1998) which indicated relatively recent mangrove expansion.

Observed changes in soil organic carbon content primarily related to decomposition over time. However, total carbon store values did not differ significantly between vegetation types, which may be related to differing accumulation time periods, or the methodological approach adopted. Additionally, new vegetation community mapping indicated that previously observed patterns of mudflat formation and landwards mangrove transgression are continuing, suggesting that while carbon sequestration levels may increase with projected sea-level rise, the long-term resilience and provision of ecosystem services by saltmarsh may be limited.

Degree Type

Thesis

Degree Name

BEnvSci (Hons)

Department

School of Earth & Environmental Science

Advisor(s)

Kerrylee Rogers

Keywords
Carbon stable isotopes, 210Pb, coastal wetlands, mangrove, saltmarsh, sea level rise

UNIVERSITY OF WOLLONGONG

Vegetation community and sediment dynamics at Ukerebagh Island, Tweed Heads

Campbell Young

A thesis submitted in partial fulfilment of the Bachelor of Environmental Science Advanced (Honours)

School of Earth and Environmental Sciences

Faculty of Science, Medicine and Health

University of Wollongong

October 2016

Declaration

The information in this thesis is entirely the result of investigations conducted by the author, unless otherwise acknowledged, and has not been submitted in part, or otherwise, for any other degree or qualification.

Campbell Young

24 October 2016

Acknowledgements

This honours year has been the hardest, but ultimately, the most rewarding year of my academic career. None of this would have been possible without the unfailing support and feedback from my UOW supervisor, Kerrylee Rogers. You took my project on last-minute and never held back from giving me much-needed critical feedback and support, even via Skype from the United States, to ensure this project was a success.

I would also like to thank my ANSTO supervisor, Debashish Mazumder. Thanks, Deba, for always making sure that I had enough time to get my analyses done, for being available to chat about possible future study directions, and for always making me welcome at Lucas Heights.

To the fieldwork team – Kerrylee, Neil Saintilan, and Jeff Kelleway – thank you for the supreme effort you put in at Tweed Heads. 16 hour days of coring and subsampling aren't easy for anyone! Also, thank you, Neil, for feedback and direction when I needed it, and Jeff for support for abstracts and $\delta^{13}C$ values to back up my conclusions.

Thank you to AINSE for supporting this work through an Honours Scholarship and recognising the significance of this work in relation to coastal wetlands in Australia.

Thank you to Atun Zawadzki and Brodie Cutmore at ANSTO for their tireless assistance in determining ^{210}Pb and ^{137}Cs dates, and their tolerance whenever I asked obvious questions or needed clarification. I'd also like to thank Jenny van Holst and Robert Chisari from ANSTO for their assistance and direction in getting samples ready for elemental analysis.

A big thank you to the PhD students at UOW who helped me with any questions I had about laboratory techniques or carbon stable isotopes. Kirti Lal and Chris Owers, your support and feedback has been greatly appreciated. Thanks for making time for me whenever I needed it.

Thanks to Marina McGlinn, for always enquiring about my progess and making sure I wasn't going crazy.

Thanks to my mates, especially Jack and Kai, for sticking around for coffees and chat at any time of the day, and my housemates, for making sure I didn't take everything too seriously.

Finally, I'd like to thank my family, especially my parents, for listening to my concerns, and for letting me come home to work and eat when I ran out of money. Your support has been invaluable.

Abstract

An increasing trend of mangrove expansion into saltmarsh communities has been observed in south-eastern Australia as part of a worldwide trend of woody vegetation encroachment on grasslands (Saintilan & Rogers 2013). Changes in coastal wetland vegetation communities as a result of sea-level rise are likely to alter 'blue carbon' sequestration rates, depending on sediment supply, primary productivity and the inherent ability of vegetation to adjust to regional hydrologic and geomorphic changes. The rate of sediment supply, both mineral and organic, many not meet the requirements to fill 'accommodation space' created by relative sea-level rise (Woodroffe *et al*. 2016). Changes in hydrological and sediment supply characteristics may be influenced by anthropogenic modifications to the estuary, including channel dredging, ocean breakwall construction, and land use change. This study investigated multi-decadal sedimentation rate changes and long-term vegetation community evolution at Ukerebagh Island, a coastal wetland within the sub-tropical Tweed River estuary on the NSW-Queensland border.

$^{210}Pb/^{137}Cs$ analysis indicated that considerable acceleration of sedimentation rates has occurred throughout the latter part of the 20th century, in line with recorded sea level rise. However, any contributing effects of the operation of the Tweed River Sand Bypass, a sand pump assisting longshore drift, cannot be distinguished from sea-level rise related increases in sedimentation. Down-core variation in carbon stable isotope ($\delta^{13}C$) values were used to infer shifts between C_3 (mangrove) and C_4 (saltmarsh – Sporobolus virginicus) communities. Sediments in mangrove communities indicated the continuous influence of mangroves on soil carbon, while saltmarsh sediments displayed a marked shift between C_3 and C_4 signatures, suggesting the former presence of either mangroves or C_3 saltmarsh species. Mixed cores exhibited an intermediate $\delta^{13}C$ signature, indicating the joint contribution of mangrove and saltmarsh to soil organic carbon. Variations in $\delta^{13}C$ correspond to time series analysis of vegetation distribution by Saintilan (1998) which indicated relatively recent mangrove expansion.

Observed changes in soil organic carbon content primarily related to decomposition over time. However, total carbon store values did not differ significantly between vegetation types, which may be related to differing accumulation time periods, or the methodological approach adopted. Additionally, new vegetation community mapping indicated that previously observed patterns of mudflat formation and landwards mangrove transgression are continuing, suggesting that while carbon sequestration levels may increase with projected sea-level rise, the long-term resilience and provision of ecosystem services by saltmarsh may be limited.

Table of Contents

List of Figures

List of Tables

List of Equations

Abbreviations

ANOVA – Analysis of variance

CIC – Constant Initial Concentration

CRS – Constant Rate of Supply

DEM – Digital Elevation Model

GLM – Generalised Linear Model

IPCC – Intergovernmental Panel on Climate Change

LiDAR – Light Detection and Ranging

MH – Marker horizon

NPP – Net primary production

RSLR – relative sea level rise

RTK GPS – Real Time Kinematic Global Positioning System

SAR – Sediment accumulation rate

SET – Sediment elevation table

SLR – sea-level rise

SOC – soil organic carbon

% C – percentage of carbon in dry soil sample (determined by elemental analysis

$\delta^{13}C$ - Carbon-13 isotope concentration. Reported relative to Vienna Pee Dee Belemnite (VPDB) per mille (-‰).

Chapter 1. Introduction

Coastal ecosystems are some of the most significant, and most heavily used and threatened natural systems on the Earth (Barbier *et al.* 2011). Their proximity to, and use by, urban populations puts them at significant risk of continued degradation and removal (Howard *et al.* 2012). The contribution of climate change and other anthropogenic activities to the decline in the health and extent of coastal ecosystems poses a significant threat to their continued contribution to the functioning of the Earth's life support system - ecosystem services (Costanza *et al.* 1997).

1.1. Ecosystem services – coastal wetlands

The three key coastal wetland vegetation communities – seagrass, mangrove and saltmarsh - are responsible for a vast range of ecosystem services, including soil erosion control and coastal storm protection (Costanza *et al.* 2008; Gedan *et al.* 2011), water purification and detoxification (Zedler & Kercher 2005), food-web linkages and provision of nursery environments for a range of species (Mazumder *et al.* 2006; Hollingsworth & Connolly 2006; Mazumder *et al.* 2011) and most importantly in terms of their effect on climate, carbon sequestration (e.g. Zedler & Kircher, 2005; Barbier *et al.* 2011; Donato *et al.* 2011; Mudd 2011; Deegan *et al.* 2012; Howard *et al.* 2014; Beaumont *et al.* 2014; Grenfell *et al.* 2016). Intergovernmental Panel on Climate Change (IPCC) sea level rise forecasts suggest that there will be significant declines in the extent of these coastal ecosystems and, accordingly, significant declines in ecosystem services associated with productivity, carbon sequestration and waste treatment (Craft *et al.* 2009; Beaumont *et al.* 2014; Wang *et al.* 2014; Bornman *et al.* 2016). Due to the significant role that coastal habitats play in sequestering carbon (Chmura *et al.* 2003; Gedan *et al.* 2009; Choi & Wang, 2004; Duarte *et al.* 2013) the degradation of these ecosystems via relative sea level rise (RSLR) has the high likelihood of exacting both a social cost via greenhouse gas contribution, and an economic cost via loss of biodiversity support and coastal protection (Pendleton *et al.* 2012; Beaumont *et al.* 2014).

1.2. Trends in research

Over the last two decades the importance of coastal wetlands in sequestering carbon has become apparent. The quantification of 'blue carbon' – that is, the potential for marine ecosystems to sequester atmospheric carbon dioxide (Nellemann *et al.* 2009) – has become an important consideration due to the disproportional role of these areas in regards to below-ground carbon storage (McLeod *et al.* 2011; Pendleton *et al.* 2012; Duarte *et al.* 2013; Beaumont *et al.* 2014; Kelleway *et al.* 2016). Subsequently, there has been a concerted effort to understand

the causative relationships between sea level rise, anthropogenic modifications, sediment accumulation rates, vegetation community dynamics, and carbon storage in saltmarsh and mangrove communities across a range of locations (Kirwan & Mudd 2012; Saintilan & Rogers 2013; Krauss *et al.* 2014; Woodroffe *et al.* 2016). Two regions that have been of particular interest are the saltmarshes of the north-eastern United States (e.g. Orson *et al.* 1992; Roman *et al.* 1997; Hartig *et al.* 2002; Goodman *et al.* 2007; Deegan *et al.* 2012; Watson *et al.* 2016) and the consequence of increased rates of RSLR in comparison to Holocene averages; and the estuarine wetlands of south-eastern Australia (e.g. Saintilan 1998; Saintilan & Williams 1999; Rogers *et al.* 2006; Hickey & Bruce 2010; Saintilan & Mazumder 2010; Lovelock *et al.* 2011; Alderson *et al.* 2013; Saintilan *et al.* 2015; Lovelock *et al.* 2015; Saintilan & Rogers 2015).

The use of carbon stable isotopes, particularly carbon-13 (^{13}C) has increasingly been used to determine the source of soil organic carbon and provide insights into belowground carbon cycle dynamics in terrestrial and marine sediments (Ehleringer *et al.* 2000). Due to the variation in ^{13}C signature ($\delta^{13}C$) between C_3 and C_4 photosynthesising plants, historical shifts in vegetation communities can be quantified via stable carbon isotope analysis (Ehleringer *et al.* 2000; Staddon 2004, Garten *et al.* 2007).

1.3. Rationale

Ukerebagh Island, in the Tweed River estuary in north-east NSW, has been the focus of an effort to understand vegetation and sediment dynamics in south-east Australian coastal wetlands over the last eighteen years. Beginning with photogrammetric surveys of the island and the installation of surface elevation tables (SETs) and marker horizons (MHs), a number of studies have demonstrated that there has been a significant change in the distribution of vegetation communities on the island throughout the 20th century (Saintilan, 1998; Wilton, 2002) and this trend may be related to variations in estuarine sediment supply, artificial adjustments to estuary conditions, and relative sea-level rise (Rogers, 2004; Saintilan *et al.* 2013; Rogers *et al.* 2014). However, there are no multi-decadal records of sedimentation rates or of soil organic carbon characteristics on the island.

Accordingly, the application of $^{210}Pb/^{137}Cs$ dating, a commonly used centennial-scale sedimentation rate indicator in coastal wetlands (e.g. Rogers *et al.* 2005; Andersen *et al.* 2011; Sanders *et al.* 2012; Smoak *et al.* 2013; Hill & Anisfeld 2015) was identified by Rogers *et al.* (2014) as a possible method of increasing the temporal scale of geomorphic change observations at Ukerebagh Island, in addition to advocating the inclusion of ecological change detection methods in determining coastal wetland response to climatic perturbations. Furthermore, the vegetation communities at Ukerebagh Island are primarily composed of

Sporobolus virginicus, a C_4 saltmarsh grass, and *Avicennia marina and Rhizophora stylosa,* C_3 mangroves, implying that $\delta^{13}C$ isotopic analysis is an ideal method for investigating changes in soil organic carbon (SOC) contribution (e.g. Craft *et al.* 1988; Middleburg *et al.* 1997; Staddon, 2004; Cheng *et al.* 2006; Zhou *et al.* 2006; Tanner *et al.* 2007; Johnson *et al.* 2007; Sanders *et al.* 2010; Saintilan *et al.* 2013).

1.4. Project Aims

This study, developed in collaboration with the Australian Nuclear Science and Technology Organisation (ANSTO), aims to contribute to a significant body of data from previous studies undertaken at Ukerebagh Island on the Tweed River, New South Wales. It concentrates on the relationships between sediment supply, climate change, carbon supply and storage, and relative sea-level rise, to build a picture of the long-term sediment and vegetation dynamics at the study site. The key aims of this study were to:

- Reconstruct the long-term changes in coastal vegetation on the island through the use of carbon stable isotope analysis. More specifically, the study will quantify the changes in vegetation by analysing the concentration of $\delta^{13}C$ in sedimentary deposits and identifying the photosynthetic pathways of previous vegetation. Temporal changes between the isotopic signature of the C_3 and C_4 pathways will be used to determine the presence of either mangrove *(A. marina* and *R. stylosa*) or saltmarsh *(S. virginicus*), respectively.
- Reconstruct the rates of sediment accretion throughout the 20th century via the analysis of ^{210}Pb and ^{137}Cs decay.
- Determine whether the current trends of vegetation succession and sedimentation at the study site are contrary to the long-term trends identified by the isotopic analysis and if so, identify possible drivers for recent changes.

To achieve these aims, the following hypotheses were tested:

H1: $\delta^{13}C$ signatures from surface sediment samples will correspond to the isotopic signature of the in-situ vegetation;

H2: Down-core $\delta^{13}C$ signatures will reflect historical shifts in vegetation community extent from saltmarsh to mangrove;

H3; Down-core $\delta^{13}C$ signatures will therefore reflect longer-term evolution of the site with respect to Holocene sea-level rise;

H4: Soil carbon concentration and soil carbon density are influenced by the conditions under which they were produced, e.g. soil carbon content in areas inferred to be from mangrove via $\delta^{13}C$ will be higher than that from inferred saltmarsh areas;

H5: Variations in multi-decadal sediment accretion rates will reflect recorded sea-level rise; and

H6: Variation in sediment accretion rates correspond to hydrological and sedimentological changes occurring within the estuary (i.e. installation of the Tweed River Sand Bypass).

Through the assessment of these hypotheses, this study will provide further insight into the long-term carbon sequestration trends on Ukerebagh Island and as an analogue for other Australian coastal wetlands where there is no significant difference in photosynthetic pathway between saltmarsh and mangrove species. It shall also provide an indication of the short-term effects of abrupt changes to an estuarine depositional environment and the implications this has for changes in vegetation patterns and blue carbon storage in coastal wetlands.

1.5. Thesis outline

Including Chapter 1 - Introduction, this thesis will be comprised of seven chapters. Chapter 2 - Literature Review - explores the key role of coastal wetlands for carbon sequestration, their response to climatic and hydrogeomorphological stimuli and current global and regional trends in vegetation and sediment dynamics. Chapter 3 – Regional Setting – outlines the hydrological, geomorphic and climatic characteristics of the study site and provides a history of the vegetation and land use changes both within the estuary and at Ukerebagh Island specifically. The implementation of controls on sedimentation along the Tweed estuary coastline is also discussed. Chapter 5 - Methods - details specifics of the fieldwork, analytical and statistical processes used in the research process. Next, Chapter 5 - Results and Discussion - presents the results of the analytical methods outlined in Chapter 4. Chapter 6 – Discussion - evaluates the results in the context of related regional and global coastal wetland features and identifies any limitations in the approaches utilised in this study. Lastly, Chapter 7 - Conclusion - outlines the implications for further research and the importance of these results in the context of increasing climate change and sea level rise, and recommends further approaches based on the findings contained therein.

Chapter 2. Literature review

This literature review shall be divided into three main sections, concentrating on: 1) the importance of coastal wetlands in the context of carbon storage and the geomorphic and biological processes which contribute to sequestration; 2) current global and local trends in coastal wetlands, especially with reference to south-east Australia and the impacts of sediment supply and relative sea-level changes; and 3) the application of isotopic techniques to wetland carbon and sediment dynamic analysis. There is a significant body of research regarding the importance of 'blue carbon' as a component of global carbon sequestration, sediment and vegetation dynamics in south-eastern Australian coastal wetlands, and isotopic analysis of sedimentation rates and vegetation community dynamics, all of which will inform this literature review and the corresponding fieldwork and analysis.

2.1. Carbon sequestration in wetlands

2.1.1. The global carbon cycle

The global carbon cycle is an interlinked process that encompasses carbon production and storage, climatic effects and human interactions (Field *et al.* 2004) (Figure 2.1).

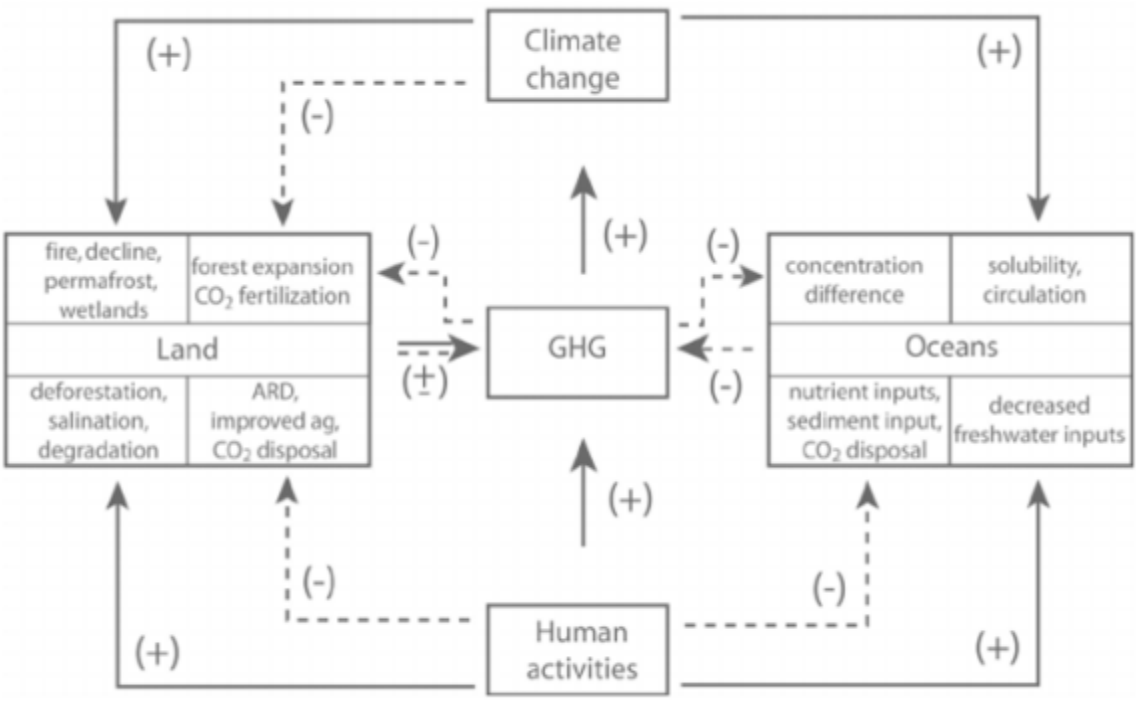

Figure 2.1: A schematic representation of the coupled carbon-climate-human system and the links among them, determining the global cycling of carbon. Solid lines and (+) indicate positive feedbacks, which accelerate climate change, dashed lines and (-) indicate negative feedbacks (carbon sequestration). GHG = greenhouse gases, ARD = afforestation/reforestation/deforestation (from Field *et al.* 2004).

It is a highly complex system that involves long-term processes such as carbon sequestration in forests, soils, and wetlands, and short-term impacts from the burning of fossil fuels (Tereshin *et al.* 2015) and large-scale deforestation (Landry *et al.* 2015). The earth's wetlands are inextricably linked to the global carbon cycle – they are the location of highly specialised evolution and the sequestration of significant levels of organic and inorganic carbon. Carbon sequestration is the process by which atmospheric carbon is captured through photosynthesis and stored long-term in biomass, soils, or the oceans (Sedjo & Sohngen, 2012). The burning of biomass and fossil fuels, in association with widespread deforestation, is increasingly contributing to carbon emissions via the release of previously sequestered carbon and the destruction of carbon sinks. Since the advent of the Industrial Revolution, the release of carbon to the atmosphere has had increasingly dangerous effects on the carbon-climate balance (IPCC 2013). Vegetated terrestrial ecosystems are vital to the global carbon cycle for the sequestration of carbon via photosynthesis and their removal will have severe consequences for the levels of carbon dioxide within the atmosphere, and accordingly, the severity of climate change impacts (Cramer *et al.* 2004).

2.1.2. Contribution of carbon to wetland evolution

Vegetation in coastal wetlands has many roles – it provides a habitat for a wide range of marine macro- and micro-invertebrates (Alongi, 2009; Mazumder, 2009; Ross *et al.* 2009; Mazumder *et al.* 2010), migratory birds (Spencer *et al.* 2009; Houston *et al.* 2012), and most importantly in this case, sequesters carbon from the atmosphere. Key reasons for the efficiency of wetlands as a carbon sink are low decomposition rates and high levels of biological productivity (Hogarth, 1999; Kirk, 2004).

There are five main categories of carbon in coastal wetlands – plant biomass carbon, dissolved organic carbon, particulate organic carbon, microbial biomass, and decomposed gaseous products such as methane and carbon dioxide (Kayranli *et al.* 2009) (Figure 2.2). Their relative proportions are dependent on the conditions within the estuary – e.g. carbon accumulation is highly sensitive to environmental conditions and disturbances such as temperature, precipitation, fire or flood (Table 2.1).

Net primary production

Net primary production (NPP) is defined as the remaining carbon incorporated into the cells, tissues and organs of a plant after the remainder has been utilised for photosynthesis (Dise, 2009). The photosynthetic process removes inorganic carbon in the form of CO_2 from the atmosphere and converts it to organic carbon, with approximately half of this being oxidised by

the plant through respiration, and the remainder being built into the structure of the organism (Dise, 2009). There are a number of key environmental drivers that control levels of NPP in wetlands (Table 2.1), the chief factors being temperature, radiation, water, toxins and nutrients (Kirk, 2004).

NPP is highly dependent on hydrological characteristics, such as tidal inundation frequency and duration, and water flow rate (Kirk, 2004). Hydrological conditions in coastal wetlands are often closely linked to climatic conditions such as temperature, precipitation and evapotranspiration and partly explain links between carbon retention efficiencies and hydrological/climatic variables (Coletti *et al.* 2013). Inundation frequency is generally a greater influence on NPP than duration, with maximum productivity occurring under intermediate inundation conditions (Kirk, 2004). This is a result of equilibrium between the flushing effects of periodic inundation and the control on oxygen availability for aerobic respiration (Kirk, 2004).

The influence of increasing temperature on NPP may have contradictory effects. Higher temperatures may increase both NPP rates and accordingly maintain carbon storage levels (Dise, 2009; McLeod *et al.* 2011). Conversely, increasing temperatures may also increase both aerobic and anaerobic respiration, resulting in higher levels of CO_2 emissions and decreasing levels of sequestered carbon (Chmura *et al.* 2003; Mitra *et al.* 2005; Dise, 2009; Kirwan & Blum,

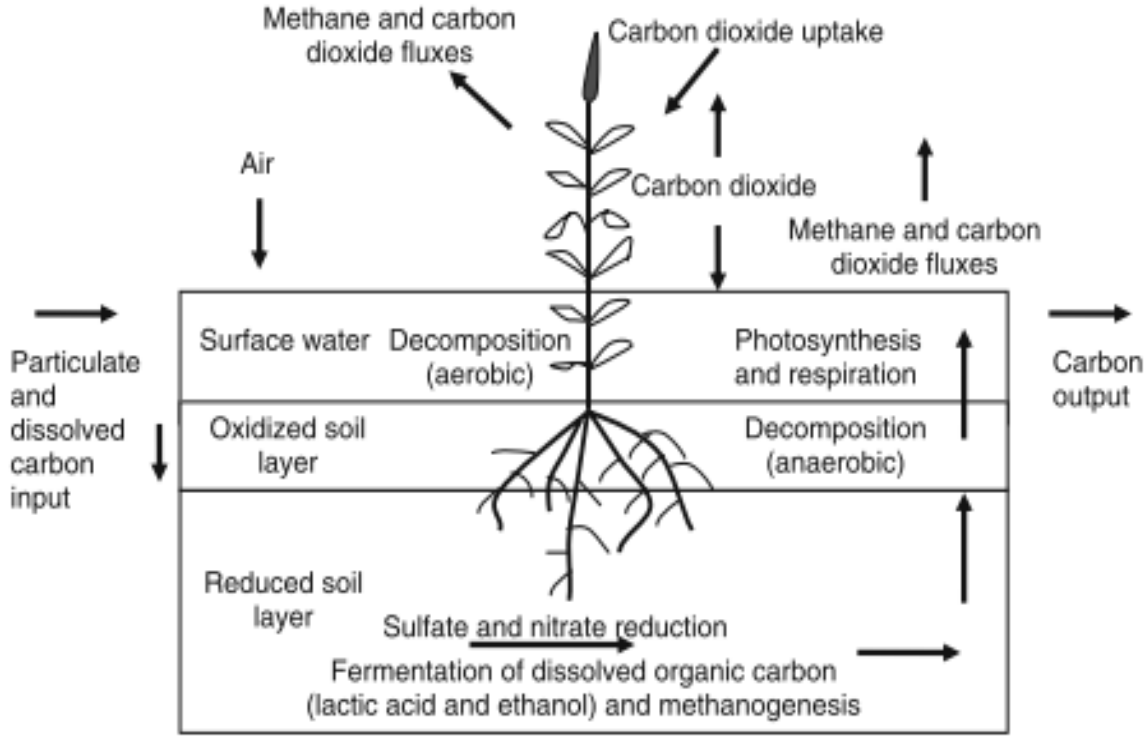

Figure 2.2: A simplified schematic diagram showing the major components of the carbon cycle in wetlands and the development of net primary production (NPP) (from Kayranli et al. 2009).

2011). Kelleway *et al.* (2016) suggests that under changing climatic conditions and rising sea levels, encroachment by higher NPP mangroves into saltmarsh areas may increase below- and above-ground carbon stores and mitigate effects of global warming. The key questions in this case is to consider whether increased productivity in wetlands will compensate for the associated increase in respiration (McLeod *et al.* 2011), and whether potential increases in carbon sequestration fully compensate for the loss of ecosystem services provided by upper-intertidal vegetation communities. The global distribution of peats, from tropical regions to permafrost, suggests that the ability of wetlands to shift carbon from the short-term to the long-term carbon cycle (Barbier *et al.* 2011) has balanced under differing climatic regimes over millennia (Whiting & Chanton 2001; Limpens *et al.* 2008). Nutrient concentrations, especially nitrogen and phosphorus, can be limiting on NPP (Kirk, 2004), as in other terrestrial vegetation communities, but also have important links to decomposition and mineralisation rates as a component of the chemical quality of plant litter (Verhoeven, 2009; Kayranli *et al* 2010).

Table 2.1: Major processes involved in carbon storage and release in wetlands, and major environmental drivers influencing those processes (from Gorham, 1995 in Dise, 2009).

Processes	Environmental drivers
Net primary production (NPP)	Temperature
Aerobic respiration	Precipitation
Anaerobic respiration	Atmospheric CO_2
DOC/DIC/POC leaching	Nutrients
Abiotic oxidation (primarily through fire)	Dissolved oxygen and other electron acceptors
Hydrology	Fire

Decomposition

Litter decomposition in coastal wetlands is a complex process which involves both biochemical processes - the conversion of complex organic compounds into simple inorganic compounds; and physical processes - the leaching of inorganic compounds affected by physical factors such as those listed in Table 2.1 (Zhao *et al.* 2015). The proportion of carbon from NPP that is released through aerobic respiration varies greatly depending on wetland type and local climatic conditions– it can be as low as 5%, but is more generally over half, and in extreme cases up to 95% (Dise, 2009). The speed of the decomposition process is extremely important for N and P nutrient cycling, and accordingly, plant growth and wetland productivity (Bridgman & Lamberti, 2009; Zhao *et al.* 2015). Climate is generally the ultimate control over two key determinants of the rates of decomposition – temperature and moisture gradients (Bridgman & Lamberti, 2009). Soil pH and hydrology are also highly important factors in determining decomposition rates (Bridgman & Lamberti, 2009).

Decomposition rates eventually slow as the redox potential in the soil declines and other electron acceptors such as sulfates, nitrates, Fe and Mn are utilised by decomposers preferentially in the place of oxygen (Kirk, 2004; Verhoeven, 2009) (Table 2.2). In this case, anaerobic decomposition becomes the dominant process for breaking down soil organic carbon (SOC). When these reductive conditions are dominant, decomposer microorganisms derive less energy per unit of carbon and accordingly, decomposition rates slow (Kirk, 2004). Because many decomposer organisms are obligate aerobes, and therefore are limited to more aerated areas of sediment, the lack of oxygen means that the rates of decomposition are extremely low in these areas (Verhoeven, 2009). The constantly saturated nature of intertidal coastal wetlands provides the impetus for these low rates of anaerobic decomposition and ensures that high levels of carbon storage are maintained. Lower macrofauna activity also contributes to the slower fragmentation of plant litter, and the breakdown of large refractory molecules such as lignin is retarded by the lack of aerobic fungi and bacteria (Verhoeven, 2009). However, increased vertebrate herbivory can significantly reduce aboveground biomass (van Wijnen *et al.* 1999) while increasing microbial biomass and slowing both microbial biomass and carbon turnover (Yu & Chmura 2010; Olsen *et al.* 2011). Grazing can significantly modify canopy structure and nutrient cycling, and therefore can potentially affect carbon uptake and respiration in saltmarshes (Wilsey *et al.* 2002).

Carbon emissions

Of the processes in Table 2.2, methanogenesis is the last process to be undertaken on the redox gradient and is obligatory once all inorganic oxidants in the sediment have been used up (Kirk, 2004). The CH_4 produced by methanogenic bacteria generally escapes the soil via ebullition - the spontaneous formation of bubbles from volatile solutes in a supersaturated solution (Kirk, 2004, Dise, 2009). The higher volatility of CH_4 in relation to other gases emitted from methanogenic sediments (e.g. CO_2, N_2) means that ebullition is a higher relative contributor to CH_4 fluxes than diffusion, which is dominant in CO_2 flux (Kirk, 2004). While some CO_2 leaves coastal wetlands via the conversion of CH_4 to CO_2 by methane-oxidising bacteria in the thin oxic zone near the surface (Kirk 2004; Dise 2009; Verhoeven 2009), wetlands are generally seen as a net sink of CO_2 and a net source of CH_4 (Brix *et al.* 2001). Therefore, the balance of CH_4 and CO_2 exchange can provide an index of a wetland's net greenhouse gas contribution (Whiting & Chanton 2001). As with NPP and decomposition, temperature, pH and inundation/soil saturation are important controls on gaseous emission/exchange ratios (i.e. CO_2/CH_4) and emission mechanisms (ebullition/diffusion) (Whiting & Chanton 2001; Limpens *et al.* 2008).

Table 2.2: Coupling between the carbon cycle and the anaerobic nitrogen, manganese, iron and sulphur decomposition cycles along a declining redox gradient. The final process, methanogenesis, contributes the majority of gaseous carbon emissions from coastal wetlands and is more pronounced in inundated wetlands where there is no oxic layer in the sediment (from Verhoeven, 2009).

Process	Redox mV
A. Fermentation:	
$C_6H_{12}O_6 \rightarrow 2CH_3CH_2OCOOH$	Less than 250
$C_6H_{12}O_6 \rightarrow 2CH_3CH_2OH + 2CO_2$	
Saccharomyces sp.	
B. Denitrification	
$C_6H_{12}O_6 + 4NO_2^- \rightarrow 6CO_2 + 6H_2O + 2N_2$	Less than 250
$2NO_3^- + 2CH_2O \rightarrow N_2O + H_2O + H_2O + 2HCO_3$	
$N_2O + H_2O \rightarrow N_2 + H_2O$	
Pseudomonas denitrificans, Bacillus spp., *Alcaligenes* sp.	
C. Dissimilatory nitrate reduction to ammonium	
$C_6H_{12}O_6 + 4NO_2^- + 4H^+ \rightarrow 6CO_2 + 6H_2O + 4NH_4^+$	Less than 250
Clostridium sp., *Bacillus* sp.	
D. Manganese reduction	Less than 225
$MnO_2 + 2e^- + 4H^+ \rightarrow Mn2+ + 2H_2O$	
Pseudomonas sp.	
E. Iron reduction	Less than 120
$Fe(OH)_3 + e^- + 3H^+ \rightarrow Fe^{2+} + H_2O$	
Pseudomonas sp.	
F. Sulfate reduction	Less than -75
$2CH_3CH_2OCOO + SO_4^{2-} + 3H^+ \rightarrow 2CH_3COO^- + 2CO_2 + 2H_2O + HS^-$	
$2CH_3COO^- + SO_4^{2-} \rightarrow 2CO_2 + 2H_2O + HS^-$	
Desulfovibrio sp., *Desulfomaculum* sp.	
G. Methanogenesis	Less than -250
$CO_2 + 8e^- \rightarrow CH_4 + H_2O$	
$CH_3COO^- + 4H^+ \rightarrow 2CH_4 + 2H_2O$	
Methanobacillus sp., *Methanobacterium* sp.	

Although brackish and saltwater wetlands are usually dominated by fermentation and sulphate reducing anaerobic conditions, mangroves are an exception to this because of their high rates of litter input, sediment subsidence and prolonged inundation (Verhoeven, 2009). Mangroves also leak oxygen from their root systems, creating a thin oxic zone in the rhizosphere (Alongi 2005), which can account for a small percentage of carbon mineralisation (Alongi *et al.* 2000; Alongi *et al.* 2005; Kristensen 2008). However, this zone rarely penetrates greater than 1 mm into the surrounding sediment (Kristensen 2008). Some evidence also suggests that P soil concentrations regulate CH_4 production (Medvedeff *et al.* 2015). Methanogenic bacteria generally favour higher temperature and pH conditions (Dise 2009, Olsson *et al.* 2015). Additionally, vascular plants

may act as a conduit for methane to escape sediment via passive plant-mediated transport (Dise, 2009). Wetlands are highly labile carbon sinks, meaning that changing environmental conditions can result in soil oxidation and the release of CO_2 (Mitra *et al.* 2005). Anthropogenic perturbations such as water table lowering and wetland drainage have the potential to release large levels of previously sequestered carbon in the form of CO_2 (Limpens *et al.* 2008; Liu *et al.* 2016).

2.1.3. Coastal wetlands in context – sequestration potential

Coastal wetlands are responsible for sequestering a disproportionate amount of carbon in relation to their total land area (Duarte *et al.* 2005; Dise, 2009; McLeod *et al.* 2011; Howard *et al.* 2014) and have far greater net primary production values than drylands for similar climate zones (Kirk, 2004). Although the approximately 49 million hectares they cover – between 2% and 6% of total land area (Kayranli *et al.* 2009; Pendleton *et al.* 2012) - are a crucially important location for blue carbon storage, they are increasingly under threat from anthropogenic processes. These processes include the destruction of mangrove forests for mariculture, agriculture, urban expansion, and forestry (Valiela *et al.* 2001), and coastal eutrophication, mosquito control, tidal restriction, urban expansion loss of sediment supply and agricultural conversion in mangroves and saltmarsh (Adam 2002; Wilton 2002; Gedan *et al.* 2011; Deegan *et al.* 2012; Howard *et al.* 2014; Ma *et al.* 2014). Climate change is also implicated in wetland vegetation distribution changes, with temperature increases implicated in the polewards extension of mangrove habitat (Duarte *et al.* 2013) and associated declines in saltmarsh extent (Osland *et al.* 2013; Saintilan *et al.* 2014). Sea-level rise is detrimentally impacting saltmarsh extent across continents (Warren & Niering 1993; Moorhead & Brinson 1995; Adam 2002; Kirwan *et al.* 2010; McKee *et al.* 2012) and increasing the areal extent of mangroves (Ray *et al.* 2011; McKee *et al.* 2012; Yang *et al.* 2013; Rogers *et al.* 2014; Swales *et al.* 2014; Kelleway *et al.*2016; Woodroffe *et al.* 2016).

There are a number of studies indicating the level of carbon stocks contained within coastal wetland environments. Although there is a high degree of uncertainty in these measures due to the lack of precision in methodology, carbon stocks for key blue carbon ecosystems have been included in IPCC (2013) coastal wetlands inventory processes (Table 2.3) and are increasingly being appreciated for their importance in sequestering carbon in marine environments (Donato *et al.* 2011; McLeod *et al.* 2011; Breithaupt *et al.* 2012; Fourqurean *et al*. 2012a; Beaumont *et al.* 2014; Kelleway *et al*. 2016). Compared to terrestrial vegetation ecosystems such as tropical forests, which accumulate carbon at rates such as 2.3-2.5 t C km^{-2} yr^{-1}, coastal wetlands have the ability to perform the same role at a rate from 30 to almost 100 times more efficiently (60-210 t

C km^{-2} yr^{-1}) (Pidgeon, 2009, in Irving *et al.* 2011). This equates to a large proportion of the total world carbon stored in terrestrial soil reservoirs – approximately $15x10^4$ kg (Kayranli *et al.* 2009).

Table 2.3: Mean and range values of soil organic carbon (to 1 m depth) for tidal salt marsh, mangrove and seagrass ecosystems, and CO_2 equivalents. These values indicate the wide range between sequestration values both within and between coastal wetland vegetation communities (IPCC 2013, in Howard *et al.* 2014).

Ecosystem	Carbon stock (MgC ha^{-1})	Range (MgC ha^{-1})	CO_2Mequiv ha^{-1}
Mangrove	386	55-1376	1415
Tidal saltmarsh	255	16-623	935
Seagrass	108	10-829	396

Because these environments generally accrete vertically with increasing sea levels, they effectively 'lock up' (Pendleton *et al.* 2012) large amounts of carbon. For example, the landward encroachment of mangroves into areas previously occupied by intertidal salt marsh in south-east Australia has dramatically increased belowground carbon stocks as a function of the increased carbon sequestration potential of mangroves, and infers that mangrove encroachment may actually benefit levels of blue carbon storage (Kelleway *et al.* 2016).

As seen in Table 2.3, there is a large variation in measured levels of carbon stocks across vegetation communities. Although there is a need to review the precision and accuracy of techniques used to determine carbon stocks (Petrokofsky *et al.* 2012), the wide range in storage values is chiefly attributed to the local environmental conditions in which carbon is stored. As relative sea level rise (RSLR) increases, it is likely that levels of carbon sequestration will increase with increased sediment accretion rates in tidal saline wetlands such as mangroves and saltmarshes (Chmura *et al.* 2003; Hill & Anisfeld 2015). However, Chmura *et al.* (2003) also states that this will only occur to a certain threshold point. Once RSLR exceeds upper accretion rate limits, the effectiveness of blue carbon areas in sequestering carbon will be nullified, and lateral erosion will effect a change from carbon sink to carbon source. The level of permanent storage may also be dependent on stand age – numerous studies by Alongi *et al.* (1998, 2001, 2004) indicate that older mangrove forests have higher levels of carbon preservation. This is in addition to other local variables including nutrient availability, plant species composition, and local geomorphic settings (Lovelock *et al.* 2014).

The likelihood of these feedbacks having a significant role in increasing carbon sequestration rates may be offset by the rate at which coastal wetland ecosystems are being destroyed. Anthropogenic influences mentioned earlier, such as urban, agricultural and forestry expansion, have been responsible for the loss of between one-half and one-third of seagrass meadow and mangrove forest areal extent (Duarte *et al.* 2005), and up to 50% of salt marsh in the United States alone (Kennish 2001).

2.1.4. Accretion dynamics

Sediment dynamics within wetlands have important implications for ecosystem services, extent and longevity of habitat types, short- and long-term sediment storage, and the formation and evolution of wetland systems themselves (Baker *et al.* 2009). An important distinction needs to be made between the two broad types of sediment that contribute to sediment dynamics within wetlands. Allochthonous (external) sediments are mostly mineral in nature, although often

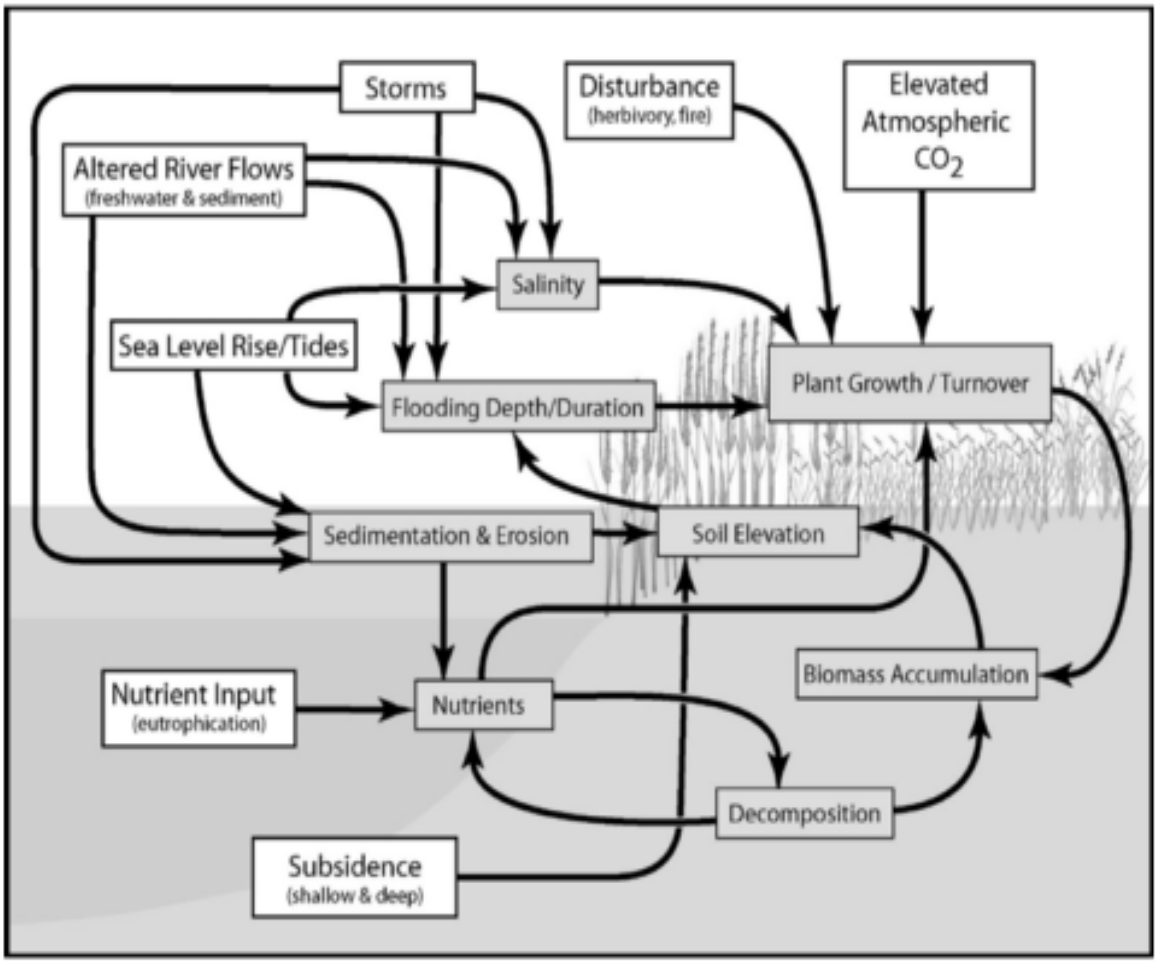

Figure 2.3: A conceptual model illustrating the complex linkages and feedbacks between natural processes and the effects of anthropogenic disturbances on coastal wetlands development and dynamics (from Cahoon & Guntenspergen, 2010).

contain an externally derived carbon component (i.e. wrack) (Cifuentes *et al.* 1996; Bouillion *et al.* 2008; Yang *et al.* 2013). Allochthonous material is supplied to the wetland via hydrodynamic forces, while autochthonous sediments are biogenically derived (French, 2006; Baker *et al.* 2009; Saintilan *et al.* 2013; Krauss *et al.* 2014; Maynard *et al.* 2014). Declining flow velocities as moving water enters wetlands reduces sediment transport capacity and results in the settling of sediment within wetland vegetation (Baker *et al.* 2009). Tidal deposition of sediment is not the only contributor to wetland accretion - above-ground plant mass contributes indirectly via litter-fall, and below-ground root and rhizome production contributes to soil volume (Hill & Anisfeld 2015). Grain size and particle settling velocities also determine the nature of sediment accretion (Baker *et al.* 2009).

Generally, the building of sediment within coastal wetlands is in response to some external stimulus, such as sea-level rise (SLR) or subsidence which results in a relative sea-level rise (RSLR) (Cahoon & Guntenspergen 2010; Kirwan *et al.* 2010; Woodroffe *et al.* 2016). However, the magnitude of a wetland's accretion response depends on a number of factors, such as rates of RSLR, tidal regime, suspended sediment concentration, and vegetation response to flooding. Changes in wetland elevation levels are not only a factor of sediment accretion – below-ground processes such as autocompaction, groundwater, dilation, water stage processes, root production and peat decomposition, and subsidence also contribute to elevation change (Cahoon & Lynch 1997; Cahoon *et al.* 1999, 2006; Rogers *et al.* 2005; French, 2006; Lovelock *et al.* 2011; Rogers *et al.* 2006) (Figure 2.3). In addition to the processes listed above, sediment transport in mangroves is controlled by several other interrelated processes including tidal pumping, flocculation, tidal prism, cyanobacterial and algal mat production, and physiochemical reactions that destroy flocs of cohesive sediment (Hogarth, 1999; Alongi, 2009). The ultimate control is generally local hydrodynamic conditions (Sanders *et al.* 2012), especially the hydroperiod, which is a coefficient of tidal inundation settings and is closely related to elevation (Crase *et al.* 2013; Woodroffe *et al.* 2016). Because sediment accretion is so closely linked to changes in RSLR, net deposition in an area cannot continue indefinitely and will decline as the mangrove area is inundated less frequently and the available accommodation space is infilled (Alongi, 2009; Woodroffe *et al.* 2016) (Figure 2.4).

Mangrove community establishment and development is closely linked to sediment transport, erosion and accumulation dynamics (Alongi *et al.* 2005). Generally, mangroves colonise an area when geomorphic conditions change to suit them, and from this point continue to enhance sedimentation (Woodroffe 1992; Swales *et al.* 2015; Woodroffe *et al.* 2016). Sedimentation is then accentuated via three key mechanisms – tidal current impedance, sediment binding and the addition of locally generated organic matter.

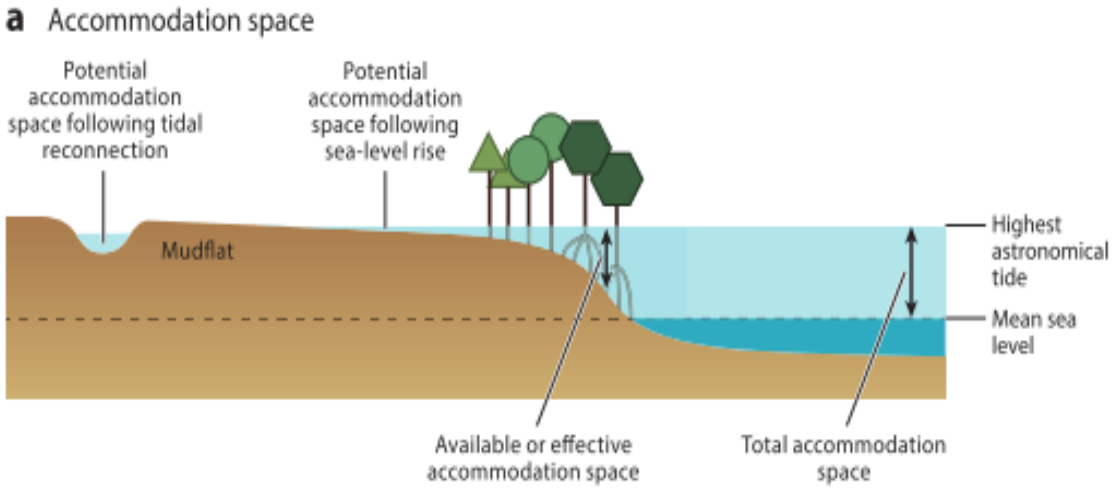

Figure 2.4: Schematic representation of the accommodation space related to tidal variations available for sediment accretion in mangrove wetlands (from Woodroffe, 2016).

The proportion of allochthonous versus autochthonous-derived sediment, and accordingly, soil carbon source, can be influenced by seaward distance and geomorphic setting (Donato *et al.* 2011). Mangrove wetlands in sediment-rich areas tend to expand laterally to colonise deltaic mudbanks, taking advantage of allochthonous sediment accumulation, while mangroves in sediment-starved areas principally build substrate biogenically (Alongi, 2009; Donato *et al.* 2011; Yang *et al.* 2013). The complex aerial root systems of mangroves, in addition to the proliferation of pneumatophores, inhibit tidal flows as a function of their friction forces (Furukawa & Wolanski 1996; van Santen *et al.* 2007) and cause soil particles to settle when water velocity increases (Kathiresan 2003). Mangrove size and shape has a significant impact on the level of sedimentation, with complex root systems much more effective at facilitating the deposition of fine particles (Alongi, 2009; Krauss, 2014). Fine sediments form flocs as a result of turbulence around surrounding vegetation and eventually settle out during slack high-tides, and therefore cannot be re-suspended (Furukawa & Wolanski, 1996). However, local geomorphic, hydrodynamic (e.g. flood vs. ebb tide dominated systems) and vegetation characteristics strongly influence the degree of sedimentation (Yang *et al.* 2014). For example, in *Avicennia* forests, sedimentation rates correlate with pneumatophore density and actively contribute to sediment deposition (Hogarth, 1999). Tidal pumping can seasonally affect levels of sediment accumulation (Woodroffe *et al.* 2016) and hydroperiod can influence the degree of sedimentation (Krauss *et al.* 2014) and mangrove species zonation (Crase *et al.* 2013). Benthic mats composed of algae also contribute to sediment accretion, acting as sediment binders and promoting organic matter accumulation (Hogarth 1999; Alongi 2009; Krauss *et al.* 2014;

Woodroffe *et al.* 2016). There is also some evidence that belowground biomass also contributes to maintaining soil surface elevation (Lovelock *et al.* 2015).

The main external controls on saltmarsh are sea level, tidal variations and sediment supply, along with internal sediment autocompaction and the influence of vegetation (Cahoon *et al.* 1999; Allen 2000). In the majority of cases in Australia, saltmarshes typically occupy higher intertidal areas, are inundated less frequently than mangrove habitats and as such, accretion rates are generally lower relative to tidal position (Saintilan *et al.* 2009; Rogers *et al.* 2013). Exceptions to this trend occur where mangroves are absent from the lower intertidal area or when *Spartina alterniflora* competes directly with mangrove systems (Patterson & Mendelssohn 1991; Howard *et al.* 2015). Interactions between hydrology and geomorphology also control the development of intertidal flats and accordingly, levels of saltmarsh establishment within an estuary (Saintilan & Rogers 2013). They typically occur in sheltered environments where fine sediments can accumulate without significant disturbance, and as a result, sedimentation rates are inextricably linked to sea level and tidal oscillations (Fagherazzi *et al.* 2012). Kirwan *et al.* (2010) also highlights the significant influence of suspended sediment concentrations on the resilience of coastal wetlands under increased sea levels. Tidal range is the main determinant in saltmarsh vertical extent, while horizontal extent is largely dependent on local topography and geomorphology (Adam 2009). Vertical accretion is widely recognised as a key influence on wetland stability, although short term perturbations such as storms or droughts can have significant influences on elevation, accretion and tidal dynamics (Roman *et al.* 1997; Rogers *et al.* 2013). As with mangroves, litterfall and below-ground biomass contributes to accretion, and results in higher levels of tide-borne sediment accumulation (Stumpf 1983; Hill *et al.* 2015).

2.2. Current wetland trends – global, regional and local

The current factors affecting mangrove and saltmarsh wetlands are the result of complex interplays between natural processes and the effect of anthropogenic processes. Changes in vegetation communities and variations in SAR are directly linked to the effects of human-induced development within wetland areas and other factors such as RSLR. Factors that influence vegetation community patterns and sediment accretion rates occur on the macro-, meso- and microscale (Figure 2.5). This section explains some of the current observed trends within coastal wetlands globally and regionally.

2.2.1. Accretion trends

The extent to which the fluctuations in sea level change associated with global warming are affecting accretion rates and carbon sequestration in wetlands remains unknown in large areas

of coastline around the world (McLeod *et al.* 2011). It has been suggested that elevated CO_2 levels may contribute to increased productivity in saltmarsh and mangrove (Cherry *et al.* 2009; McKee & Rooth 2008) and paradoxically aid some coastal wetlands by increasing biogenic contributions to elevation building (Langley *et al.* 2009). Notwithstanding this, it is important that the contribution of biological processes contributing to elevation change is further identified for inclusion in assessing the impacts of RSLR. Kelleway *et al.* (2016) used vegetation community changes to suggest that the increased productivity associated with the encroachment of mangroves may significantly increase blue carbon stocks in Australian coastal wetlands and in this way, mitigate some of the detrimental effects of increased climatic change.

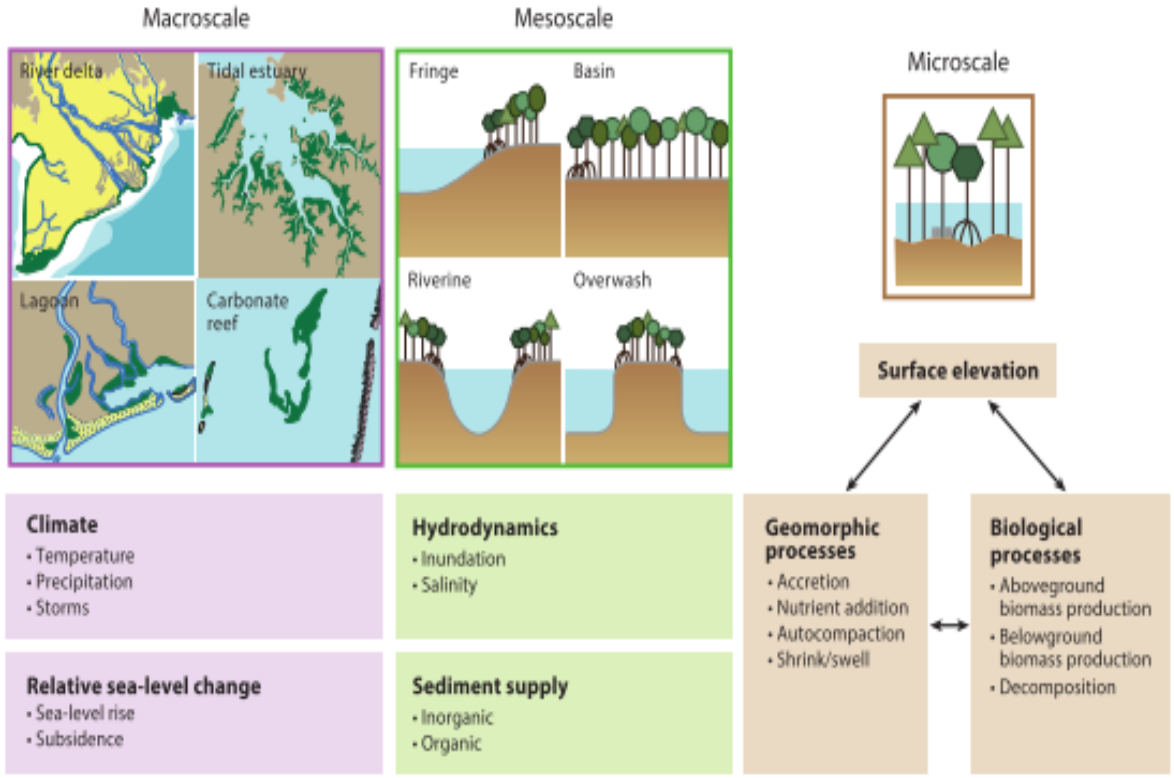

Figure 2.5: Coastal wetland environments at the macro-, meso- and microscale, and the varying external and internal processes that influence vegetation community zonation and sedimentation dynamics (from Woodroffe *et al.* 2016).

Climate-induced sea level rise is not the only contributor to changes in RSLR. The relationship between RSLR and wetland surface elevation involves feedbacks between groundwater levels, sedimentation, NPP, water level and inundation depth (Rogers *et al.* 2014). As RSLR increases, the frequency and amplitude of associated tidal events increases and may subsequently increase flood event frequency and erosion rates in saltmarshes and mangroves (Woodroffe, 1995; Silliman *et al.* 2009). The response of coastal wetlands to climate-induced changes in relative sea-level will most likely be determined by their ability to maintain a sediment budget which can successfully infill newly-created accommodation space (McKee *et al.* 2012; Woodroffe *et al.*

2016). This suggests two possible primary responses to accelerated RSLR: an apparent sediment balance, where accretion rates appear to match RSLR; and a sediment deficit, where the adjustment of local geomorphic conditions will be insufficient to fill accommodation space.

Palaeoenvironmental studies have indicated that wetland accretion rates can persist in the face of rapid sea-level rise, either displacing landward or accreting substrate rapidly enough to match RSLR (Krauss *et al.* 2014; Woodroffe *et al.* 2016) However, wetlands are more likely to keep pace with RSLR if integrated over long time periods – evidence from significant peat deposits in the Caribbean suggests that mangrove forests have kept pace with Holocene sea level rise via biogenic accretion (McKee *et al.* 2007), and via tidal redistribution of sediments in the Top End of Australia (Woodroffe 1990). Smoak *et al.* (2013) presents evidence that mangrove forests in the Florida Everglades have successfully maintained accretion rates either matching or exceeding local rates of SLR with the assistance of sediment derived from storm surges. The inclusion of storm surge deposits, however, is dependent on other local factors such as seasonal variation in vegetation productivity and the longer-term influence of storm events comprises a significant knowledge gap (Rogers *et al.* 2013).

If sediment supply, and consequently, rates of vertical land development, is continually less than RSLR, wetland accretion rates will also fail to keep pace and will become progressively drowned (Ellison & Stoddart 1991, in Woodroffe *et al.* 2016). The burial of mangrove peats below calcareous sands in Belize, and peats underlying wetlands in the Everglades, suggests that in some cases sediment supply has not kept pace with RSLR and wetlands have degraded and disappeared (Woodroffe *et al.* 2016). Coastal subsidence in Louisiana, coupled with eustatic sea level rise, has led to high rates of marsh degradation and disappearance (DeLaune & White 2013). The discrepancy between new accommodation space and sediment supply indicated that efforts to restore Mississippi Delta wetlands lost since the 1930s would require the redeposition of several decades' worth of river sediment load, which is highly improbable. Contemporary empirical evidence such as this, albeit on such a large scale, suggests that the restriction of fluvial sediment supply can have significant impacts on the ability of coastal wetlands to adjust to RSLR. The construction of works such as upstream dams limits the supply of allochthonous sediment via reduced fluvial transport (Ganju & Schoelhamer, 2010; McKee *et al.* 2012; Ma *et al.* 2014; Wang *et al.* 2014). It is also possible that works such as breakwaters and tidal power installations (O'Laughlin & van Proosdij, 2013) will reduce tidal amplitudes within basins and subsequently reduce sediment supply to wetland surfaces.

2.2.2. Relative sea level rise - vegetation community dynamics

A general shift of woody plant encroachment into grasslands globally in recent decades has been strongly reflected in vegetation community changes in wetlands (Saintilan & Rogers 2015). Wetland expansion has most commonly been observed in mangrove vegetation communities, with RSLR and associated accretion rates allowing landward mangrove expansion at the expense of freshwater and saltmarsh communities (Saintilan & Williams, 1999; Doyle *et al.* 2010; Krauss *et al* 2014; Rogers *et al.* 2013; Howard *et al.* 2015). Changes in vegetation patterns are directly related to accretion rates (Woodroffe *et al.* 2016) and geomorphic stability (Orson & Howes, 1992). Accordingly, these factors determine the progression of vegetation according to their biological limits.

Other influencing factors that influence vegetation community change include tolerance to inundation and salinity (Crase *et al.* 2013; Howard *et al.* 2015), geomorphic and human-enforced landward expansion limits (Hartig *et al.* 2002; Gedan *et al.* 2009) and other climatic effects such as increased CO_2 levels, rainfall variations, and temperature changes (McKee *et al.* 2012). Vegetation communities can exhibit a range of responses to RSLR, which are highly dependent on the nature of sediment supply to the wetland (Simas *et al.* 2001). RSLR can increase the dispersal and survival of mangrove propagules and seedlings (Rogers 2004), evidenced by the strong relationship between RSLR and upslope mangrove migration.

The distribution of saltmarsh and mangrove is also subject to limitations from physicochemical factors. Harsh conditions in the upper intertidal area such as high salinity and nutrient availability are contributors to community zonation (Saintilan *et al.* 2009). Tidal hydrodynamics and hydroperiod also strongly influence site-specific relative distribution of mangroves and saltmarsh (Saintilan *et al.* 2009; Crase *et al.* 2013; Woodroffe *et al.* 2016), and as a consequence, climate-induced changes in these factors that are not accompanied by increases in sediment supply will have significant implications for plant community zonation in wetlands.

In areas where saltmarsh is the dominant wetland vegetation, such as on the Atlantic coast of the United States, there is indications that wetlands will drown and erode as a consequence of the changes in hydrodynamic conditions associated with RSLR (Kirwan *et al.* 2010; Mudd, 2011). Under these conditions, marshes will likely migrate landwards to higher elevations until they meet anthropogenically enforced limits (Moorhead & Brinson, 1995; Simas *et al.* 2001; Hartig *et al.* 2002; Gedan *et al.* 2009) or topographical settings which prevent colonisation of intertidal species (Saintilan *et al.* 2009; Di Nitto *et al.* 2014; Phan *et al.* 2015). At lower elevations where sediment supply is insufficient, the plant community will lose the ability to accrete biogenically (van Wijnen & Bakker, 2001; Kolker *et al.* 2009) and trap sediment via declining flow velocities

(Baker *et al.* 2009). A number of studies have focused on sedimentation rates within North Sea saltmarshes in Scandinavia. The backbarrier saltmarsh in Skallingen (west Denmark) has been the subject of research since the 1930s and data currently indicates that with a higher sea level rise, vegetation will eventually drown as a consequence of an inability to increase sediment loads (Bartholdy *et al.* 2010; Andersen *et al.* 2011). SLR also has the potential to erode the seaward edge of saltmarshes. The Venice lagoon (Day *et al.* 1998) has experiences increased in wave energy and tidal prism as the result of increased RSLR, and are subsequently eroding laterally at high rates. Wetland vegetation inhabiting deltas across all climate zones and continents is under severe threat from the coupled forces of anthropogenically-induced changes in sedimentation regimes and climate-induced SLR (Syvitski *et al.* 2009).

2.2.3. Coastal wetland modelling and projections

Multiple efforts have been made to constrain the internal and external influences on wetland accretion dynamics so that landscape-change trends in the future can be assessed. Woolnough *et al.* (1995), Temmerman *et al.* (2003), Soares (2009), Kirwan *et al.* (2010), Brain *et al.* (2012) and Rogers *et al.* (2012) amongst others have developed multi-dimensional models to predict future trends in sediment accretion as current SLR trends continue. Temmerman's non-linear regression model (2003) takes into account the intensity of tidal inundation and flow length distances, while more complex ecogeomorphic models that consider feedbacks between wetland vegetation and geomorphic processes have delivered considerably different results to simple 'bathtub' models which assume constant elevation and do not account for the ability of wetlands to accommodate changes in relative sea level (Rogers *et al.* 2012).

2.2.4. Coastal wetland trends – south-east Australia

The global trends in coastal wetlands are reflected by the current changes occurring along the south-eastern coast of Australia – a pattern of mangrove encroachment into saltmarsh areas has been observed at multiple sites along the eastern seaboard, in a range of geomorphic settings (Saintilan & Williams, 1999; Saintilan & Rogers, 2013; Kelleway *et al.* 2016). Through the development of an estuarine mapping protocol, Wilton (2002) demonstrated mangrove incursions into saltmarsh at nine study sites, including coastal embayments, barrier estuaries, and drowned river valleys (Table 2.4). This was in addition to an earlier review of 28 studies by Saintilan & Williams (2000) which demonstrated a consistent trend of mangrove encroachment into previous saltmarsh areas across all types of study areas. Anthropogenic factors contributing to the landward expansion of mangroves include alterations in tidal regime as a result of barrage construction and dredging in barrier estuaries (Saintilan & Williams, 1999). Studies from Botany Bay (Hickey & Bruce 2010) have investigated the links between tidal inundation extent and

vegetation distribution, contributing to further understanding of species vulnerability and vegetation community change as the result of alterations in hydrological parameters.

Lack of precipitation is also a vitally important factor in the determination of coastal wetland trends on the south-eastern coast of Australia. Significant sediment autocompaction can be attributed to drought conditions, and is another contributor to mangrove encroachment into saltmarsh (Rogers *et al.* 2006). Regional climatic trends are highly important for determining drought conditions. For example, the drought conditions observed in Rogers *et al.* (2006) were attributed to an *El Niño* phase of the Southern Oscillation Index. Increases in the intensity and frequency of storm events is a major contributor to coastal erosion and can be attributed to a combination of a positive SOI and a negative phase in the Pacific Decadal Oscillation (PDO) (Proudfoot & Singh Peterson, 2011). Studies in Queensland have indicated that rainfall variability influences landward mangrove expansion (Eslami-Andargoli *et al.* 2009, 2010) however, the autocorrelation of rainfall with sea-level fluctuations makes it difficult to determine the strength of individual drivers (Rogers *et al.* 2014).

Table 2.4: Percentage declines of absolute saltmarsh areas in NSW (from Wilton, 2002).

site	percentage decline in saltmarsh area based on original areal extent	
		smallest proportion
Black Neds Bay	12%	
Ukerebagh Island	17%	
Courangra Point	38%	
Tilligerry Creek	40%	
Currambene Creek	48%	
Cararma Inlet	57%	
Towra Point	62%	
Brisbane Water islands	71%	
Careel Bay	97%	greatest proportion

2.3. Coastal wetland analysis techniques

Multiple techniques can be used to quantify rates of vegetation community change, sediment accretion and carbon sequestration in coastal wetlands and reconstruct palaeoenvironmental conditions. Palaeoecological approaches such as pollen and spore signal interpretation (Bunting & Whitehouse 2008, Ellison 2008), radiocarbon dating of sediments and fossil materials (Choi *et al.* 2001; Brevik *et al.* 2004; Choi & Wang 2004; Pigati *et al.* 2010; Kermode *et al.* 2016) and foraminifera/diatom stratigraphy analysis (Gehrels 1999; Allen 2000; Cundy *et al.* 2000; Gehrels *et al.* 2001; Bao *et al.* 2007) and sedimentological approaches such as anthropogenic marker

identification and geochemical tracers (Payne *et al.* 1997; Mesnage *et al.* 2002; Covelli *et al.* 2006) are often used in combination to infer ecological and geomorphic histories. In this literature review, the main focus is on the use of both radioisotopes and stable isotopes to determine the nature of past sediment accretion rates, estuarine conditions and vegetation communities.

2.3.1. Soil carbon isotopes

The three main isotopes of carbon are ^{12}C (98.9%), ^{13}C (1.1%), and the radioisotope ^{14}C (trace amounts) (Faure & Mensing, 1986; Farquhar *et al.* 1989). A wide range of current and past environmental conditions that impact soil carbon storage can be inferred from the presence of the second-heaviest isotope, ^{13}C, as a component of SOC (Garten *et al.* 2007), and as such, the analysis of ^{13}C is a significantly useful tool for reconstructing coastal wetland history.

Photosynthetic pathways

Terrestrial plants can generally be divided into 3 groups according to their photosynthetic pathways – C_3, C_4 and CAM (Crassulacean acid metabolism) – and because of differing discrimination against ^{13}C in biochemical pathways (Staddon, 2004; Marshall *et al.* 2007), photosynthetic pathways can be identified via $\delta^{13}C$ values (Craft *et al.* 1988; Choi & Wang, 2001). Although C_4 plants have a predicted vegetated land surface coverage of 18%, including important crop species (Still *et al.* 2003), the C_4 pathway (Hatch & Slack, 1970) is used by less than 4% of terrestrial plant species.

In C_4 plants, CO_2 is originally fixed in the mesophyll cells by cytosolic phosphoenolpyruvate carboxylase (PEPC) into HCO_3^- and then re-released and concentrated in the bundle sheath cells. At equilibrium, the heavier ^{13}C is concentrated in HCO_3^- (Farquhar *et al.* 1989). However, CO_2 leakage from the bundle sheath cells means that partial fractionation by the Rubisco enzyme – the main photosynthetic pathway in C_3 plants – occurs (O'Leary 1988: Farquhar *et al.* 1989; Kubasek *et al.* 2013). This results in a less depleted $\delta^{13}C$ value (-9‰ to -17‰) compared to C_3 plants, where full Rubisco fractionation of CO_2 occurs and $\delta^{13}C$ values range from -20‰ to -40‰ (Staddon 2004). The difference between the mean $\delta^{13}C$ values in C_3 and C_4 vegetation is ~ 13%, allowing unambiguous identification of photosynthetic pathways (Sharp, 2007) (Figure 2.6).

Stable carbon isotope tracing - $\delta^{13}C$ signatures

The species composition of vegetation within a wetland is a significant factor in determining $\delta^{13}C$ concentrations in soil organic matter (SOM), and as a result, changes in these concentrations over time can be used to identify the sources of organic carbon in the sedimentary record (Cheng et al. 2006; Sharp 2007). The $\delta^{13}C$ signature of soil CO_2 usually matches the SOM signature, indicating that little isotopic fractionation occurs during decay and the signature can be used to identify the contribution of vegetation types and algae to soil organic matter chronologically (Sharp 2007). However, there are a number of factors that may confound the identification of vegetation contribution to SOC. Progressive down-core enrichment due to preferential microbial decomposition of lighter carbon sources must be taken into account when analysing chronological SOM records (Ehleringer *et al.* 2000; Garten *et al.* 2007). Temporal (i.e. seasonal) and spatial variation may also influence $\delta^{13}C$ values within species (Cloern *et al.* 2002; Dubbert 2012; Sun *et al.* 2016). The 'Seuss effect' – the decrease of both $\delta^{14}C$ and $\delta^{13}C$ values in atmospheric CO_2 due to anthropogenic activity (Keeling 1979) –

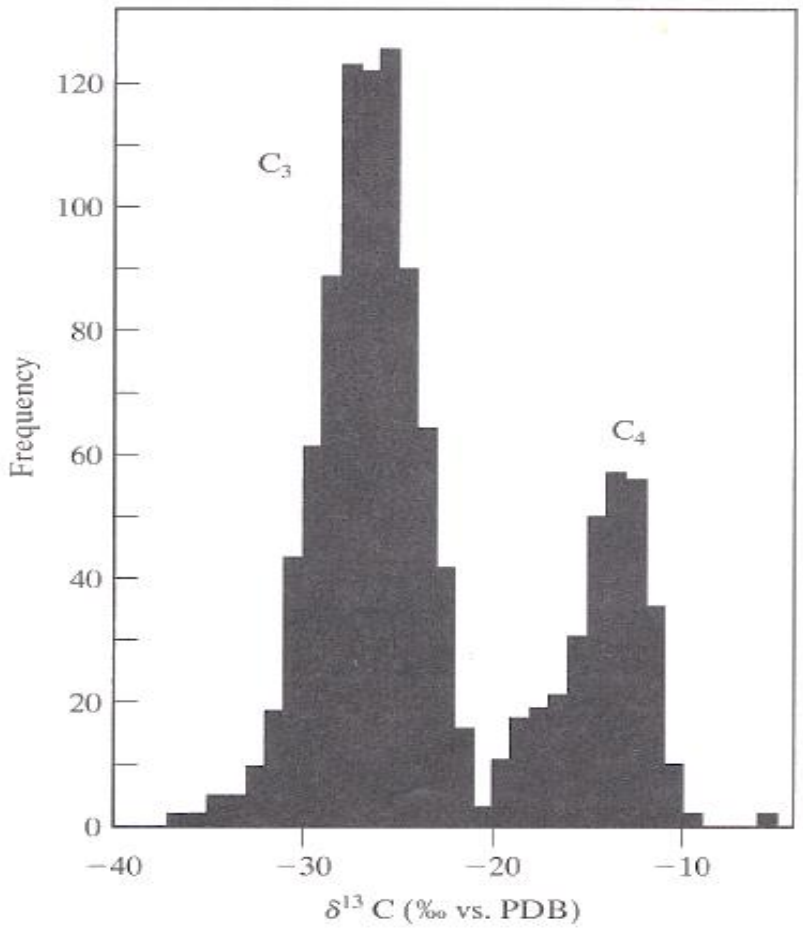

Figure 2.6: Differences in $\delta^{13}C$ values between C_3 and C_4 plants. Mean values are -25‰ PDB for C_3 and -12‰ PDB for C_4 plants (from Sharp, 2007).

may also confound down-core SOC values (Hornibrook *et al.* 2000; Verburg, 2007; Bostrom *et al.* 2007) Lastly, the incorporation of both allochthonous and autochthonous carbon in the soil profile, especially as hydrological and sediment supply conditions vary, may influence $\delta^{13}C$ values (Whitaker *et al.* 2015).

Past usage in wetland studies

$\delta^{13}C$ measurement in wetland studies has been used as an analogue for a wide range of wetland environmental conditions, including salinity regime and its effects on soil organic carbon stability (Chmura & Aharon 1995; Williams & Rosenheim, 2015), levels of coastal eutrophication (Oczkowski *et al.* 2014), RSL and palaeoenvironmental change (Johnson *et al.* 2006; Tanner *et al.* 2007; Lim *et al.* 2010; Khan *et al.* 2015), organic matter exchange and cycling (Bouillon *et al.* 2008) and most importantly, changes in the source of sediment organic matter (Craft *et al.* 1988; Cifuentes *et al.* 1996; Choi *et al.* 2001; Wang *et al.* 2004; Cheng *et al.* 2006; Zhou *et al.* 2006; Zhang *et al.* 2010; Bianchi *et al.* 2013; Saintilan *et al.* 2013). One of the key focuses of this literature review is the quantification of historical fluctuations in C_3 and C_4 vegetation, often used alongside other indicators of RSLR (Johnson *et al.* 2007). Carbon stable isotopes have previously indicated the dominance of particular vegetation communities and the contribution of allochthonous and autochthonous sources to carbon accumulation (Saintilan *et al.* 2013).

2.3.2. Sediment dynamics

Surface elevation tables (SETs) and marker horizons (MHs)

A method often utilised to determine the influence of vertical accretion and below-ground processes over a short timescale is the surface elevation table technique combined with marker horizons (SET-MH) (Figure 2.7), a permanent, non-destructive method for analysing wetland elevation change in shallow coastal environments (Cahoon *et al.* 2002; Webb *et al.* 2013; Callaway *et al.* 2014; Rogers *et al.* 2014). The SET instrument - a portable mechanical levelling device used to provide a constant reference plane - is inserted into a permanent benchmark in the ground and fibreglass pins are extended from the instrument to the surface (Howard *et al.* 2014). This arrangement allows for repeated measurements over time, reflecting changes in soil surface elevation (Callaway *et al.* 2013) Surface marker horizons are also used for short-term vertical accretion studies – this involves placing a powder such as feldspar on the soil surface and taking a short core. Measurement of the position of the marker horizon from the soil surface allows extrapolation of short-term average sedimentation rates (Rogers *et al.* 2014).

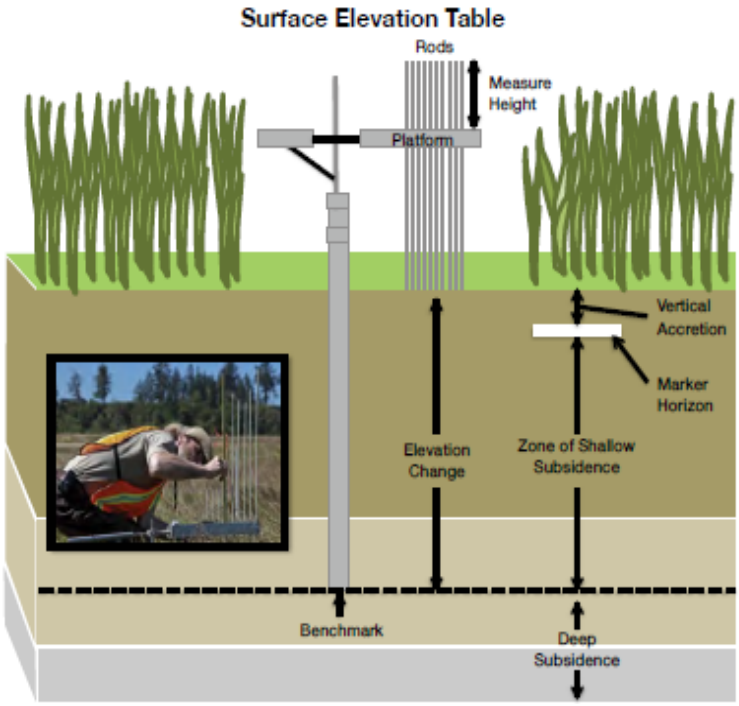

Figure 2.7: Diagram of a surface elevation table (SET) and marker horizon method used to detect changes in soil surface elevation (from Howard *et al.* 2014).

<u>^{210}Pb chronology</u>

One of the most common techniques for dating medium-term (25-150 years) sediment accretion rates and depositional processes is the use of fallout ^{210}Pb (Abril & Brunskill, 2014), a naturally occurring radionuclide and member of the ^{238}U decay chain (Bellucci *et al.* 2007):

Equation 2.1: The ^{238}U decay chain.

$$^{238}U \rightarrow {}^{226}Ra \rightarrow {}^{222}Rn \rightarrow {}^{218}Po \rightarrow {}^{214}Bi \rightarrow {}^{214}Po \rightarrow {}^{210}Pb$$

This technique was developed in the 1960s and has been applied to a broad range of environmental studies, including glacier ice, lacustrine and marine sediments (Abril & Brunskill, 2014). The ^{210}Pb is supplied to sediment via ^{226}Ra decay (Nittrouer *et al.* 1979) to ^{222}Rn ($t^{1/2}$ = 3.8 days) which then decays to ^{210}Pb through intermediate nuclides and leaves the atmosphere via precipitation onto the sediment surface (Begy *et al.* 2011) and from catchment (Figure 2.8). This ^{210}Pb is then assumed to be relatively undisturbed due to the lack of significant sediment resuspension and secondary transport (Wang *et al.* 2016). This excess, or unsupported, ^{210}Pb that is washed from the environment is in addition to the supported ^{210}Pb already present via the continuous decay of U-series elements within the sediment (Begy *et al.* 2011). Supported ^{210}Pb can be determined by establishing the ^{226}Ra content of the sample via gamma spectrometry, as these isotopes are in equilibrium and will decrease with the ^{226}Ra half-life ($t^{1/2}$ = 1600 years) (Appleby & Oldfield, 1978). Total ^{210}Pb content is usually determined by

measuring its daughter isotope ^{210}Po through alpha spectrometry (Robbins & Edgington, 1975; Kirchner & Ehlers, 1998). Therefore, unsupported ^{210}Pb, and accordingly, sediment deposition chronology, can be calculated from the difference between ^{226}Ra and ^{210}Po.

The two main calculation methods, Constant Rate of Supply (CRS) (Appleby & Oldfield, 1978) and Constant Initial Concentration (CIC) (Robbins & Edgington, 1975), assume a constant rate of ^{210}Pb supply to sediments over time and a limited post-depositional mobility of sediments, respectively. To independently validate ^{210}Pb results, an artificial fallout radionuclide whose chronological atmospheric peak is readily known can be used as a time marker, such as ^{137}Cs ($t^{1/2}$ = 30.17 ± 0.03 yr) analysis via gamma spectrometry (Abril & Brunskill, 2014).

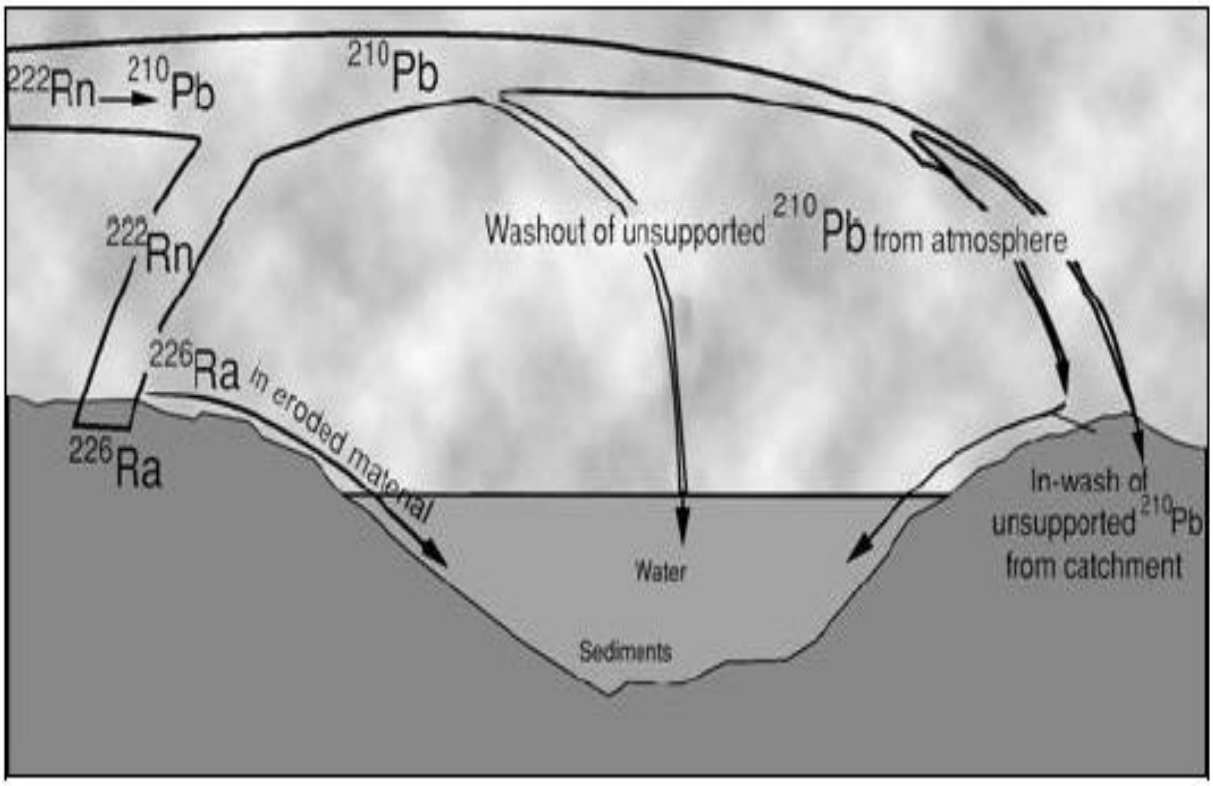

Figure 2.8: A simplified diagram illustrating the movement of unsupported and supported 210Pb into lake and wetland sediments via atmospheric washout, erosional material, and catchment in-wash (from Appleby & Oldfield, 1984).

2.4. Summary of Key Points

The health of coastal wetlands is vitally important for global carbon sequestration and so an increased understanding of the processes that contribute to carbon storage in wetland soils has been compiled in recent decades. Furthermore, there is an ever-expanding body of research documenting the encroachment of mangroves into areas previously colonised by saltmarsh, and causal factors such as hydrologic and geomorphic changes, anthropogenic impacts and inter-

annual and inter-decadal climatic variations. The use of analytical techniques which provide a multi-decadal record of sedimentation rates, carbon storage and vegetation community shifts provide further insight into historical trends and can be linked with causal environmental factors.

Chapter 3. Regional Setting

3.1. Regional context

Ukerebagh Island is located within the estuary of the Tweed River, on the NSW-Queensland border on the eastern coast of Australia (28°11'S, 153°33'E) (Figure 3.1). The island consists of intermixed mangrove and saltmarsh ecosystems and is a small part of the wider Tweed River wetland system. The Tweed River estuary is typical of the wetland environments found on the south-eastern coast of Australia, consisting of a mesotidal environment with mangrove and saltmarsh intertidal vegetation underlain by Quaternary alluvial deposits (Rogers *et al.* 2006). Vegetation trends on the islands reflect a wider trend globally and along the south-eastern coast of Australia where mangroves and woody vegetation are encroaching on the traditional range of saltmarsh vegetation (see Section 2.2.4).

3.2. Geomorphology and hydrology

The Tweed River estuary is classified by Roy *et al.* (2001) as an open, trained mature wave-dominated barrier estuary, typical of the depositional environments within drowned valley systems that were created post-Holocene sea-level rise that are prevalent along the coastline of the Australian continent (Sloss *et al.* 2006). The dominant geological units in the area are the Neranleigh Fernvale Group and the Lamington Volcanics (Saintilan, 1998). The Tweed River itself has a catchment area of 1054 km^2 and a total estuary area of 22.7 km^2 (NSW Office of Environment and Heritage, 2012). The main arm of the Tweed extends approximately 60 km, with the tidal limit located 2 km upstream from Murwillumbah (Rogers, 2004). The estuary can be divided into three main areas – the fluvial channel, encompassing the main course of the river extending towards the estuary from the south; the tidal channel, including the tidally influenced section of the estuary and Ukerebagh Island, and the broadwaters to the west, namely Cobaki and Terranorra (Saintilan 1998). The remainder of the estuarine area consists of low elevation alluvial plains on which the township of Tweed Heads is located, shielded by the sandy coastal barrier (Rogers *et al.* 2014). The Tweed River estuary is semi-diurnal, with a tidal range of 2.1 m (Rogers *et al.* 2014). The tidal prism in the estuary indicates a local tidal range of 1.55 m on the ebb flow and 1.02 m on the flood flow, 1.2 km upstream from the entrance (NSW Office of Environment and Heritage, 2012). Long-term water level trends from the nearest water level gauge at Letitia Spit (Station number: 201429) as calculated by Rogers *et al.* (2014) indicate an relative sea-level increase of 4.24 ± 0.16 mm y^{-1} between December 1987 and June 2013.

The sedimentology in each area is highly influenced by depositional characteristics and hydrological influences - the tidal channel is dominated by reworked marine sands, while the

intertidal environments in the fluvial channel are characterised by catchment-derived, flood-discharge shaped silts and clays (Saintilan, 1998). The Broadwaters are typical of the coastal lakes found along the NSW coast and are former low-lying coastal land inundated at around 6000 BP, and are being infilled by both flood-tidal sedimentation and fluvially-derived sediments (Saintilan, 1998). The formerly highly dynamic islands within the estuary, including Ukerebagh, Greenbank and others, have become highly consolidated over the last century (Saintilan, 1998).

The study site, Ukerebagh Island, is typical of low-relief tidal delta islands and is primarily composed of marine sands (Rogers *et al.* 2014). The island sits within the tidal channel area (Saintilan, 1998) and is enclosed by Terranora Creek, the Tweed River channel, and Ukerebagh Passage, approximately 1.5 km from the channel entrance (Rogers, 2004). The estuary was mapped by Druery and Curedale (1979) and it was determined that the estuary flows through a dual marine sand barrier and has now filled the original palaeo-estuarine basin. The estuarine delta is now slowly prograding across the dual barrier system, carrying a mantle of thin alluvial

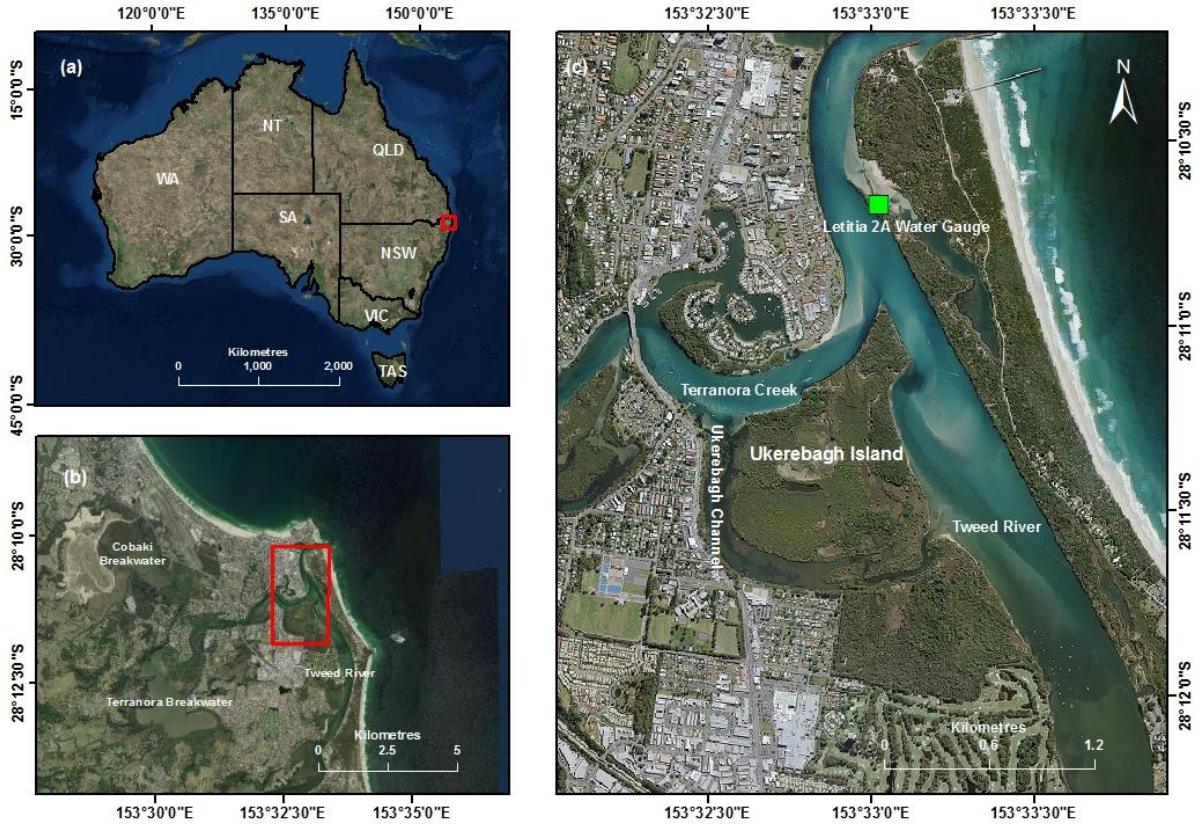

Figure 3.1: The study site (a) within Australia, (b) within the wider Tweed River estuarine area and (c) within the tidal prism near the river entrance.

deposits (Druery & Curedale, 1979, in Wilton, 2002).

Surface elevation trends at Ukerebagh Island from 2002-2014 have been quantified by Rogers *et al.* (2014) and although negligible, were calculated to be significantly greater in mangrove areas, compared to saltmarsh. Mangrove surface elevation increased at a rate of 1.40 ± 0.03 mm yr^{-1}, while saltmarsh elevation increase was 0.17 ± 0.09 mm yr^{-1} (Figure 3.2). Significant correlating trends identified in this study include climatic and hydrological factors such as antecedent rainfall and antecedent water levels, factors with strong associations to interannual climatic variations such as the Southern Oscillation Index (Rogers *et al.* 2014). However, these rates lag behind recorded sea-level rise from Letitia Spit. Sand is supplied to the estuarine barrier via the process of longshore drift, with an estimated 500,000 m^3 yr^{-1} moving along Letitia Beach near the river entrance. Cross-shore sediment transport superimposed on this process is responsible for the formation of offshore subaqueous bars, and is exacerbated by spring and storm surge tides (Acworth & Lawson, 2012). 'Slug' movement of sand around the heads in the area has also been recorded, with these movements occurring during periods of high wave energy and

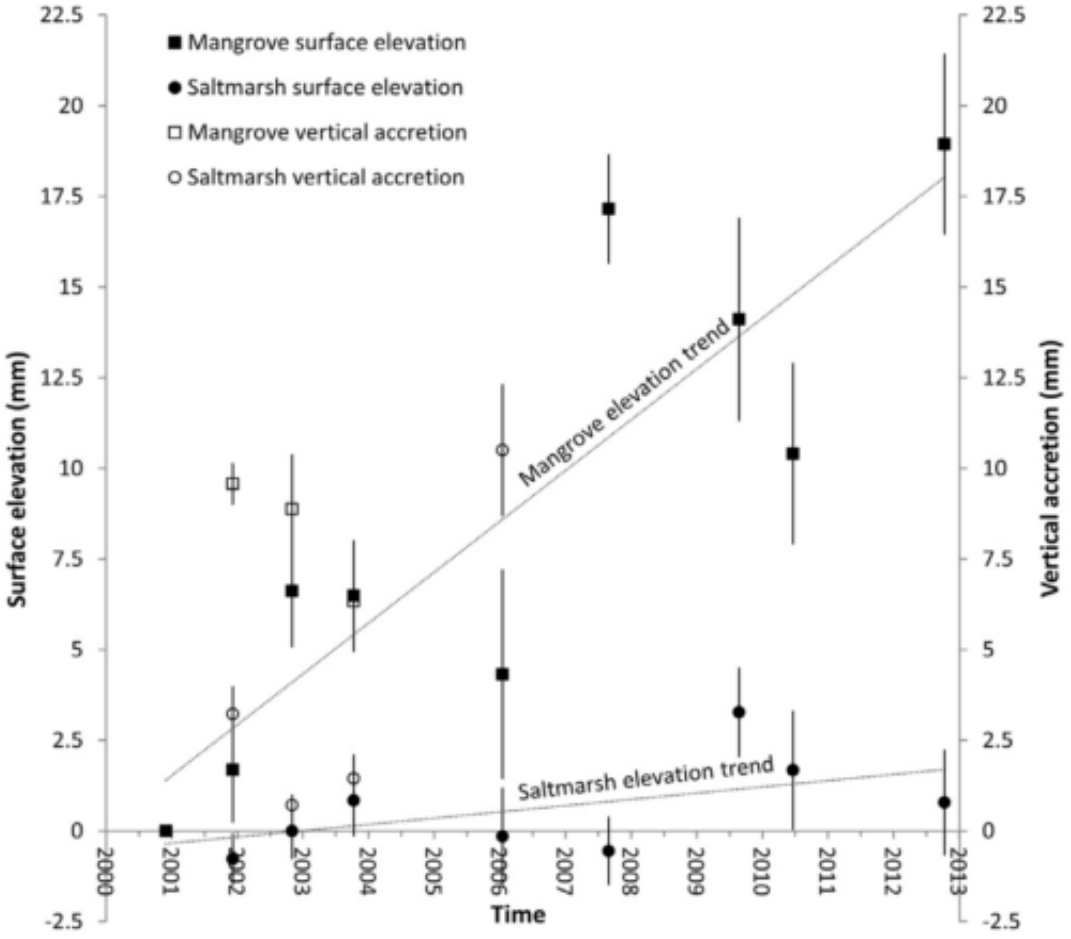

Figure 3.2: 12-year surface elevation trends at Ukerebagh Island (from Rogers *et al.*2014). Mangrove surface elevation and vertical accretion rates were well in excess of those in saltmarsh.

accelerated longshore transport, and creating temporary imbalances in sediment budget (Acworth & Lawson, 2012).

3.3. Climate

The Tweed River catchment is humid and subtropical (Saintilan, 1998), with mean daily maximum temperatures 4.6°C and the mean daily minimums of 15.9°C, as measured at Coolangatta Airport (BOM, 2016). Mean annual rainfall as measured at Coolangatta Airport is 1519.5 mm. The eastern coast of Australia is subjected to the effects of the El Nino Southern Oscillation (ENSO), including the study site. Variations in the Southern Oscillation Index (SOI), such as a negative SOI value (indicating an El Nino episode), result in the warming of the central and eastern tropical Pacific ocean and a reduction in rainfall over eastern and northern Australia (Rogers, 2004). A strong relationship between positive SOI, negative Pacific Decadal Oscillation (PDO), and spring tides has been shown to be an indicator of higher intensity and frequency of storm events (Proudfoot & Singh Peterson, 2011).

The region experiences a wet season from December to April, in which approximately 60% of the total annual rainfall is usually recorded. Periodic cyclonic weather systems may contribute up to 250 mm of rain in 24-hour periods (NSW Department of Public Works, 1991).

3.4. Vegetation

Ukerebagh Island is home to five mangrove species - *Aegiceras corniculatum, Avicennia marina, Bruguiera gymnorrhiza, Excoecaria agallocha* and *Rhizophora stylosa*, which inhabit the lower intertidal zone; and two salt marsh species, predominantly *Sporobolus virginicus*, with small amounts of *Juncus krausii* at higher elevations. *Casuarina glauca* is also present at the highest part of the intertidal range (Rogers *et al.* 2014). The estuary as a whole contains approximately 475 ha of saline coastal wetland environments (Rogers *et al.* 2014).

Mangroves have expanded rapidly at both their landward and seaward margins over the last 80 years throughout the Tweed Estuary, as indicated by photogrammetric mapping undertaken by Saintilan (1998). In the period 1930-1994, mangrove extent within the estuary increased by 75% (33 ha) (Saintilan, 1998). These expansions were attributed to prograding intertidal flats, as well as vertical accretion of the seaward edge of the intertidal zone (Wilton, 2002) and some colonisation of low-relief dredge spoil areas (Saintilan, 1998). Wetland habitat mapping undertaken by Wilton (2002) indicated that between 1948 and 1998, 17% of the original areal extent of saltmarsh on Ukerebagh Island disappeared – of this, 35% was lost to mangrove incursion and 13% lost to terrestrial incursion (Figure 3.3), with the remainder disappearing at the expense of expanding channel area. In terms of the overall changing vegetation patterns,

around 49% of the original saltmarsh habitat was lost to waterways, terrestrial vegetation, mangroves, or mixed habitat areas. A total of 3.4 ha of saltmarsh habitat was estimated to be replaced by mangrove over this time period (Rogers, 2004).

The earlier photogrammetric survey by Saintilan (1998) observed that saltmarsh extent within the Tweed estuary increased in the period 1930-1971, and began to decline thereafter. As of 1998, the total saltmarsh area within the estuary was still in excess of total saltmarsh areal extent at 1930 (Saintilan, 1998). Wilton (2002) calculated that Ukerebagh Island showed a net loss of mangrove habitat, largely due to erosion on the island's eastern bank as a result of boating activities and channel dredging. The trends observed by these previous studies have continued throughout the last decade, with a trend of increasing mangrove extent (11.68%) and decreasing saltmarsh extent (25.93%) identified in the period 2000-2012 (Pacific Wetlands Environmental Consultants, 2012).

Heap *et al.* (2001) placed the Tweed River estuary in the 'modified' (i.e. <65% remaining natural cover) category of their estuarine classification scheme, while it has also been estimated that 90% of the original coastal lowland vegetation within Tweed Shire has been cleared for urban development (Pressey & Griffith 1987).

Ukerebagh Island is unusual among the intertidal coastal vegetation communities of the eastern Australian coast in that the saltmarsh community is comprised only of *S. virginicus,* a C_4 plant, in comparison to the mangrove community, which is wholly comprised of C_3 plants. Previous

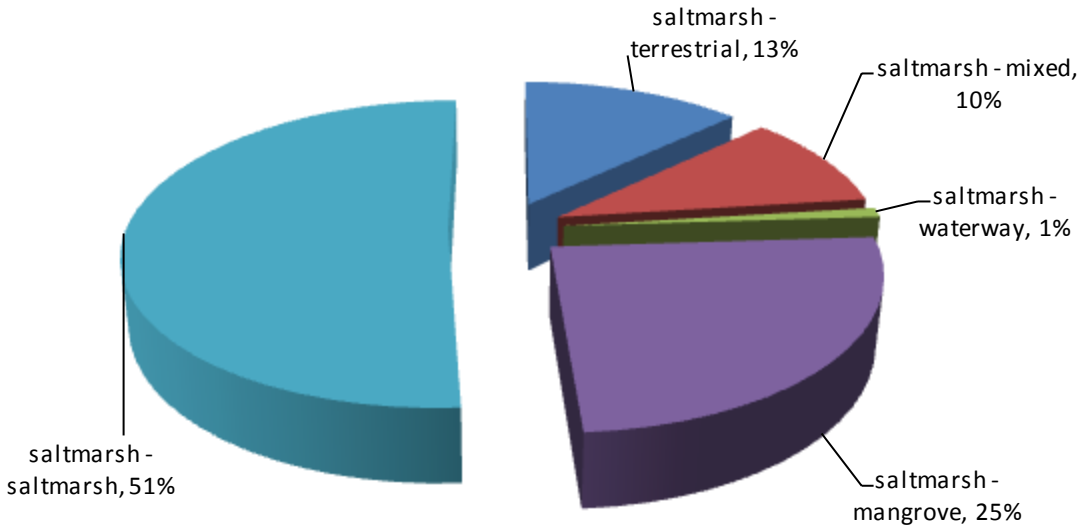

Figure 3.3: Percentage (%) changes of vegetation coverage on Ukerebagh Island 1948-1998 (from Wilton, 2002).

studies overseas have used the differences in $\delta^{13}C$ signatures in sediment to characterise changes in vegetation communities (see section 2.3.1) but this approach has not previously been utilised in Australia.

3.5. Current and past management practices

The Tweed River estuary has been subject to several anthropogenic processes since European settlement, most of which are common to estuaries along the south-eastern coast of Australia. The estuary has been subjected to large periodic episodes of channel dredging from the 1870s onward (Wilton, 2002) with the majority of this work occurring in the late 1950s and early 1960s. Significant amounts of marine channel sands have previously been dumped as dredging deposits on the northern fringes of Ukerebagh Island (Wilton, 2002) (Figure 3.3). Dredging within the main channel has lowered water levels within the estuary and increased tidal amplitude, extending the seaward expansion of mangrove seedlings (Saintilan, 1998). An amplification of tidal hydraulics has also been attributed to dredging events, with resultant siltation of the tidal delta distributaries (Druery & Curedale 1979, in Saintilan, 1998). Altered tidal amplification has also promoted landward expansion of mangroves (Saintilan, 1998).

The entrance breakwater at the river mouth was originally constructed over the period 1891-1904 and has been continually maintained to allow access for shipping since 1961 (NSW Department of Public Works, 1991) with the entrance walls extended further seaward in the

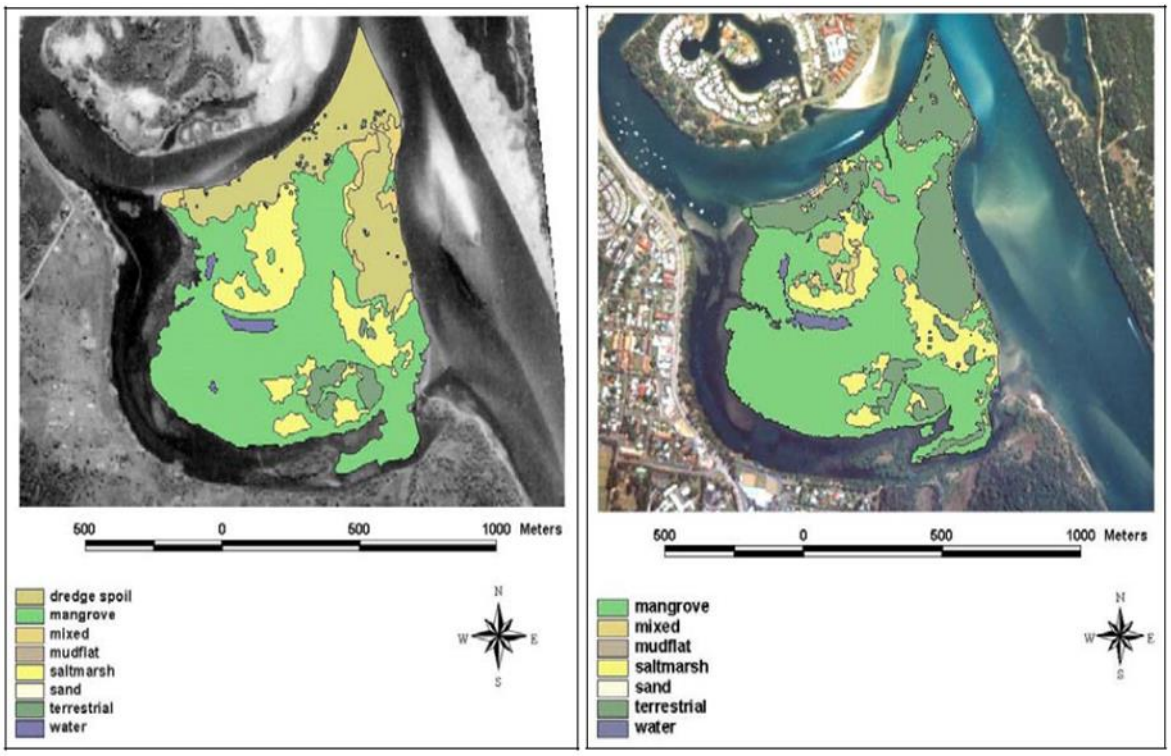

Figure 3.4: Changes in vegetation communities on Ukerebagh Island, 1948-1998 (from Wilton, 2002).

early 1960s (Castelle *et al.* 2009). Channelisation of sugarcane fields to aid surface drainage and the construction of canal estates have also contributed to higher levels of sedimentation within the estuary (Saintilan, 1998).

The recurring need to maintain an open channel led to the design and implementation of the Tweed River Sand Bypass Project, a joint scheme between the New South Wales and Queensland Government intended to restore and maintain beach amenity along the southern Gold Coast, and maintain a navigable entrance to the Tweed River (Lawson *et al.* 2001). Sediment travelling along the coast via longshore drift and accumulating against the southern entrance breakwall would be pumped underground from a pier 250 m south of the southern breakwall and deposited at four outlets: Snapper Rocks East, Snapper Rocks West, Kirra Point and Duranbah Beach (Dyson *et al.* 2001) (Figure 3.5). Previously, the interruption of approximately 500,000 m^3 yr^{-1} of littoral drift was responsible for significant erosion on northern beaches, and as sand accreted; it would eventually pass the entrance and begin to impact navigation conditions (Dyson *et al.* 2001). The problems attributed to northwards transfer of sand were first quantified by Druery & Curedale (1979) in the NSW Public Works Department 'Tweed River Dynamics Study' report (NSW Department of Public Works, 1991) and an agreement was reached between the State Governments in 1994 to construct a sand bypass pump (Tweed River Sand Bypassing Project, 2014). The sand bypass system is designed to deliver, on average, 500,000 m^3 yr^{-1} of sand to the southern Gold Coast beaches every year, to account for the net littoral drift amount experienced in the region, along with a reserve capacity to clear sand during storm events (Lawson *et al.* 2001). Environmental approvals for both states were carried out

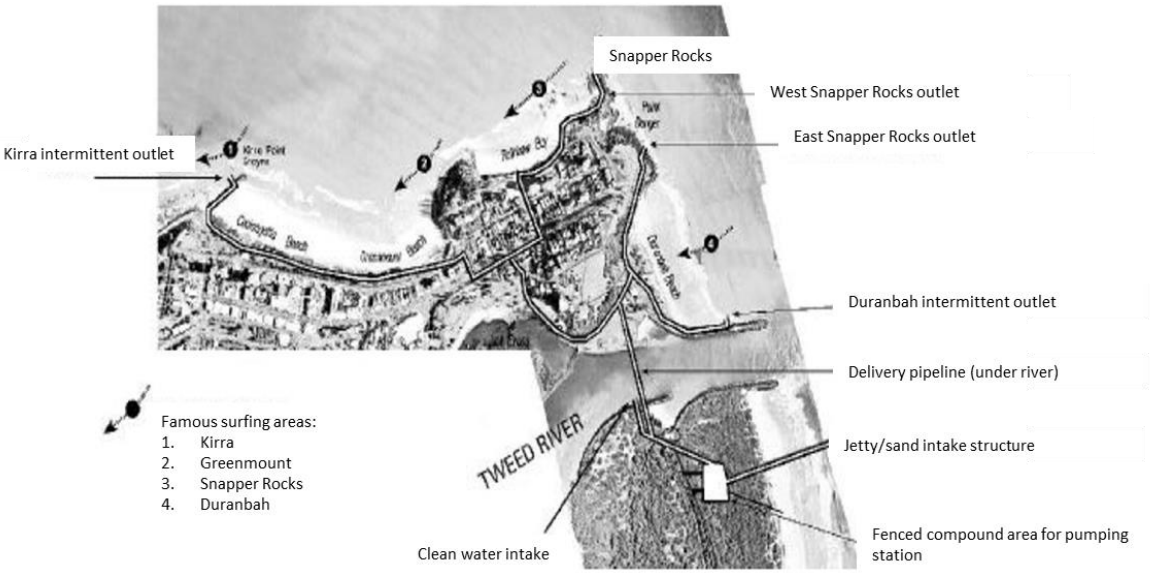

Figure 3.5: The Tweed River Sand Bypass System, showing the Tweed River entrance and breakwalls, the sand intake structure and the four sand pump outlets on the southern Gold coast beaches (from Dyson *et al.* 2001).

and implemented via an Environmental Impact Statement/Impact Assessment Study (Hyder *et al.* 1997), which outlined a range of hydrological, ecological and geomorphic monitoring activities to be conducted periodically.

Although the project has been successful in terms of supplying the prescribed amounts of sand to the northern beaches and mitigating beach erosion (Patterson, 2011), the sand bypass has also potentially influenced the hydrodynamic and sediment conditions within the estuary itself. Of particular concern is that the supply of sediment to the estuary from the channel entrance has been limited and as a result, may be contributing to the deceleration of sedimentation rates at Ukerebagh Island (K. Rogers, pers. comm. 2016). Although monitoring activities are carried out within the estuary, there is a lack of information as to the full effects of the sand bypass on estuary conditions and further investigation is required.

As previously mentioned, high levels of urban development have resulted in the clearing of significant quantities of lowland coastal vegetation, such as saltmarsh on Greenbank Island (Saintilan, 1998), and accordingly, limiting further landward expansion of coastal vegetation as RSLR pushes suitable intertidal vegetation conditions further landward.

3.6. Previous studies

The first studies into changes in vegetation patterns on the island were undertaken by Saintilan (1998) for the period 1930-1994 and noted mangrove expansion onto dredging spoil and some landward expansion into saltmarsh areas. This was supplemented by further studies by Wilton (2002) and Rogers *et al.* (2014) which utilised GIS aerial photo interpretation for the period 2000-2012 and compared the rates of vegetation distribution dynamics to water level and rainfall variables. This study also utilised an SET network put in place in November 2000 that has been periodically analysed for changes in surface elevation (Rogers, 2004, Rogers *et al.* 2006; Rogers & Saintilan, 2008; Rogers *et al.* 2014). The study indicated that the main control on mangrove elevation trends at Ukerebagh Island is the tidal prism, which in turn is defined by inundation depth, hydroperiod, and distance from the primary tidal channel, and indicated that climatic perturbations may confound analyses of elevation response. Rainfall was found to be a key driver of surface elevation variability, as a consequence of inter-annual and inter-decadal climatic perturbation patterns such as ENSO and PDO (Rogers, 2004; Rogers *et al.* 2014).

Since 2000, the NSW Department of Lands and the Queensland Environment Protection Authority have conducted an Estuarine Vegetation Monitoring Program (Pacific Wetlands Environmental Consultants 2012), which has also consistently identified a trend of increasing mangrove extent and saltmarsh decline.

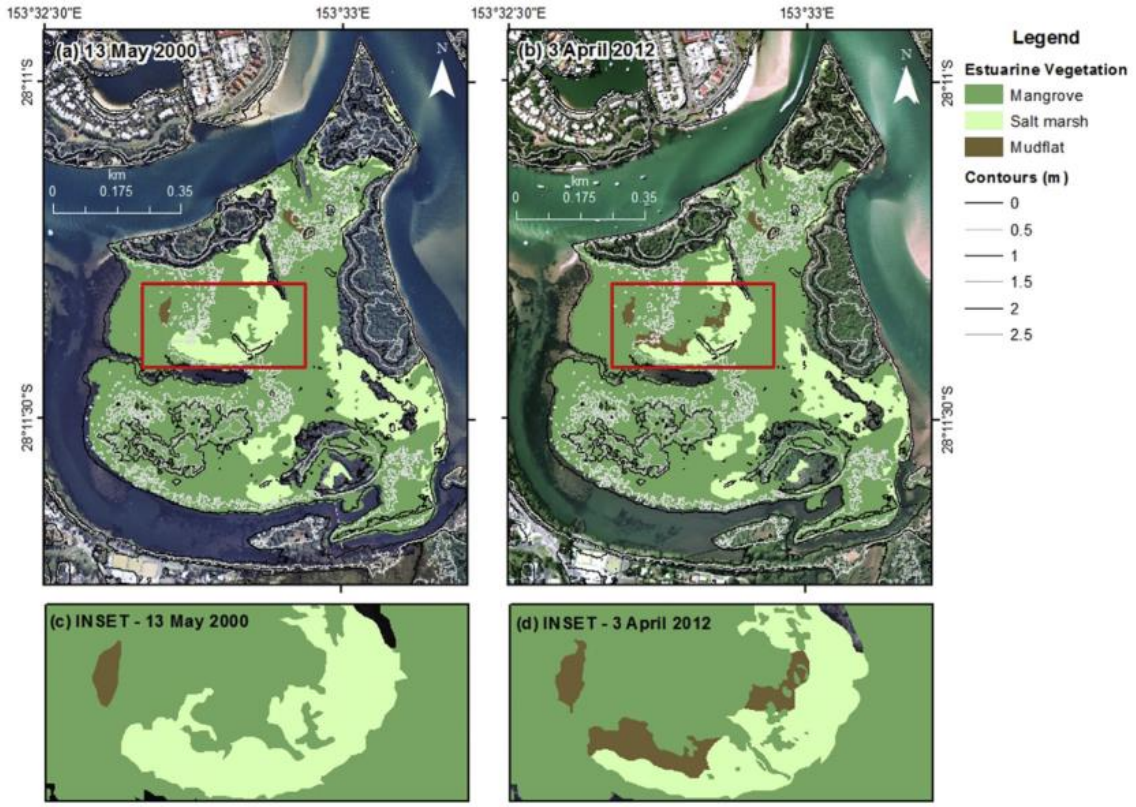

Figure 3.6: Comparison of estuarine vegetation extent on Ukerebagh Island from (a) 2000 and (b) 2012, and the extent of mudflat development post-saltmarsh loss in (c) 2000 and (d) 2012 (from Rogers *et al.* 2014).

Mangrove expansion was also observed to be preceded by the formation of unvegetated mudflats in areas previously occupied by saltmarsh (Figure 3.6). Further investigation into the inundation and salinity tolerances of the dominant vegetation species on the island was suggested. As the tidal prism will expand with increasing sea-level rise, this suggests that the vegetation trends on the island will continue into the 21st century. To date, there have been no studies on whether the operation of the Tweed River Sand Bypass and the presence of the breakwalls have significantly altered the nature of sediment supply to Ukerebagh Island and the rest of the estuary.

Chapter 4. Methodology

4.1. Site selection

Sediment cores were taken at nine locations across two transects (seven for stable carbon isotope analysis, two for ^{210}Pb). Core sites were selected on the basis of their location within the vegetation dynamics on the island (Figure 4.1), with at least one core on each transect representing a) long-term mangroves, b) long-term saltmarsh, and c) mixed mangrove/saltmarsh area, where mangrove vegetation has largely replaced areas previously occupied by saltmarsh. Sample locations were recorded using RTK/Trimble GPS to record coordinates and surface elevation from the CORSnet-NSW Global Navigation Satellite System tracking stations. Cores were driven into the stratum by manual hammering to a depth of 1.5 m (Figure 4.2); this depth was selected in order to examine long-term changes in carbon isotope and sequestration dynamics, and to ensure the maximum dating range for ^{210}Pb could be examined. Cores were extracted using a fixed piston vacuum method and capped and labelled in situ. Carbon cores were subsampled in 2 cm slices at every 5 cm for the first 30 cm of the core, and then at 10 cm thereafter until core end. These samples were bagged and labelled, then kept

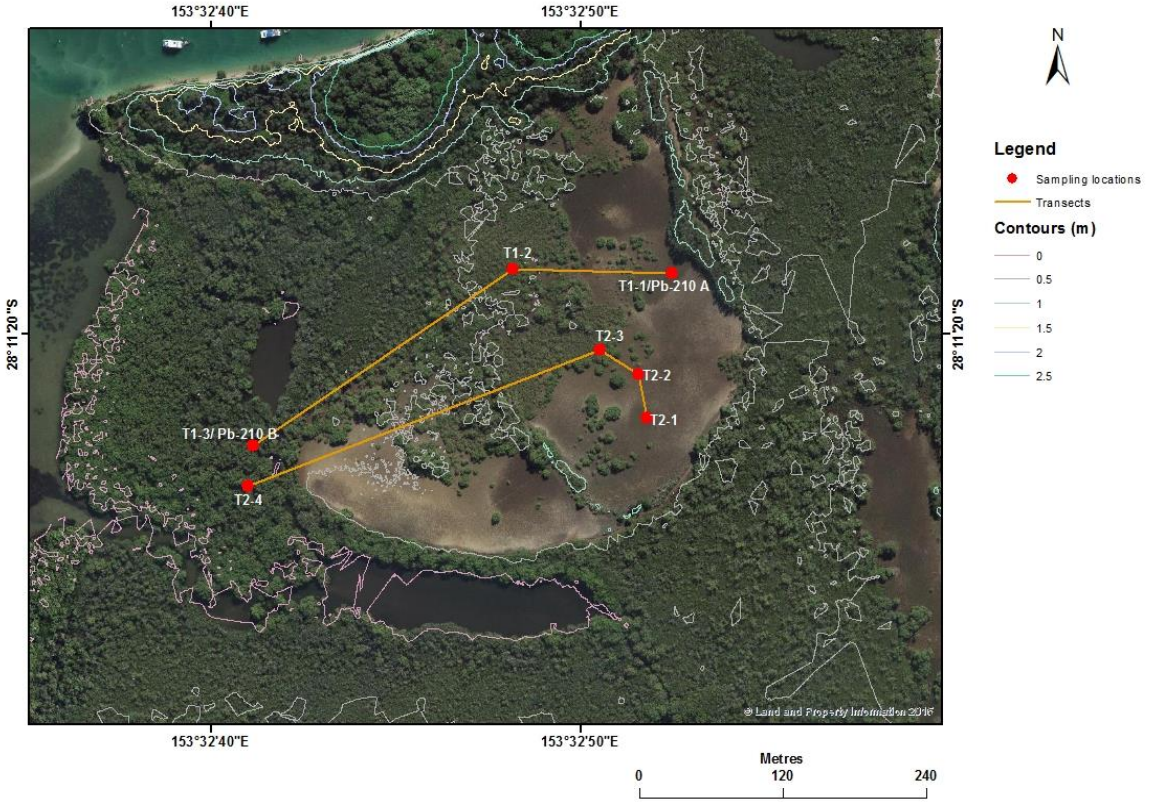

Figure 4.1: Sample transects and locations at Ukerebagh Island. δ^{13}C cores are labelled as transect no.-core no. (e.g. T1-1) and saltmarsh and mangrove ^{210}Pb cores are labelled Pb-210 A and Pb-210 B respectively. Contours are provided for sample location height reference.

Figure 4.2: Core insertion in saltmarsh area adjacent to saltmarsh SET at Ukerebagh Island.

at 3-5^{o}C until further analysis. ^{210}Pb cores were kept capped and returned whole for further laboratory preparation at UOW and ANSTO.

4.2. General soil characteristic analysis

4.2.1. Sediment grain size

Grain size analysis was performed at the University of Wollongong using a Malvern Mastersizer 2000. Where applicable, samples were sieved to remove any organic material or material with diameter >1500 µm.

4.2.2. Dry bulk density and moisture content

Soil dry bulk density (DBD) was determined from the mass of a fully dried sample and its original volume (Howard *et al.* 2012). The dry bulk density equation is as follows:

Equation 4.1: Dry bulk density calculation.

$$dry\ bulk\ density\ (g/cm^3) = \frac{\text{Mass of dry soil } (g)}{\text{Original volume sampled } (cm^3)}$$

For each sample, a known volume was extracted from a core slice using a 2.4 cm diameter syringe (for slice width 1 cm, 4.58 cm^3, for slice width 2 cm, 9.16 cm^3). Soil samples were then dispensed into a pre-weighed aluminium dish and placed in a 60°C oven to dry. Samples were re-weighed after cooling after 24 hours. Samples were weighed at 24-hour intervals until the successive weight differences were less than 4%, i.e. a constant weight was determined. DBD was then determined using the above formula. Percentage moisture content was calculated as follows:

Equation 4.2: Soil moisture content calculation

$$Moisture\ content\ (\%) = \frac{\text{Mass of wet soil } (g) - \text{Mass of dry soil } (g)}{\text{Mass of wet soil } (g)} \times 100\%$$

Core compression values were applied post-hoc to both dry bulk density and core slice depths to correct for sediment compression as a result of core driving and removal at the study site. A general figure for compression was applied for the full core length (Equation 4.3). Although compaction was likely to be greater in the top section of the core where the sediment is less consolidated due to factors such as crab mounds in mangrove areas, and organic material is more predominant, we were unable to account for these variations in the sampling process. Accordingly, the compaction factor was applied along the whole core depth.

Equation 4.3: Core compaction correction equation.

$$Core\ compaction\ correction = \frac{depth\ of\ core\ at\ refusal\ point\ (m)}{length\ of\ sample\ recovered\ (m)}$$

4.3. $^{210}Pb/^{137}Cs$ analysis and sediment accumulation rates

Sample preparation was undertaken both at the University of Wollongong and at the Environmental Radioactivity Measurement Centre at ANSTO, Lucas Heights, Sydney. Sample analysis took place over a period of one week at the ANSTO facilities. Six sub-samples from the saltmarsh core and ten sub-samples from the mangrove core were processed.

4.3.1. Pre-analysis preparation

Sediment samples from 1cm sample slices were wet sieved through a 63 μm mesh to collect <63 μm fraction and dried at 60°C until dry. Samples were then ground to provide homogenous samples for analysis.

For each sample, approximately 1-2 g of sediment was weighed into a 150 mL beaker and approximately 10 dpm of ^{133}Ba and 10 dpm of ^{209}Po mixed tracer solution were added to quantify isotope levels and determine isotope recovery. Approximately 2 mL of concentrated HNO_3 was added to each beaker to disperse sediment samples and heated for at least 5 minutes on a 40-50°C hotplate. After cooling, 10mL of concentrated HNO_3 was added slowly while swirling, then 15mL more HNO_3 added. Any remaining sample on beaker sides was rinsed with 2M HNO_3. Digestion then took place on hotplate at 60°C and samples were evaporated to dryness. While digesting, drops of n-octanol were added to vigorously reacting samples as a surfactant to reduce foaming and 2M HNO_3 used to rinse sides of beakers. Samples were then cooled again. 20 mL of 10% H_2O_2 was added to cover sediment and heated at 60°C until effervescence subsided. This process was repeated until sample reactivity was reduced and the majority of organic material was removed. Samples were then left to reduce on hotplate at 60°C to approximately 25 mL volume or 30 minutes.

25 mL concentrated HCl was added to each beaker and placed on hotplate with a watchglass covering to produce an azeotrope (constant boiling point acid composition) to dissolve authigenic phases within the sediment (i.e. carbonates, sulphides, oxyhydroxides) and to leach clay and primary mineral surfaces. This reflux reaction was left to proceed overnight at 50°C. Samples were deemed to be sufficiently digested when the supernatant appeared yellow and residues were a light colour.

Cooled samples were separated from the supernatant using 50mL centrifuge tubes with 6M HCl added and centrifuged at 4500 rpm for 5 minutes. Supernatants were decanted into original beakers and solid samples were centrifuged again with 15 mL of 6M HCl. Supernatant decanting was repeated and residues were discarded.

Supernatant samples were placed on 60°C hotplates to evaporate to almost-dry, with 6M HCl used as rinsing agent. 5 mL of concentrated HCL was added and evaporation was repeated twice, to ensure removal of nitrates from sample. Samples were then cooled prior to polonium and radium isolation.

4.3.2. Polonium isolation

30 mL of 0.1M HCl and 50 mL of reagent water was added to samples that had been placed on hotplate stirrers at 70-90°C. 1 mL of 20% ascorbic acid solution was added to reduce Fe (III) to Fe (II) for plating of sample onto silver discs. 100 µm of 1M citric acid was added after three minutes to oxidise complex trace iron and chromium and 10 mg of Bi^{3+} holdback carrier to inhibit bismuth autodeposition. The pH of samples was then adjusted to approximately 1.5 using concentrated NH_4OH and cresol red indicator.

1 g of hydroxylammonium chloride was added rapidly to each sample and a polyethylene holder containing a silver disk was immediately floated in the solution. Watchglasses were placed on the top of sample beakers and left for 4-6 hours to allow autodeposition of Po on silver discs. Discs were spun periodically to remove trapped bubbles which can result in sub-optimal polonium deposition and beaker volume was maintained with reagent water.

At completion of plating, discs were removed and rinsed with reagent water into sample beaker. Disks were then rinsed with 95% ethanol over a separate waste beaker and placed on tissue to dry. Once dry, discs were labelled and taken to alpha spectrometer for ^{210}Po activity determination.

4.3.3. Radium isolation

The remaining sample solution was diluted to approximately 800 mL in a 1L beaker with reagent water and placed onto a magnetic stirrer at a high speed. 20mL of concentrated H_2SO_4 and 100 mL 20% Na_2SO_4 were slowly added respectively. 10 mL of 10 mg/L Pb^{2+} carrier in 0.1M HNO_3 was added slowly to samples dropwise from a burette above the beaker. Beakers were left overnight to allow precipitation of Pb/Ba/Ra sulphates. On the following day, supernatants were decanted slowly to prevent loss and centrifuged with 50% ethanol at 5100 rpm for 2 minutes. Supernatant was decanted and discarded and centrifuging was repeated with 50% ethanol. After second decanting and discarding of supernatant, 5mL of Na_5DTPA and one drop of thymol blue were added, and tubes were placed in ultrasonic bath to dissolve sulphate precipitates. Drops of 10M NaOH were added if necessary to increase the pH of the solution above 9 and tubes were shaken to dissolve all precipitate.

2 drops of methyl red indicator was added to samples and solutions were passed through 0.45µm disposable membrane filters into cleaned polystyrene vials. 5 mL 4% Na_2SO_4 was added to centrifuge tubes and shaken briefly to collect residual Na_5DTPA, and solution was again passed through filter. 2 mL of 1:1 acetic acid/water and 1 mL of $BaSO_4$ seeding suspension were added to solutions which then turned pink. Solutions were placed in the fridge for 30 minutes.

Smooth-surfaced Millipore 'VV' membrane filters were placed in a lock-seal Gelman filter apparatus and filters were rinsed with 50% ethanol and drained before proceeding. Vials containing the colloidal Ba/Ra sulphate precipitate were poured into filter funnels and allowed to drain completely. Vials and filter funnel walls were rinsed with 50% ethanol to ensure collection of all precipitate on the filter. Any visible crystals on the filter paper were dissolved by adding water dropwise on top of the crystal while maintaining suction. Filter papers were placed face up in small polystyrene petri dishes, labelled accordingly, and marked with a black dot on the top perimeter of the filter (not on the precipitate). Petri dishes containing the filters were placed on top of an HPGe gamma detector to collect gamma spectrum for 10 minutes, measuring ^{133}Ba recovery via the 356 keV peak. ^{226}Ra was then analysed via alpha spectrometry.

4.3.4. Sedimentation rate modelling

As dry bulk density increases with depth, dry bulk density (g cm^{-3}) was converted to cumulative dry mass (g cm^{-2}) after Appleby (2001) to account for sediment autocompaction over time (A Zawadzki, pers. comm., 2015). Both the Constant Initial Concentration (CIC) (Robbins & Edgington, 1975) and Constant Rate of Supply (CRS) (Appleby and Oldfield, 1978) were used to calculate mass accumulation and vertical accretion rates (see Appendix 2). ^{137}Cs peaks were then used to independently validate these figures via bomb spike calibration.

CRS modelling was chosen for final representation of ^{210}Pb dates and sediment accretion rates as it better represents the variable contribution of labile organic material in the upper part of the core to mass accumulation, which is relatively absent from the lower parts of the core (K .Rogers, pers. comm.)

4.3.5. ^{137}Cs calibration

Approximately 5 g of dried and ground sample was analysed for ^{137}Cs activity with the Ortec Well detector gamma spectrometry system at ANSTO. The 662 keV peak was used to determine ^{137}Cs activity. Quoted activities are at the date of counting, quoted uncertainties are at 1σ counting errors and less than (<) values are quoted at the 95% confidence interval. The detector system energy calibration was carried out using a National Institute of Standards and Technology (NIST) traceable multi-nuclide standard source and the detector system efficiency calibration was determined using IAEA reference materials including RGU-1, RGTh-1, RGK-1 and Soil-6.

4.3.6. Vertical accretion rates and statistical analysis

Vertical accretion rates were calculated by dividing incremental sample depths by the difference in age between subsequent CRS sediment ages. Absolute error for samples was calculated via the mean variation of sum in quadrature.

4.4. Soil carbon characteristics and $\delta^{13}C$ analysis

4.4.1. Sample preparation

A total of 119 samples from 9 cores were dried in a 60°C oven for 48 hours and crushed using a TEMA ring crusher. Organic material was not removed from samples for analysis but left in-situ within core. For $\delta^{13}C$ analysis, 1-2 g aliquots of dried and crushed samples were then placed in test tubes with approximately 10 mL of 1M HCL to remove carbonates via acid digestion (Mazumder *et al.* 2010). Tubes were left in fumehood for at least 48 hours, with acid re-addition every 24 hours. When digestion ceased, tubes were centrifuged and rinsed with distilled water. Washed samples were then rinsed into trays and dried in a 60°C oven until constant dry weight was reached. Samples were reground in an agate mortar and pestle and bagged and labelled for analysis at ANSTO.

4.4.2. Isotope concentration and SOC analysis

At ANSTO, powdered and homogenised samples were loaded into tin capsules and analysed with a continuous flow isotope ratio mass spectrometer (CF-IRMS), model Delta V Plus (Thermo Scientific Corporation, USA), interfaced with a Thermo Fisher Flash 2000 HT EA elemental analyser (Thermo Electron Corporation, USA). Two quality control references were included in each run. Delta (δ) units in per mille (-‰) were used to report stable isotope values relative to the international standards (Vienna Pee Dee Belemnite (VPDB)) and determined using the following formula:

Equation 4.4: $\delta^{13}C$ value calculation in parts per thousand (‰).

$$X(-‰) = \left(\frac{R_{sample}}{R_{standard}} - 1\right) \times 1000$$

$\delta^{13}C$ values from a range of sources on the east coast of Australia and the Gulf of Carpentaria were used for identification of vegetative contribution to soil carbon (Table 4.1).

Table 4.1: Measured $\delta^{13}C$ values for *A. marina, S virginicus, R. stylosa, B. gymnorrhiza* and *A. corniculatum* from a range of estuarine settings in Australia, predominantly on the eastern coast (excepting those from Loneregan *et al.* 2007 in the Gulf of Carpentaria). Asterisks (*) denote measurements where root and leaf values were not differentiated.

Site	Source	Site conditions	Species	Leaf $\delta^{13}C$ (−‰)	Root $\delta^{13}C$ (−‰)
Mills Ck	Saintilan *et al.* 2013	Fluvial muds and silts, brackish	*A. marina*	-27.9	-24.7
Allens Ck		Fluvial muds and silts, brackish	*A. marina*	-27.7	-24.6
Spencer		Estuarine silts, brackish to hyper-saline upper intertidal	*A. marina*	-27.3	-24.7
Mooney Mooney		Estuarine silts, saline to brackish	*A. marina*	-28.3	-24.3
Pittwater		Marine sand delta, sea-water salinity	*A. marina*	-28.3	-23.3
			S. virginicus	-15.36	N/A
Assorted sites (Berowra Ck, Careel Bay, Towra Pt, Georges River)	J. Kelleway (unpublished data)	Sandy/Fine-grained	*A. marina* (mature forests)	-30.60 to -28.37	-26.90 to -25.50
Southern Moreton Bay	Guest *et al.* 2004a	Upper marsh	*S. virginicus*	-14.3*	
		Lower marsh edge	*S. virginicus*	-15.0*	
Towra Point	Saintilan & Mazumder 2010	Fluvial deltaic sand	*S. virginicus*	~ -15*	
Ross River	Abrantes & Sheaves 2008	Adjacent to upstream tidal pools	*S. virginicus*	-16.3 to -15.4*	
			A. marina	-27.0±0.9*	
			A. corniculatum	-27.4 to -26.3*	
Embley River	Loneragan *et al.* 1997	Dry season	*R. stylosa*	-28.7 to -28.3*	
		Wet season	*R. stylosa*	-28.8 to -28.2*	
Southern Moreton Bay	Guest *et al.* 2004b	Range of sites	*S. virginicus*	-15.0 to -14.7*	
			A. marina	-27.4*	
			R. stylosa	-26.3*	
			B. gymnorhiza	-26.3*	
Jervis Bay (Cararma Inlet)	K. Rogers (unpublished data)		*A. marina*	-24.6 to -23.8	-24.1
Jervis Bay (Cararma Inlet)			*S. virginicus*	-15.1	-18.0 to -17.7
Botany Bay	Saintilan & Mazumder (under review)		*A. marina*	-27.63	
Homebush Bay			*A. marina*	-26.68	
Broken Bay			*A. marina*	-28.01	

4.4.1. Soil carbon density and carbon store

Soil carbon density (g cm^{-3}) was calculated by multiplying the dry bulk density of the sample slice by % carbon obtained from elemental analysis. The estimated amount of carbon in the total core was obtained by fitting a linear trend between each known soil carbon density value and assigning values to uncorrected 1 cm intervals between each known point up to a depth of 1 m.

All soil carbon density values (g cm^{-3}) were then summed to give a total core carbon value and then converted to MgC ha^{-1} to reflect reporting conventions for carbon stock assessment (Equation 4.5).

Equation 4.5: Calculation of soil carbon stock for individual cores (MgC ha^{-1}) from Howard *et al.* 2014).

$$Total\ core\ carbon\ (MgC\ hectare^{-1}) =$$

$$summed\ core\ carbon\ (g\ cm^{-3}) \times (\frac{1Mg}{1000000g}) \times (100000000\ \frac{cm^2}{1\ hectare})$$

4.4.1. Statistical analysis

Analysis of variance (ANOVA) modelling was performed to determine significant differences between single parameter means by vegetation type. Post-hoc Tukeys HSD was used to determine which vegetation types were significantly different.

Generalised Linear Model (GLM) analysis

This technique has previously been utilised in Saintilan *et al.* (2013) to characterise relationships between vegetation types, hydrological and geomorphological characteristics and soil carbon (%C, soil carbon density and $\delta^{13}C$). The statistical technique is useful for transforming non-linear distributions via a link function to a linear distribution to establish relationships between dependent variables and local contributing conditions (Saintilan *et al.* 2013).

Generalised linear models were used in this study to determine the relationship between soil carbon characteristics (%C, $\delta^{13}C$, soil carbon density and soil carbon stock), down-core depth, vegetation community type, and grain size distribution. Dependent variable datasets were checked for distribution (e.g. normal, exponential, Poisson) to determine the appropriate link function for fitting of linear distribution in the GLM. When data did not fit any regular

distributions (i.e. non-parametric data), a normal distribution was assumed as a result of the large sample size used for modelling and the high level of significance returned in the test, therefore limiting the potential for a Type I error (B. Gooden, pers. comm.).

Partition modelling

Decision tree partition modelling can be used to partition data according to relationships between X and Y values and identifies the optimum value where the means in a continuous response value change. In this study, decision tree partition modelling was used to identify the down-core depth at which the $\delta^{13}C$ signature shifts significantly for each vegetation type. T-tests were performed to determine the significance of the partition point.

4.5. Spatial analysis

4.5.1. Digital Elevation Model (DEM) analysis

A 1 m Digital Elevation Model (DEM) derived from a LiDAR C3 point cloud from an Airborne Laser Scanner (ALS50) system (NSW Land and Property Information) was used to derive a range of hydrological features at Ukerebagh Island. The DEM has a reported vertical accuracy of ± 0.3 m and a horizontal accuracy of ± 0.8 m. The 'Hydrology' (Spatial Analyst) Toolbox in ArcMap 10.2 was utilised for this purpose and a basic model constructed for raster dataset derivation (Figure 4.3).

DEM validation

To determine the accuracy of the 1 m DEM, ground control points from the site were collected for the purpose of elevation accuracy validation. Ground control points were collected using a Trimble R8 Real-Time Kinematic Global Positioning System (RTK GPS) and simultaneously corrected using CORSnet-NSW, a system of permanent satellite navigation tracking systems. Kinematic surveying with the Trimble R8 produces a horizontal accuracy of ± 10 mm + 1 ppm RMS and a vertical accuracy of ± 20 mm + 1 ppm RMS (Trimble, 2014). To avoid any bias, points that were collected at a higher density than the DEM cell size (i.e. 1 m) were removed, ensuring that analysis utilised only one RTK point per raster cell (after Bowie, 2015). These points were exported to ArcMap 10.2 and 'Extract Values to Points' (Spatial Analyst toolbox) was used to extract the DEM elevation values to the RTK point shapefile and the attribute table was exported to Excel. Linear correlation was then used to determine the agreement between RTK point and DEM values, returning an R-squared value.

Hydrology model

The DEM extent for Ukerebagh Island ('Uke_Is_DEM') was extracted from the original DEM ('Tweed_DEM') using 'Extract by Mask' with a polygon outline ('Uke_is_outline.shp'). To determine the number of anomalous flow direction cells in the output, 'Flow Direction' was applied to the DEM and 'Sink' was then applied, identifying any cells which could not be assigned

Figure 4.3: ArcMap 10.2 ModelBuilder output for derivation of hydrological characteristics from a Digital Elevation Model.

any of the 8 valid flow direction values and are therefore anomalous. The sink tool was applied to determine if the DEM had enough errors contained within and accordingly, required smoothing via the 'Fill' tool to develop a depressionless DEM.

The 'Fill' tool was subsequently applied to the original DEM ('Uke_fill_DEM') and 'Flow Direction' was recalculated ('Uke_fill_flowdir'). This dataset was then used to determine both upstream and downstream flow length via the 'Flow Length' tool ('Uke_flowlength_upstream' and Uke_flowlength_downstream') and to determine a stream network for the island via the 'Flow Accumulation' tool ('Uke_flow_accumulation').

4.5.2. Vegetation mapping

Aerial photography from 22 April 2015 was obtained from Tweed Shire Council and digitised vegetation mapping was performed via ArcMap. To enable comparison with previous vegetation mapping undertaken by Rogers *et al.* (2014), the following three categories were used for classification:

- Mangrove
- Saltmarsh
- Mudflat

Although the 'Mixed' vegetation classification has been utilised previously for this site and other estuaries along the south-east coast of Australia (i.e. the Pacific Wetlands Environmental Consultants estuarine vegetation monitoring programs), the above three vegetation communities were selected for use in this analysis for better identification of the occurrence of intermediate mudflats between saltmarsh disappearance and mangrove colonisation.

To determine the hydrological and elevation characteristics for each vegetation community, vegetation extent polygons were converted to rasters ('Polygon to Raster') and flow length, flow accumulation and elevation were extracted to separate raster files using the 'Extract by Mask' tool. Following this, the vegetation extent rasters were converted to point shapefiles ('Raster to Point'). 'Extract Multi Values to Points' was performed to create attribute tables for each vegetation community. The attribute tables from these point shapefiles were then exported as text files for statistical analysis. Figure 4.4 shows the ModelBuilder output for vegetation community attribute determination.

Oneway ANOVA analysis was performed to determine if there was a significant relationship between vegetation community type and elevation, flow length and flow accumulation. Post-hoc Tukeys HSD was again used to delineate differences between separate vegetation types.

4.5.3. Inundation characteristics

Two Onset HOBO U20 water loggers on site that had been deployed during previous fieldwork in 2015 were retrieved during the 2016 field season. One water logger was placed at mangrove SET 2 (TR1) while the other was placed at saltmarsh SET 1 (TR2) (Figure 4.5). Absolute pressure (kPa) and temperature (°C) was recorded at 15-minute intervals for the period

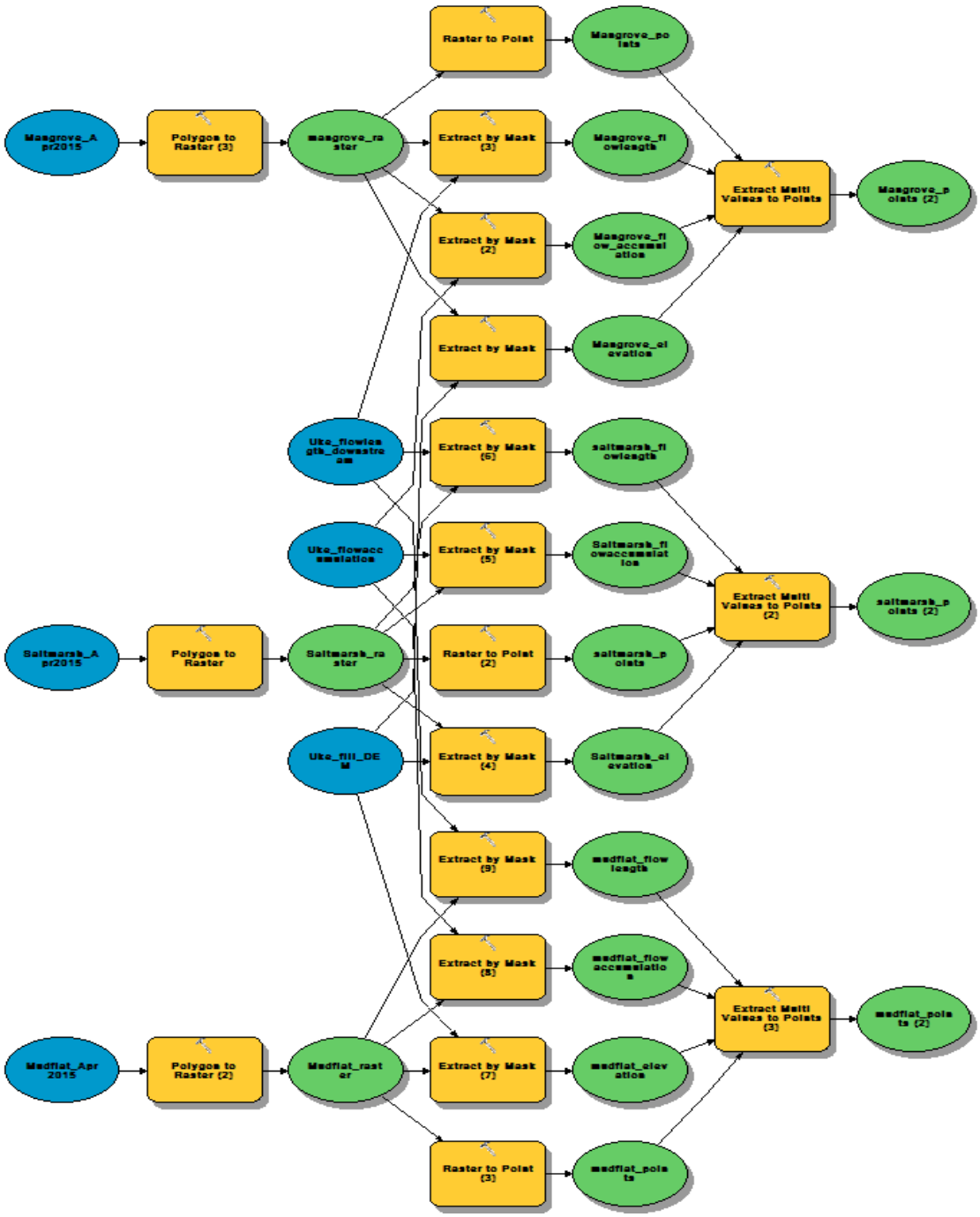

Figure 4.4: ArcGIS ModelBuilder output for extraction of hydrological and elevation characteristics of individual vegetation communities.

5/05/2015-17/12/2015 and extracted using HOBOware Pro software. To determine sensor depths, barometric compensation was performed using mean sea level pressure (MSLP) barometric data from the Coolangatta AP weather station (4.2 km NE of Ukerebagh Island) obtained from the Bureau of Meteorology. HOBOware Pro automatically calculated general statistics for each water logger (e.g. mean sensor depth and standard deviation).

Hydroperiod (i.e. the proportion of time inundated) was calculated by determining the fraction of 15 minute measurements that exceeded 0.01 m depth (Equation 3.4). Measurements between 0 and 0.01 m were disregarded to minimise errors associated with water remaining in the water logger casing (after Bowie, 2015). Mean inundation depth for the points was then calculated by determining the average of all 15 minute measurements that exceeded 0.01 m.

Equation 4.6: Hydroperiod and mean inundation depth calculations.

$$Hydroperiod = \frac{n(depth\ measurements > 0.01\ m)}{n(depth\ measurements)}$$

$$Mean\ inundation\ depth = \frac{\Sigma(depth\ measurements > 0.01\ m)}{n(depth\ measurements > 0.01\ m)}$$

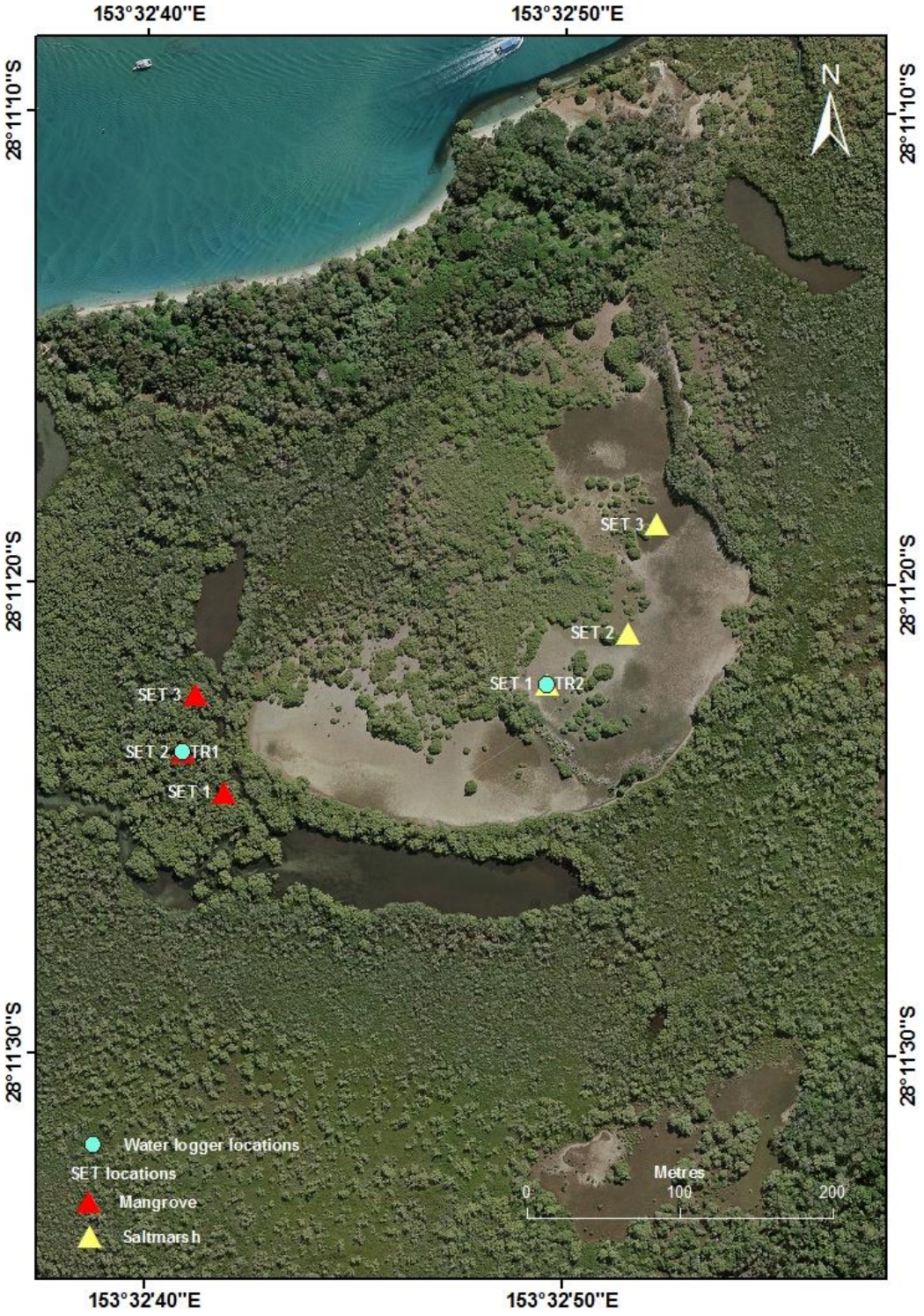

Figure 4.1: SET and HOBO water logger locations.

Chapter 5. Results

This section presents the results of 1) sediment and soil carbon characteristics, and statistical analyses; 2) ^{210}Pb sediment mass accumulation and sedimentation rate calculations, and 3) derivation of vegetation community and hydrological characteristics from remote sensing data and in-situ measurements.

5.1. Sediment and soil carbon characteristics

5.1.1. Sediment characteristics

Grain size

Mangrove cores (T1-3, T2-4, ^{210}Pb B, Figures 5.4, 5.8, 5.10) generally consisted of dark organic material interspersed with thick mangrove roots in approximately the top 40 cm of each core, after which a noticeable shift to grey sandy material was evident. Saltmarsh (T1-1, T2-1, T2-2, ^{210}Pb A, Figures 5.2, 5.5, 5.6, 5.9) and mixed vegetation cores (T1-2, T2-3, Figures 5.3, 5.7) also exhibited a highly sandy, but organic-rich, upper layer.

All cores extracted exhibited a general shift towards an increasing sand fraction down-core, with phi (ϕ) values at core bottoms ranging between 1.65 and 2.07, generally indicating that the main source material is fine-grained sand. Throughout all cores at all depths, phi values rarely exceeded 5 (coarse silt). *Cerithium novaehollandae* shell specimens, an intertidal mollusc, were found at the base of mangrove core T1-3. Surface grain size distribution indicated highly sandy

Figure 5.1: *Cerithium novaehollandae* shell found at core bottom in mangrove core T1-3.

fractions, ranging from 39.5 – 76.2% sand for saltmarsh surface values 33.8 – 68.2% in mangrove surface values and 74.6 – 75.8% in mixed surface values.

Periodic shifts in grain-size distribution down-core were observed in the majority of the cores taken, with noticeable variations in sand and silt percentage in all vegetation community types. Decreases in sand percentage approximately between 20 - 30 cm down-core are reflected across the entirety of the mangrove cores (T1-3, T2-4 and ^{210}Pb B), with decreases of similar magnitude also apparent in saltmarsh cores T2-2 and ^{210}Pb A, and mixed vegetation core T1-2. Saltmarsh cores T1-1 and T2-1 also exhibit a small decrease in sand percentage between 10 and 20 cm, while increasing with depth afterwards.

Dry bulk density and moisture content

Moisture content and dry bulk density patterns generally reflected grain size down-core, with dry bulk density increasing and moisture content decreasing. Across all cores, dry bulk density generally increases to approximately 0.7 - 1 g cm^{-3} at core bottom, with corresponding decreases in moisture content. Moisture content in all cores generally approached approximately 20% or less at core bottom and within sample depths where sand percentage approached 100%, reflecting a general moisture content and dry bulk density value for compacted sand at depth. The nature of these values suggests that uniform compaction and dewatering of sandy sediment occurs at depth. Within the organic-rich zone at the top of the cores, mangrove cores (T1-3, T2-4 and ^{210}Pb B) demonstrated dry bulk density values ranging from 0.09 g cm^{-3} to 0.36 g cm^{-3} before rapidly increasing within the lower sand-rich layer underlying organic-enriched sediment. These low dry bulk densities and the corresponding high moisture contents reflect the less compacted nature of sediments within mangrove communities. On the other hand, saltmarsh and mixed community dry bulk densities were much higher within the predominantly organic derived sample depths, with moisture contents rarely exceeding 40% and dry bulk densities occasionally below 0.5 g cm^{-3}, most noticeably at the top of saltmarsh core T1-1 and T2-1, at 60 cm depth in saltmarsh core T2-1 and T2-2 and at 15 and 30 cm in mixed core T2-3.

5.1.2. Down-core comparisons of sediment and soil carbon characteristics

Figures 5.2 to 5.10 illustrate core cross-sections, grain size distribution (sand, silt and clay percentages and phi values), moisture content and dry bulk density values, and soil carbon characteristics (%C, δ^{13}C and soil carbon density) for each core.

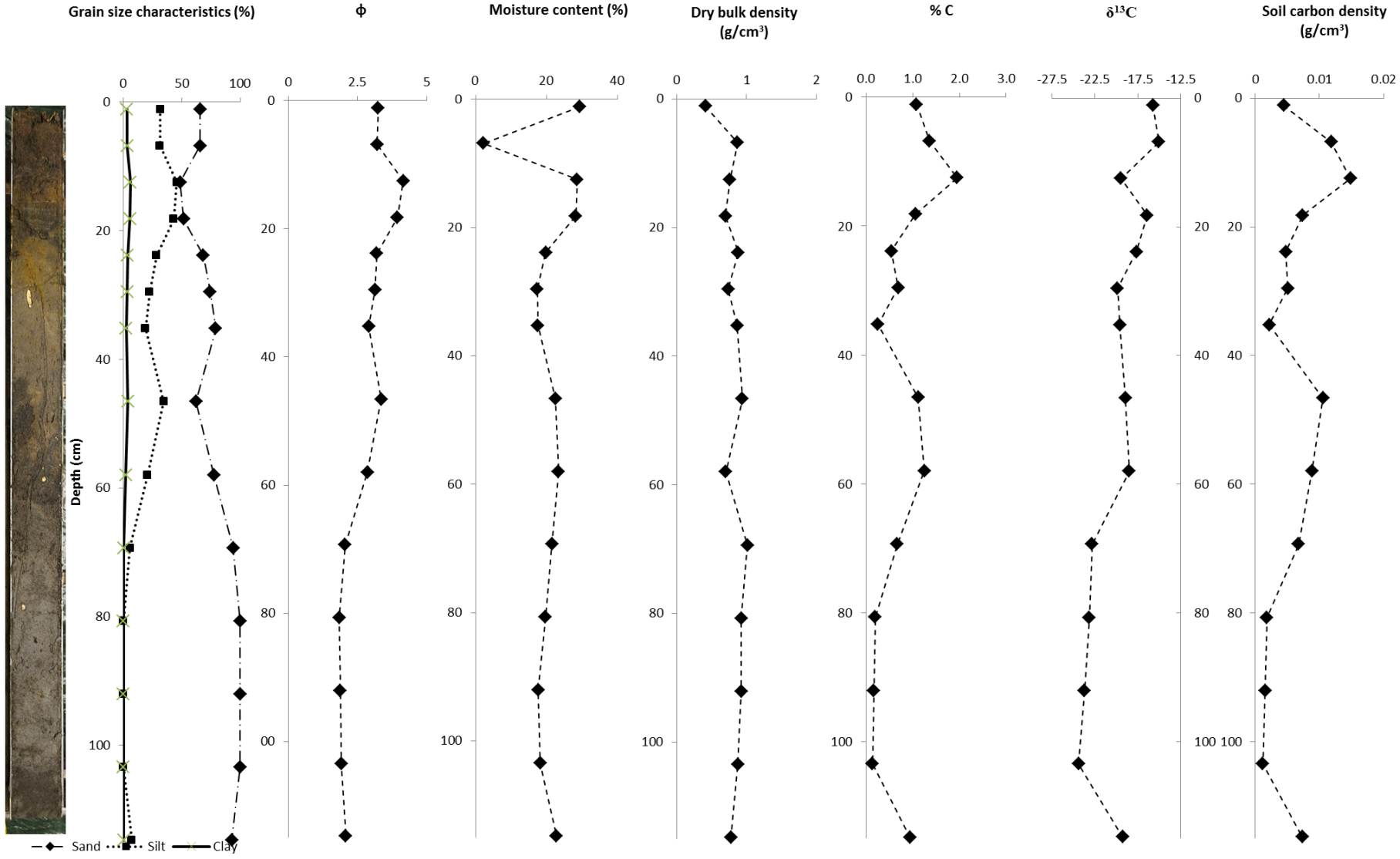

Figure 5.2: Grain size, phi, moisture content and dry bulk density, and soil carbon characteristics for saltmarsh core T1-1.

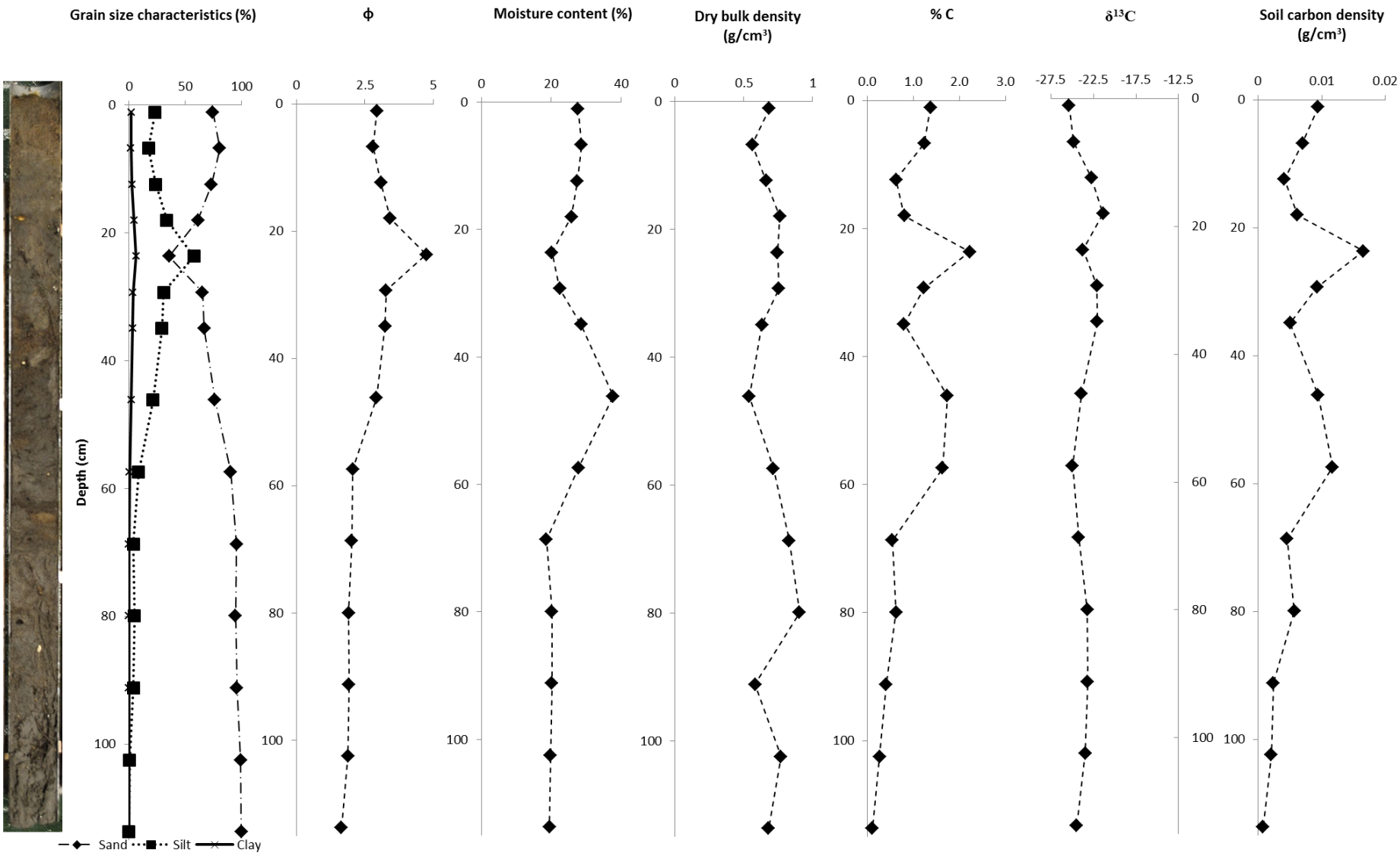

Figure 5.3: Grain size, phi, moisture content and dry bulk density, and soil carbon characteristics for mixed core T1-2.

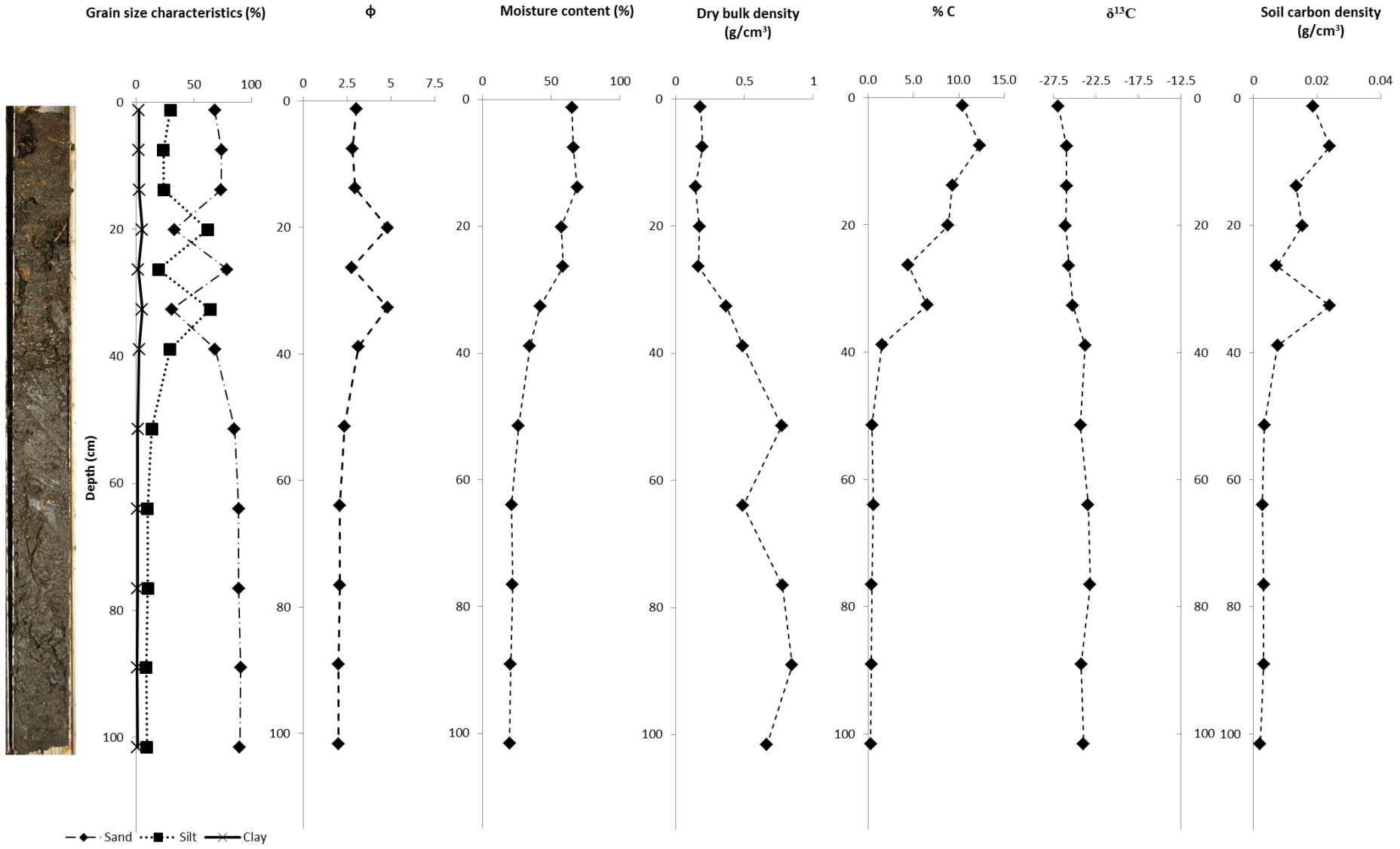

Figure 5.4: Grain size, phi, moisture content and dry bulk density, and soil carbon characteristics for mangrove core T1-3.

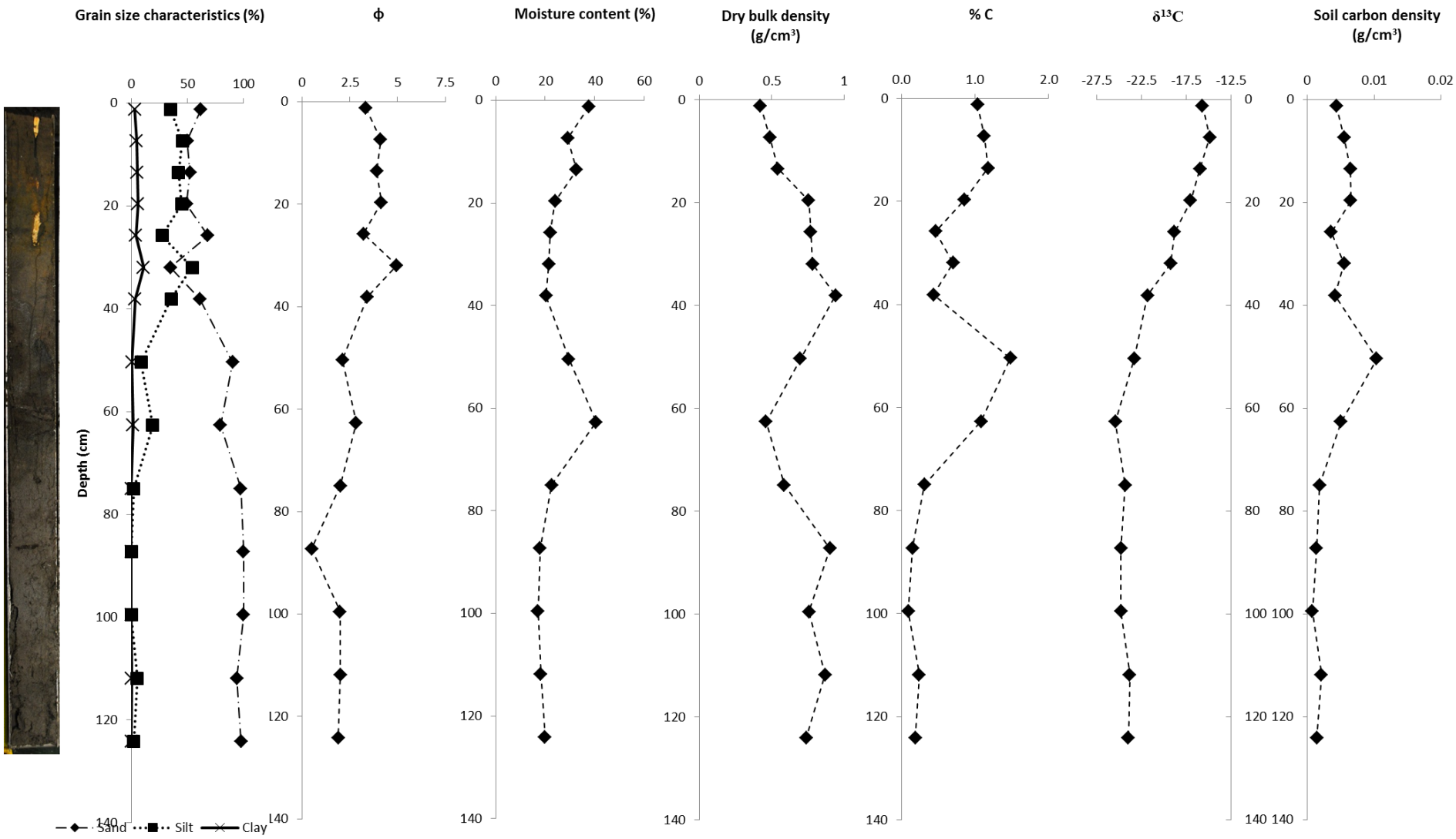

Figure 5.5: Grain size, phi, moisture content and dry bulk density, and soil carbon characteristics for saltmarsh core T2-1.

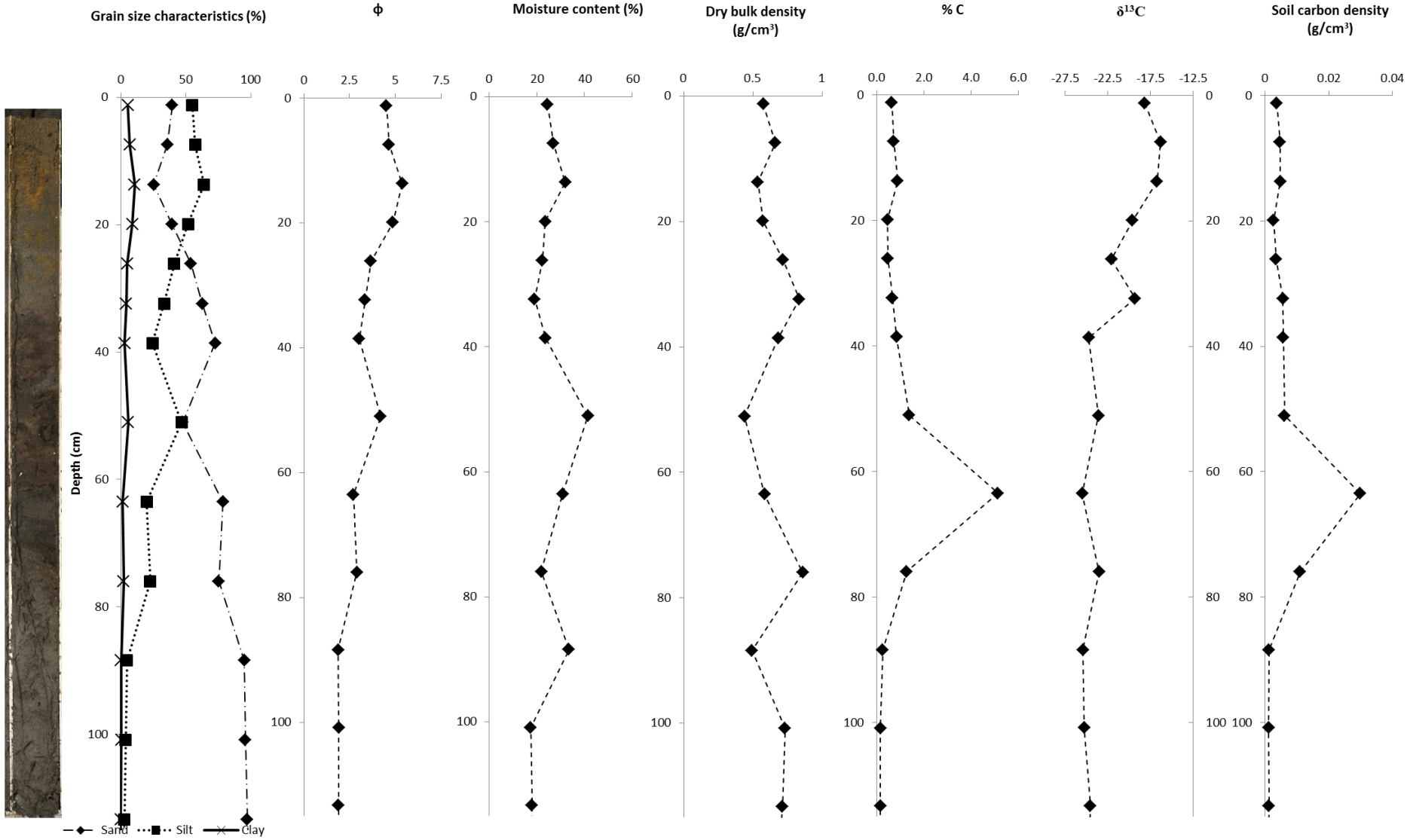

Figure 5.6: Grain size, phi, moisture content and dry bulk density, and soil carbon characteristics for saltmarsh core T2 -2.

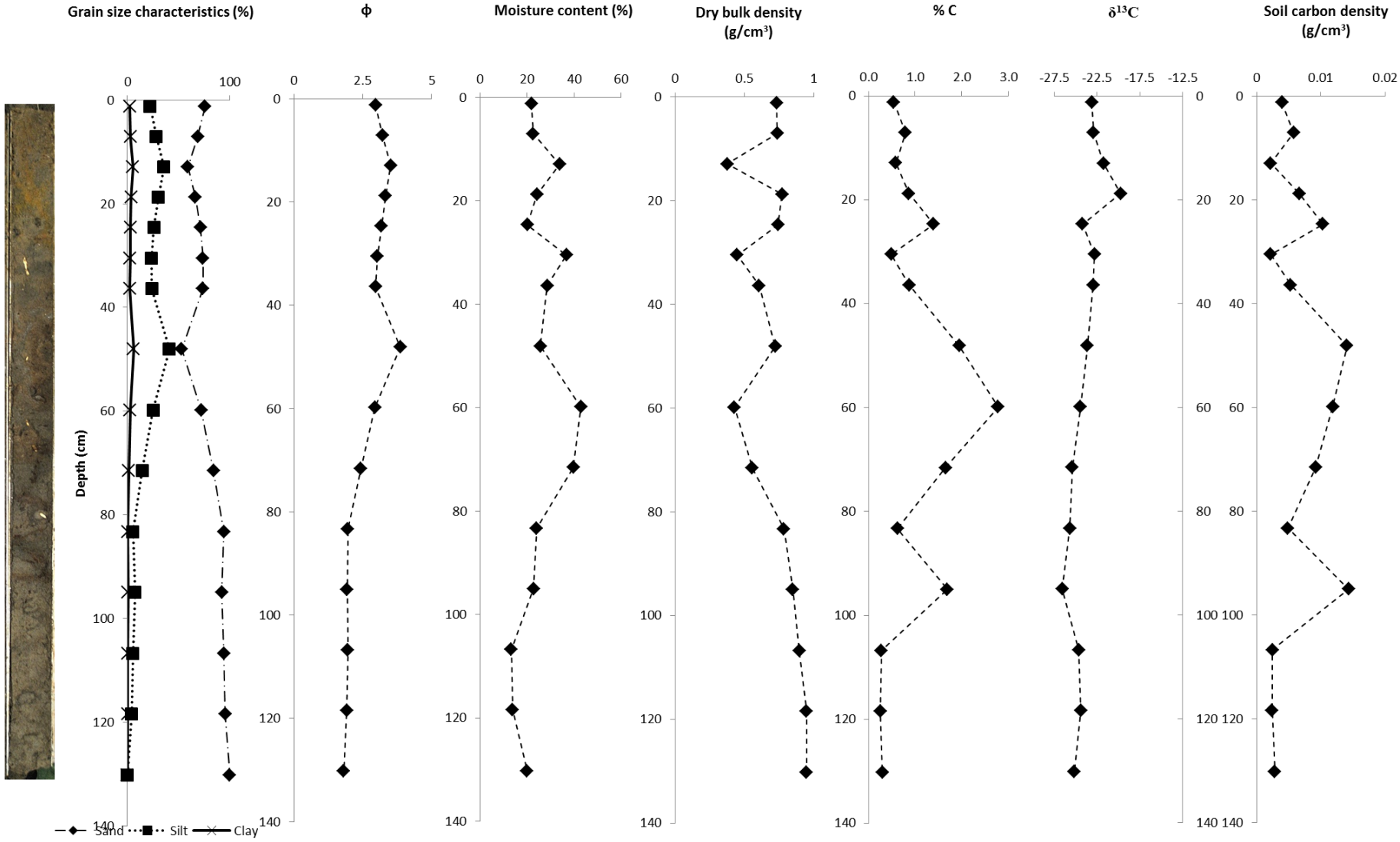

Figure 5.7: Grain size, phi, moisture content and dry bulk density, and soil carbon characteristics for mixed core T2-3.

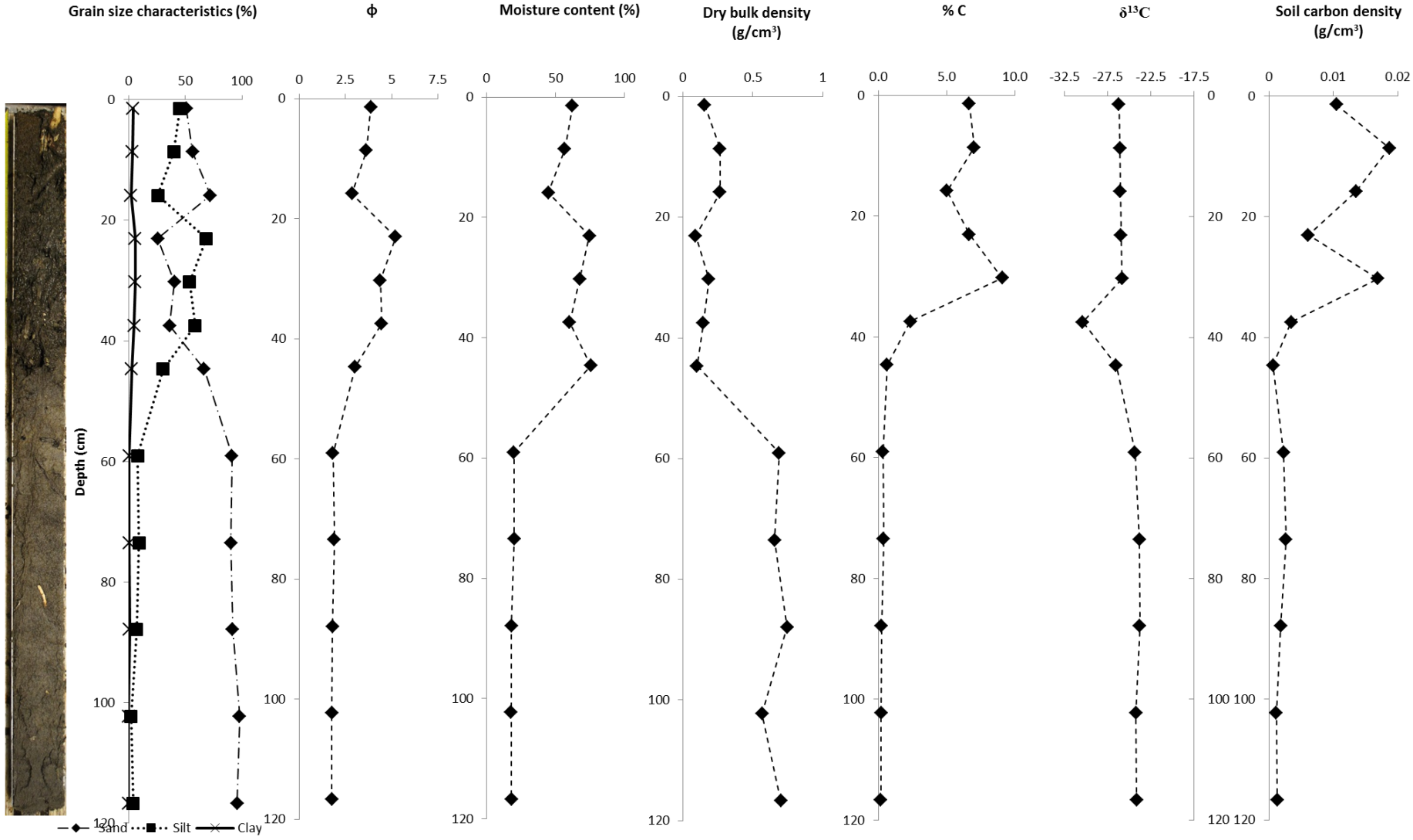

Figure 5.8: Grain size, phi, moisture content and dry bulk density, and soil carbon characteristics for mangrove core T2 -4.

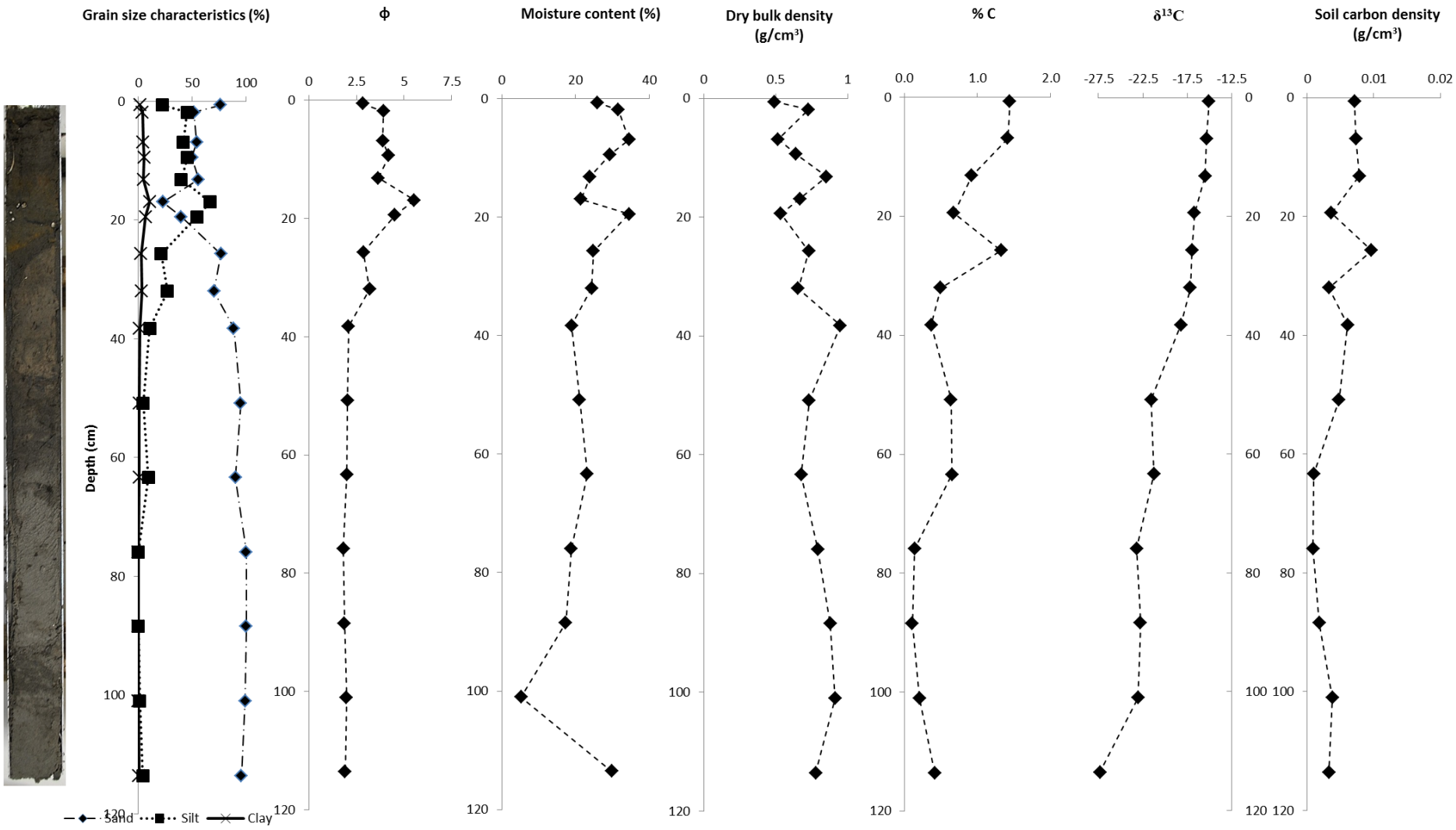

Figure 5.9: Grain size, phi, moisture content and dry bulk density, and soil carbon characteristics for saltmarsh core ^{210}Pb A.

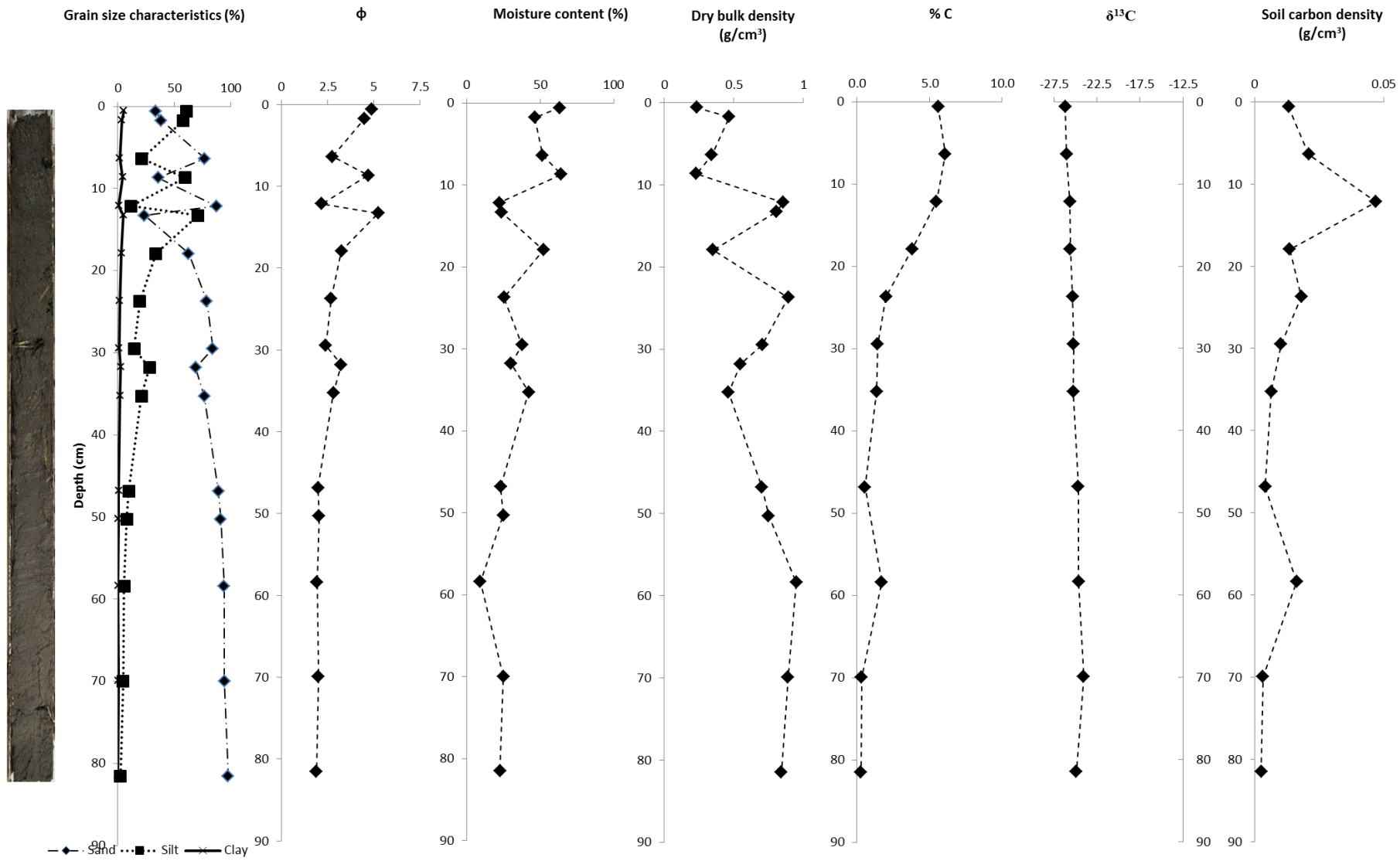

Figure 5.10: Grain size, phi, moisture content and dry bulk density, and soil carbon characteristics for mangrove core ^{210}Pb B.

5.1.3. Soil carbon characteristics

Carbon concentration and density

In all cores, soil carbon content decreased to between 0.1 - 0.3 % at core bottom. Soil carbon concentration (%C) values within the top 35 cm of mangrove cores were considerably higher than saltmarsh cores, varying from 4.4 - 12.3 % in mangrove cores T1-3 and T2-4. A lower range was observed in mangrove core ^{210}Pb B where high soil carbon content values (3.8 – 6.1%) were present within the top 19 cm of the core. Soil carbon concentration in mangrove cores was much higher than those within mixed vegetation and saltmarsh cores, where maximum values within top sediments (0 – 35 cm) did not exceed 2.2%.

When soil carbon concentration values did not fit the general trend of decreasing carbon content with depth, they generally accompanied an increase in phi values, indicating finer-grained sediment. Instances of this relationship were found in saltmarsh cores T1-1 (11 – 19 cm, 45 – 59 cm) and T2-1 (30 – 33 cm), mixed cores T1-2 (22 – 24 cm) and T2-3 (46 – 49 cm) and mangrove core T1-3 (18 – 21 cm, 31 – 33 cm). Decreases in phi values (increased grain size) often accompanied increases in soil carbon density. Down-core variation in soil carbon density reflects the mostly uniform down-core increase in dry bulk density and decomposition-related decrease in soil carbon concentration. Maximum soil carbon density values do not appear to differ greatly between mangrove, mixed and saltmarsh cores. However, oneway ANOVA indicated a significant difference between soil carbon densities by vegetation type ($DF = 118$, $F = 6.4111$, $p = 0.0023$). Post-hoc Tukeys HSD showed that while mangrove and saltmarsh soil carbon densities were significantly different, mixed vegetation values were not significantly different to either mangrove or saltmarsh soil carbon densities.

GLM results indicated that soil carbon concentration and density were significantly affected by both depth and vegetation type, in combination, as single effects and in interaction with each other (Table 5.1, Models A and B respectively). This analysis supports observations that soil carbon density, especially within active growing zones of the cores, was significantly different between vegetation types and the reduction in both soil carbon concentration and density with increasing depth. Conversely, mean grain size (micron) was not found to significantly influence carbon concentration and density (Models C and D), but significant interaction effects supported observations of lower soil carbon density when grainsize was larger and at depth, and higher carbon density for shallower depths and smaller grain sizes. A significant interaction effect was not found for mean grain size and depth for soil carbon concentration (Model C), indicating that the generally low variation in grain size with depth was not a significant controlling factor on soil carbon concentration.

Table 5.1: Results from generalised linear model analyses for $\delta^{13}C$, %C and soil carbon density (g cm^{-3}). Asterisk (*) indicates models where the chi-squared distribution was non-parametric, but normality was assumed because of high significance of results.

Model	Variables			GLM Model			Significance			
	Dependent variable	Effect variable 1	Effect variable 2	Distribution	Link function	Goodness of fit (Pearsons)	Whole model	Effect 1	Effect 2	Interaction
A	Soil carbon concentration (%C)	Depth (cm)	Vegetation type	Normal	Identity	**<.0001**	**<.0001**	**<.0001**	**<.0001**	**<.0001**
B	Soil carbon density (g cm^{-3})	Depth (cm)	Vegetation type	Normal	Identity	**1.0000***	**<.0001**	**<.0001**	**0.0148**	**<.0001**
c	Soil carbon concentration (%C)	Depth (cm)	Mean grain size (micron)	Normal	Identity	**<.0001**	**<.0001**	**0.0003**	0.5406	0.6096
D	Soil carbon density (g cm^{-3})	Depth (cm)	Mean grain size (micron)	Normal	Identity	**1.0000***	**<.0001**	**<.0001**	0.0535	**0.0209**
E	$\delta^{13}C$	Depth (cm)	Vegetation type	Normal	Identity	**<.0001**	**<.0001**	**<.0001**	**<.0001**	**<.0001**

<u>$\delta^{13}C$ signatures</u>

$\delta^{13}C$ values from the top 20 cm of the saltmarsh cores (T1-1, T2-1, T2-2, ^{210}Pb A) range between -14.8 and -19.5‰, predominantly within the range of *Sporobolus* values specified in previous studies. In all cores, $\delta^{13}C$ signature generally transitions to depleted values approximating C_3 signatures with increasing depth.

Mixed vegetation cores, while exhibiting $\delta^{13}C$ values that strongly suggest C_3 plant provenance (core T1-2, surface $\delta^{13}C$ value = -25.4‰, core T2-3, surface $\delta^{13}C$ value -23.1‰), also displayed a shift towards $\delta^{13}C$ values that were more enriched than typical C_3 signatures, suggesting the mixing effect of autochthonously derived C_3 and C_4 soil carbon. $\delta^{13}C$ signatures in mangrove cores suggested C_3 provenance throughout the whole core depths. Surface $\delta^{13}C$ signatures ranged between -26.9 and -26.2‰. All mangrove cores demonstrated a general down-core enrichment of $\delta^{13}C$ values alongside a decrease in soil carbon content and soil carbon density.

The incorporation of mangrove organic material in cores ostensibly from saltmarsh areas, or areas where saltmarsh has been historically dominant, was noted in several cores. After removal

of saltmarsh core T2-1, a mangrove pneumatophore was observed within the core top (Figure 5.5, photo inset). In mixed vegetation core T1-2, mangrove roots were recovered from within the core at a depth of 101-114 cm.

A consistent pattern across both transects and between ^{210}Pb cores was observed as core location transitioned from saltmarsh to mangrove (Figure 5.11). $\delta^{13}C$ values within the upper core shift from enriched $\delta^{13}C$ values, typical of C_4 plants, in saltmarsh, to more depleted values in mixed vegetation areas and culminating in $\delta^{13}C$-depleted values resembling C_3 signatures in the mangrove vegetation. Decreasing $\delta^{13}C$ values from saltmarsh to mangrove areas reflects the vegetation transition on the island, with the intermediate $\delta^{13}C$ values in the upper parts of mixed cores possibly indicating a mixing effect between C_3 and C_4 carbon sources. At lower depths in all cores, $\delta^{13}C$ values were depleted, suggesting a C_3 carbon source. Partitioning analysis by individual core (Figure 5.11) and by vegetation type (Table 5.2) indicated that the most pronounced variance in above and below-partition mean was found in the saltmarsh cores, with individual core partition depths ranging from 38 - 69 cm for saltmarsh, 29 – 59 cm for mangrove, and 46 – 59 cm for mixed cores.

Above-partition means for mixed cores ranged between -22 and -23‰ $\delta^{13}C$, while there was little difference between above- and below-partition means for mangrove cores. Below partition mean values for all cores were between -22 and -27‰ $\delta^{13}C$. Above and below partition $\delta^{13}C$ values in mangrove cores correspond approximately to $\delta^{13}C$ values for C_3 plants when compared to living mangrove tissue collected from other sites (Table 4.1). Similarly, above-partition values for saltmarsh closely reflect C_4 values (-18.7 to -16.4 ‰ $\delta^{13}C$), while the above-partition values from mixed cores suggest that a mixing of C_3 and C_4-derived soil carbon is resulting in an intermediate $\delta^{13}C$ signature.

Additionally, GLM analysis indicated that depth and vegetation type combined, as single effect and interaction (i.e. effects of depth on $\delta^{13}C$ are influenced by vegetation type) all have a significant effect on soil $\delta^{13}C$ (Table 5.1, Model E). The significant interaction effect ($p < 0.0001$) supports the differing extent of $\delta^{13}C$ signature variation with depth between vegetation types.

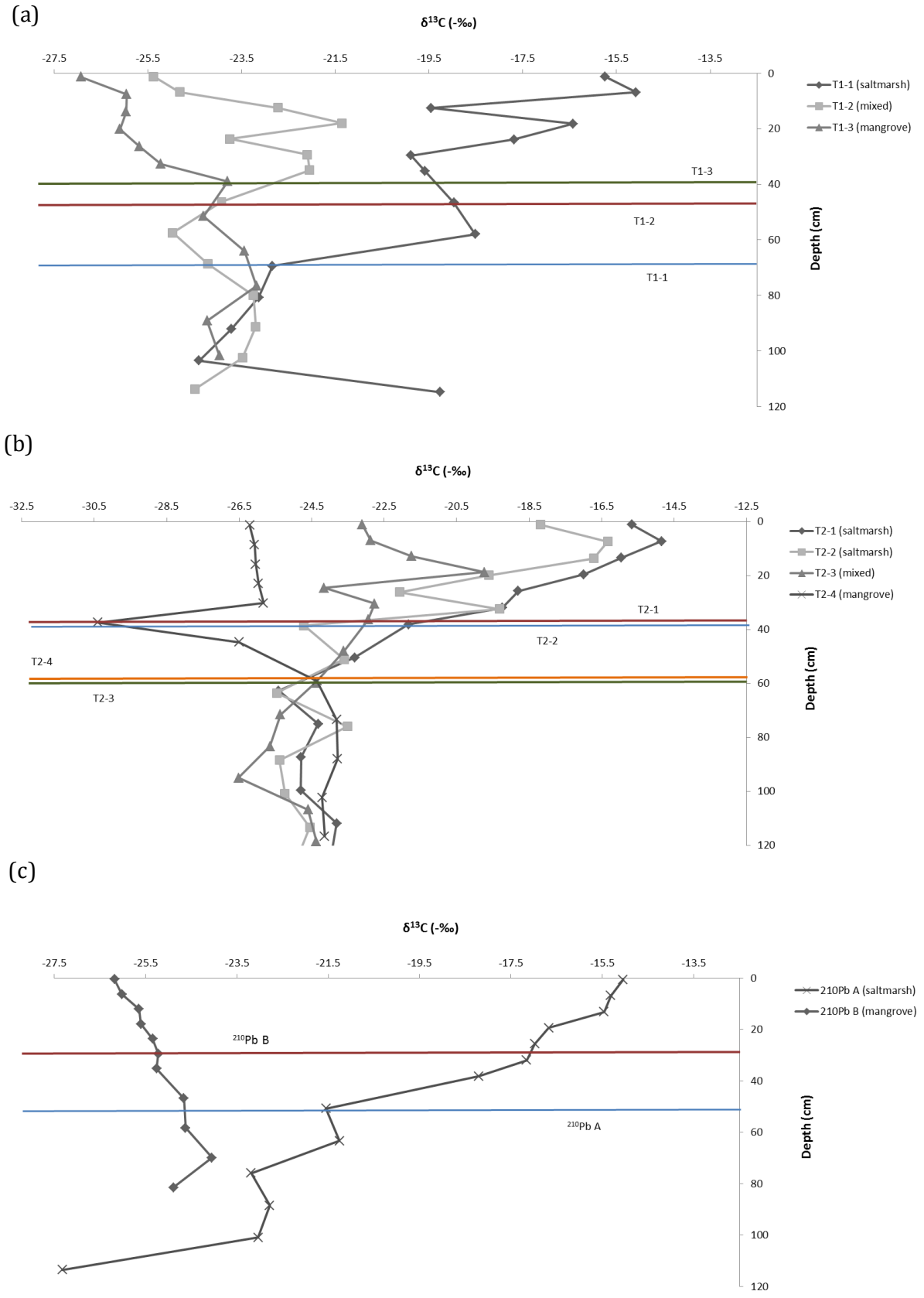

Fi¡Figure 5.11: Transect 1 (a), Transect 2 (b) and ^{210}Pb (c) δ^{13}C comparisons. Coloured lines and labels indicate popoints where mean significantly changes as determined by partition analysis.

Table 5.2: $\delta^{13}C$ values and t-test results for partitioning analysis of cores by vegetation type.

Vegetation type	Optimum depth partition (cm)	Mean $\delta^{13}C$ (-‰ ± SE) above partition	Mean $\delta^{13}C$ (-‰ ± SE) below partition	Significance
Mangrove	46.823	-25.995 ± 0.211	-24.118 ± 0.258	**p<0.0001**
Mixed vegetation	46.168	-22.896 ± 0.316	-24.517 ± 0.327	**p=0.0014**
Saltmarsh	38.60909	-17.860 ± 0.402	-23.619 ± 0.425	**p<0.0001**

.

5.1.4. Total carbon store

Total carbon store was highly variable between cores, both along transect and by vegetation type (Table 5.3). One-way ANOVA analysis of total carbon store within 8 cores (Figure 5.12) did not demonstrate a significant difference between carbon store by vegetation type (DF = 7, F = 1.8652, p = 0.2482). Mangrove core ^{210}Pb B was excluded from analysis because sampling depth did not meet requirements for analysis (minimum 1 m sampling depth).

Table 5.3: Total carbon store within sample cores classified by in-situ vegetation type. Mangrove core ^{210}Pb B was excluded from statistical analysis due to minimum sampling depth requirements.

Core name	Vegetation type	Total carbon store (MgC ha^{-1})
T1-1	Saltmarsh	50.762
T1-2	Mixed	59.371
T1-3	Mangrove	47.752
T2-1	Saltmarsh	35.431
T2-2	Saltmarsh	63.823
T2-3	Mixed	75.284
T2-4	Mangrove	27.040
^{210}Pb A	Saltmarsh	23.546
^{210}Pb B	Mangrove	88.052*

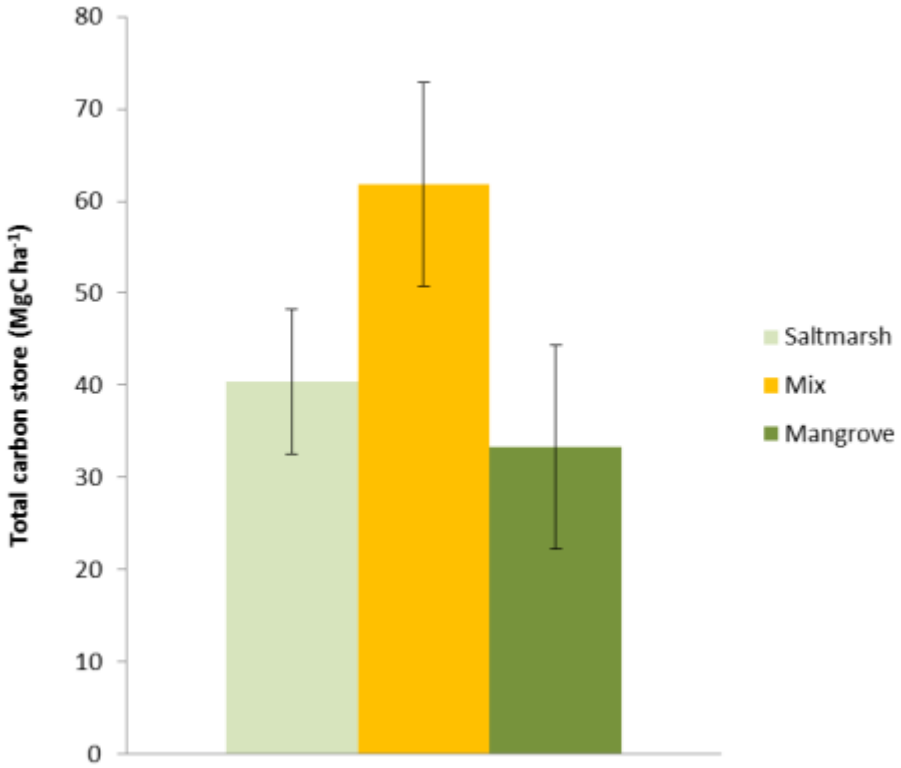

Figure 5.13: Variation in mean total carbon storage (± SE) by vegetation type.

5.1. Sedimentation rates

5.1.1. Saltmarsh sedimentation

The saltmarsh core (^{210}Pb A) exhibited an unsupported ^{210}Pb decay rate between 0 and 14.4 cm (Figure 5.13). In all samples, supported ^{210}Pb activity was less than 10 Bq kg^{-1}

^{137}Cs bomb peak calibration via gamma spectrometry indicated a broad peak (Figure 5.14) ranging from 4.3 to 6.9 cm. Although the peak is quite broad, it is in agreement with the ^{210}Pb dating profile and accordingly validates the ^{210}Pb dating (A Zawadzki, pers. comm.). CRS modelling indicated calculation of ^{210}Pb ages from 1850 to 2012 (Figure 5.15).

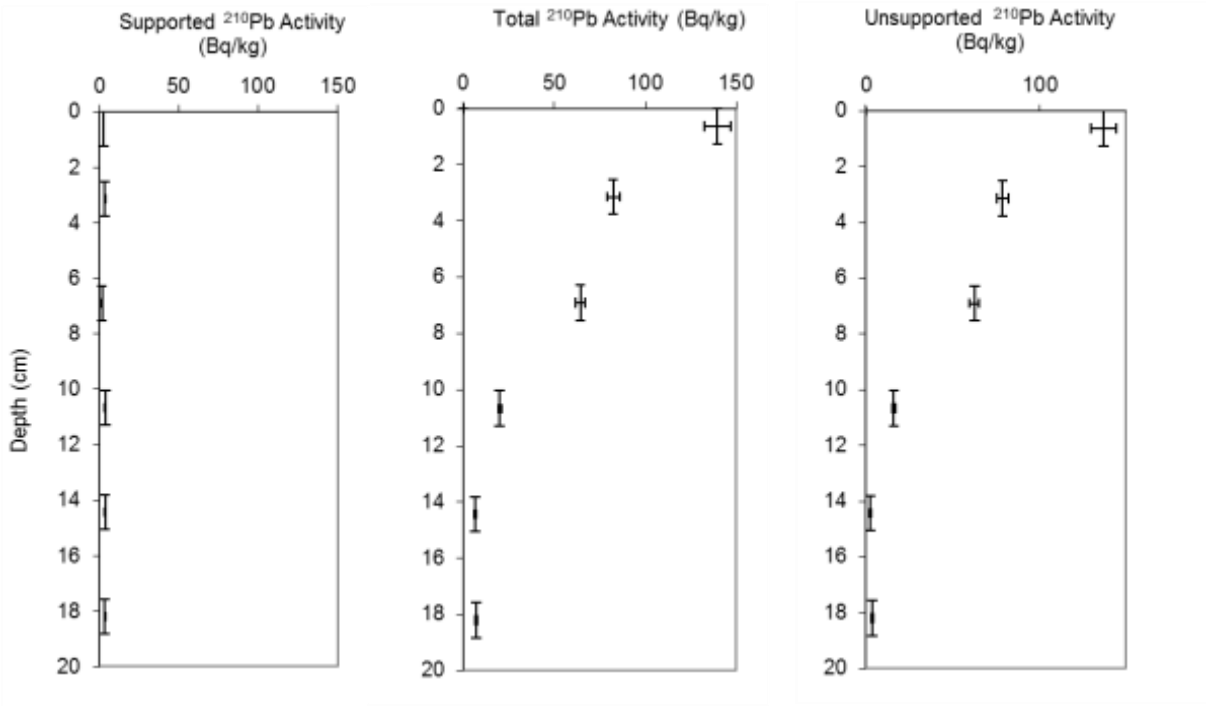

Figure 5.14: ^{210}Pb activity results for saltmarsh core ^{210}Pb A.

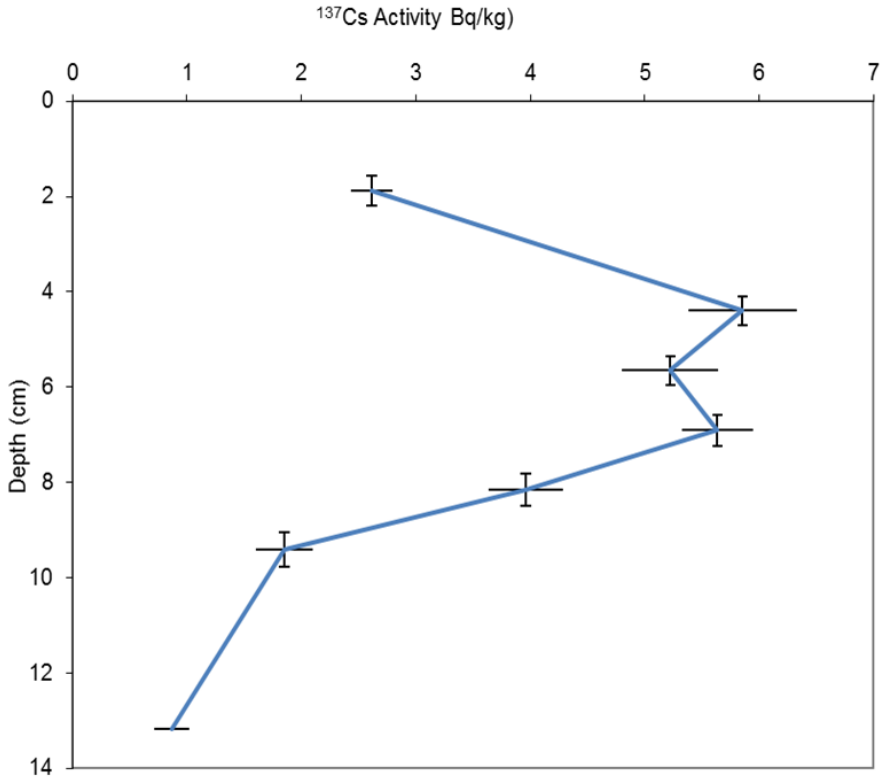

Figure 5.16: ^{137}Cs activity for saltmarsh core ^{210}Pb A.

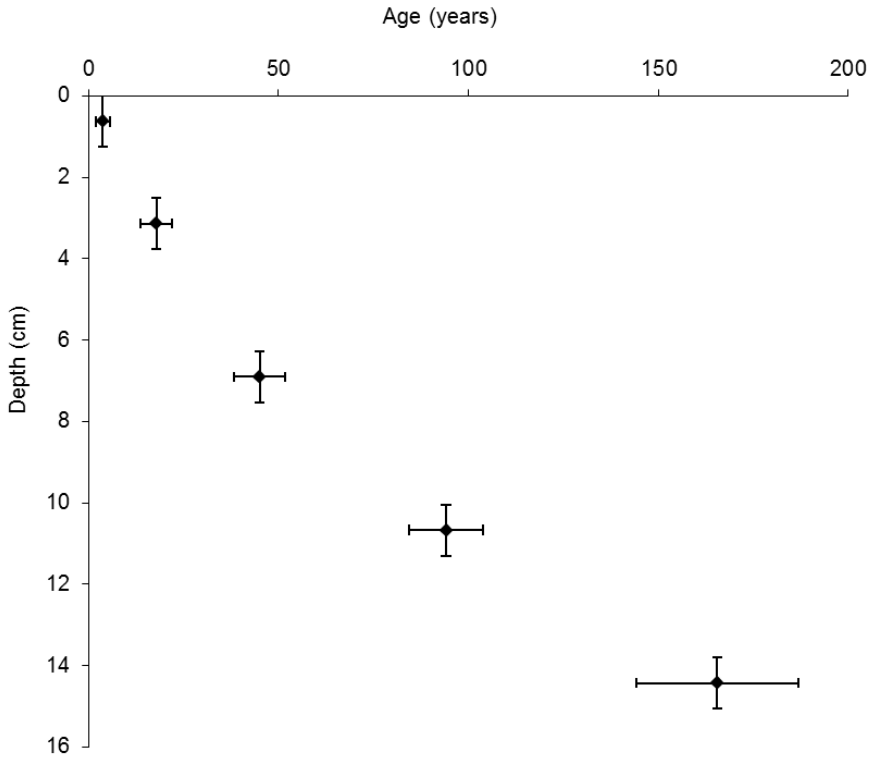

Figure 5.15: CRS modelling age vs. sample depth for saltmarsh core ^{210}Pb A.

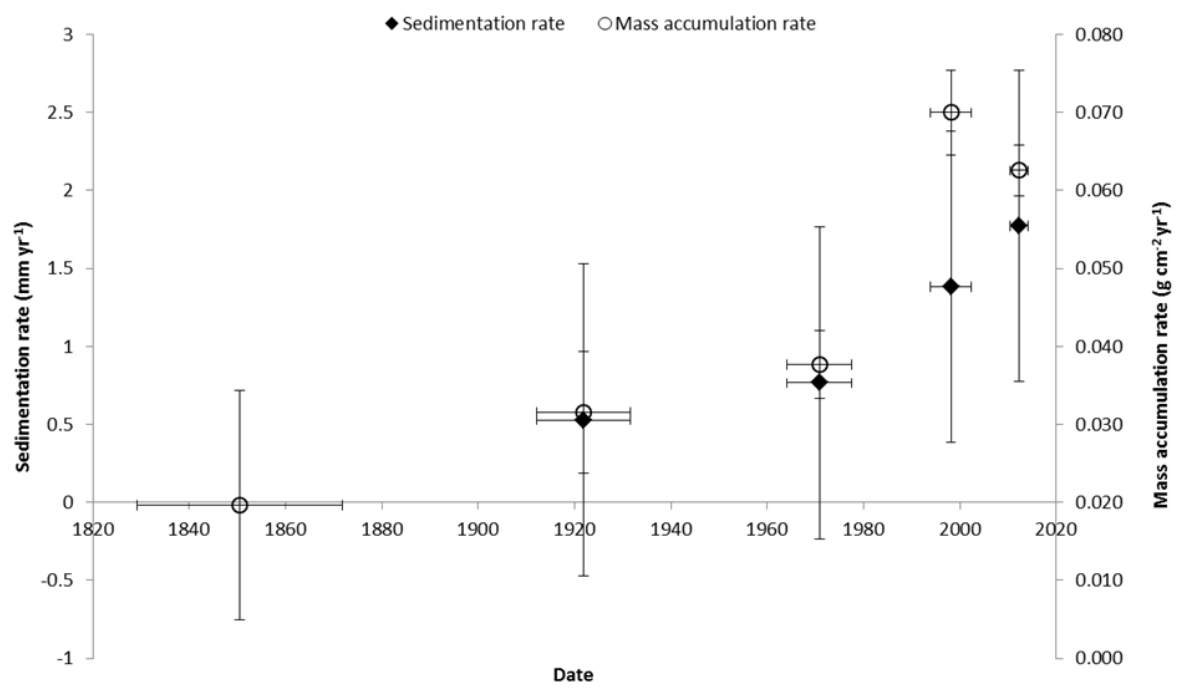

Figure 5.17: CRS sedimentation rates and mass accumulation rates for saltmarsh core ^{210}Pb A.

The saltmarsh core exhibited a steady increase in both mass accumulation and sedimentation rates over the last century (Figure 5.16). Mass accumulation was higher in younger sediments (0.020 ± 0.015 g cm^{-2} yr^{-1} at 1850, compared to 0.063 ± 0.003 g cm^{-2} yr^{-1}.at 2008).

Sedimentation rates exhibited a similar trend. Beginning with a measurement of 0.528 ± 0.21 mm yr^{-1} between 1922 and 2016, sedimentation rates accelerated to a maximum rate of 1.772 ± 0.86 mm yr^{-1}. Sedimentation accelerated faster in the second half of the 20th century, with no decreases across the period.

5.1.2. Mangrove sedimentation

Supported ^{210}Pb values were all below 10 Bq kg^{-1} in the mangrove core. However, at the bottom of the sampling range, unsupported ^{210}Pb was still quite high, fluctuating from 24 to 50 Bq kg^{-1} (Figure 5.17). Subsequently, CRS ages were calculated using samples from the top 15 cm of the core (Figure 5.18).

Because supported ^{210}Pb was so high at the lower sample depths, three samples were analysed for ^{226}Ra (substitute for supported ^{210}Pb) and ^{137}Cs using gamma spectrometry. This analysis returned ^{226}Ra results higher than the original alpha spectrometry, suggesting that the original pre-spectrometry sample digestion did not extract all of the ^{226}Ra in the sample matrix and accordingly, supported ^{210}Pb was greatly underestimated in the original alpha spectrometry.

Therefore, if supported ^{210}Pb is approximately 40 Bq kg^{-1}, as calculated in the ^{226}Ra gamma spectrometry results (Table 5.4), then the core cannot be dated below the point where supported ^{210}Pb is equal to total ^{210}Pb, at approximately 14 cm.

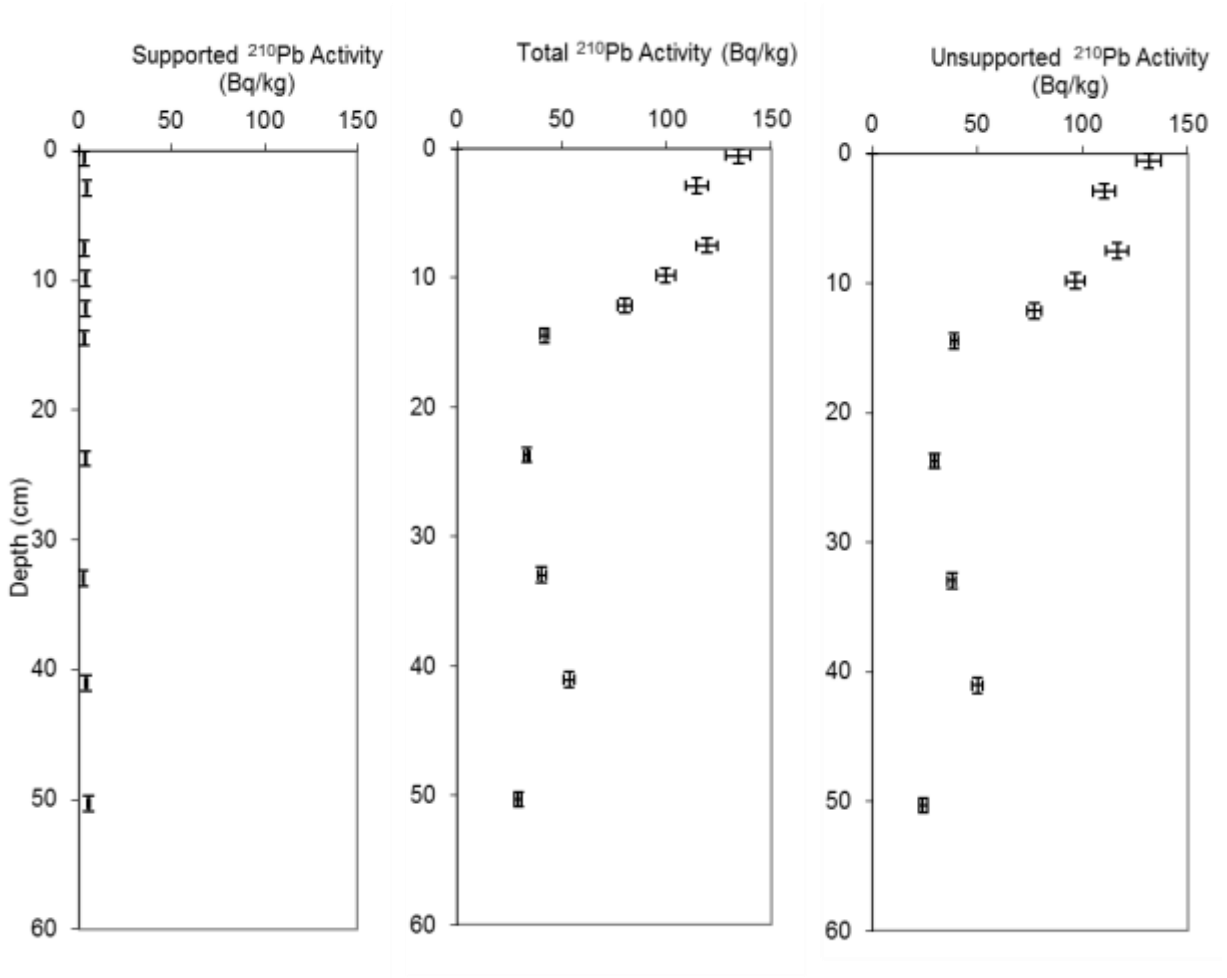

Figure 5.18: ^{210}Pb activity results for mangrove core ^{210}Pb B.

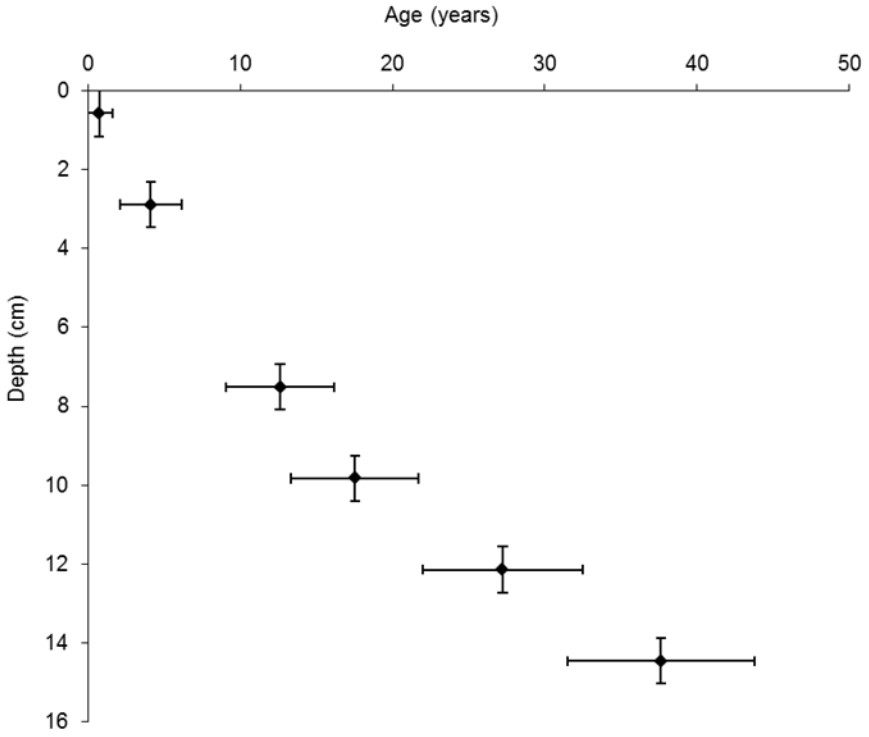

Figure 5.19: CRS modelling age vs. sample depth for mangrove core ^{210}Pb B.

Table 5.4: Gamma spectrometry results for ^{226}Ra (supported ^{210}Pb) and ^{137}Cs.

Sample ID (ANSTO)	Corrected depth (cm)	^{226}Ra (Bq kg^{-1})	^{137}Cs (Bq kg^{-1})
S716	4.6 - 5.8	38.0 ± 7.8	6.3 ± 1.3
S717	16.2 - 17.3	67.6 ± 5.6	4.9 ± 0.8
S718	20.8 - 22.0	16.6 ± 13.4	8.5 ± 1.9

Although CRS dates could only be measured to 1978, the sedimentation rates show a similar trend to the saltmarsh values. Again, acceleration in sedimentation over time was observed across the last 27 years, with a doubling in sedimentation rate coinciding with the commencement of the Tweed River Sand Bypass operation. Coefficients of determination for sedimentation rate vs. age for mangrove (R^2 = 0.8848) and saltmarsh (R^2 = 0.8689) indicated that acceleration in sedimentation rates suggest that acceleration has undergone generally consistent increases.

Mass accumulation rates were not as variable as sedimentation (Figure 5.19). The highest values (0.221 ± 0.013 and 0.221 ± 0.011 g cm^{-2} yr^{-1}) were calculated for CRS dates 1978 and 2012 respectively, with mass accumulation rates remaining steady at a rate between 0.154 and 0.166 between these two dates. As in the saltmarsh core, there is a slight decrease in mass accumulation in the last measured sample, which was dated to 2015. However, the higher mass accumulation rates at the surface indicated a similar pattern to the saltmarsh core, notwithstanding the high mass accumulation value from 1978.

Saltmarsh and mangrove mass accumulation rates and sedimentation rates showed similar patterns of sedimentation acceleration over time, and both cores showed high mass accumulation in younger sediments (Figures 5.16 and 5.19). Surface measurements in both cores, while being generally higher than historical mass accumulation, are lower relative to measurements immediately preceding them. Linear regression indicates that increases in mass accumulation and sedimentation rates show reasonably high levels of correlation (Figure 5.20), with a stronger relationship apparent in saltmarsh.

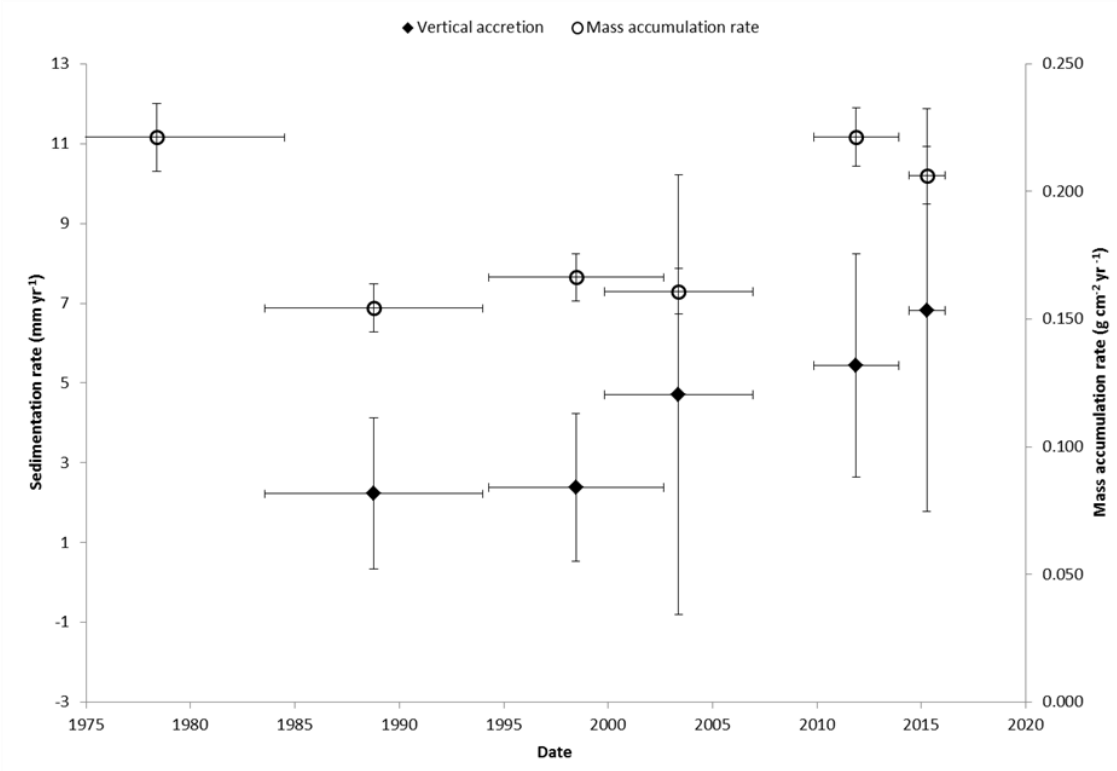

Figure 5.20: CRS sedimentation rates and mass accumulation rates for mangrove core ^{210}Pb B.

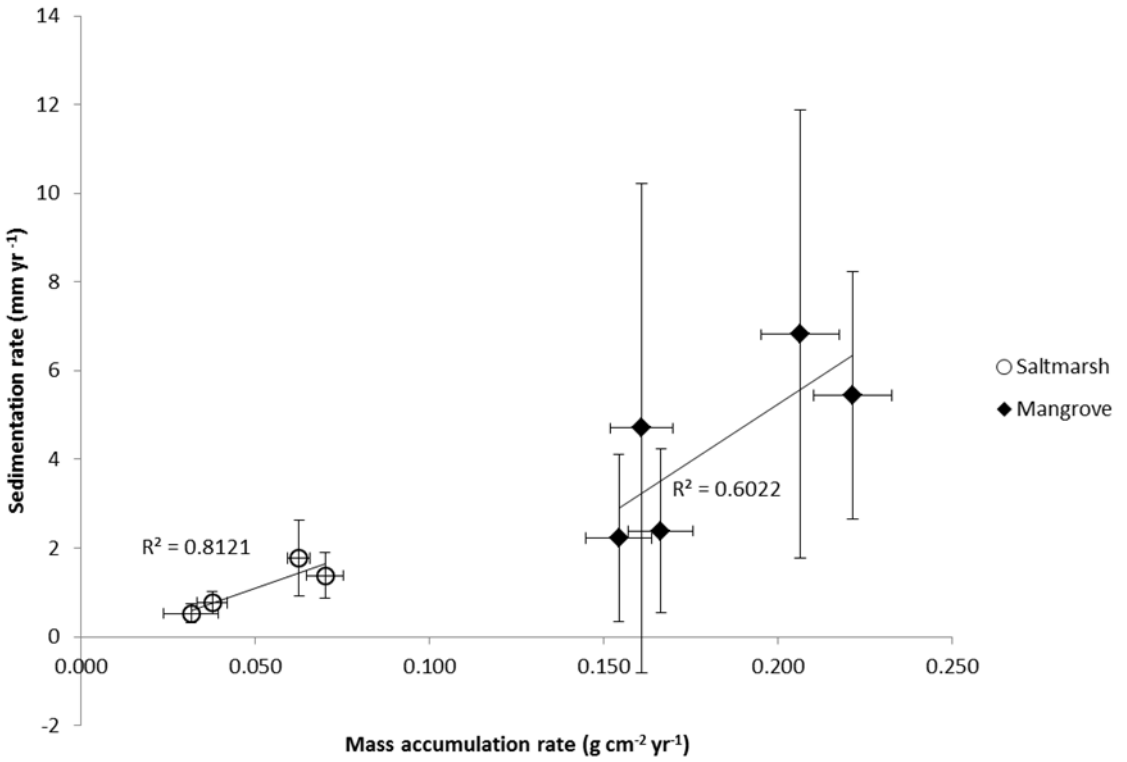

Figure 5.21: Mass accumulation rate vs. vertical accretion rate comparisons and R-squared linear correlations for mangrove and saltmarsh ^{210}Pb cores.

5.2. Spatial analysis

5.2.1. Variations in vegetation community extent

Vegetation mapping for 22 April 2015 indicates that the majority of saltmarsh and mudflat is in the central area of the island, adjacent to the small pool and channel to the south. Considerable saltmarsh flats are also present in the south-eastern portion of the island, while mangroves dominate throughout the central and southwestern portions of the island.

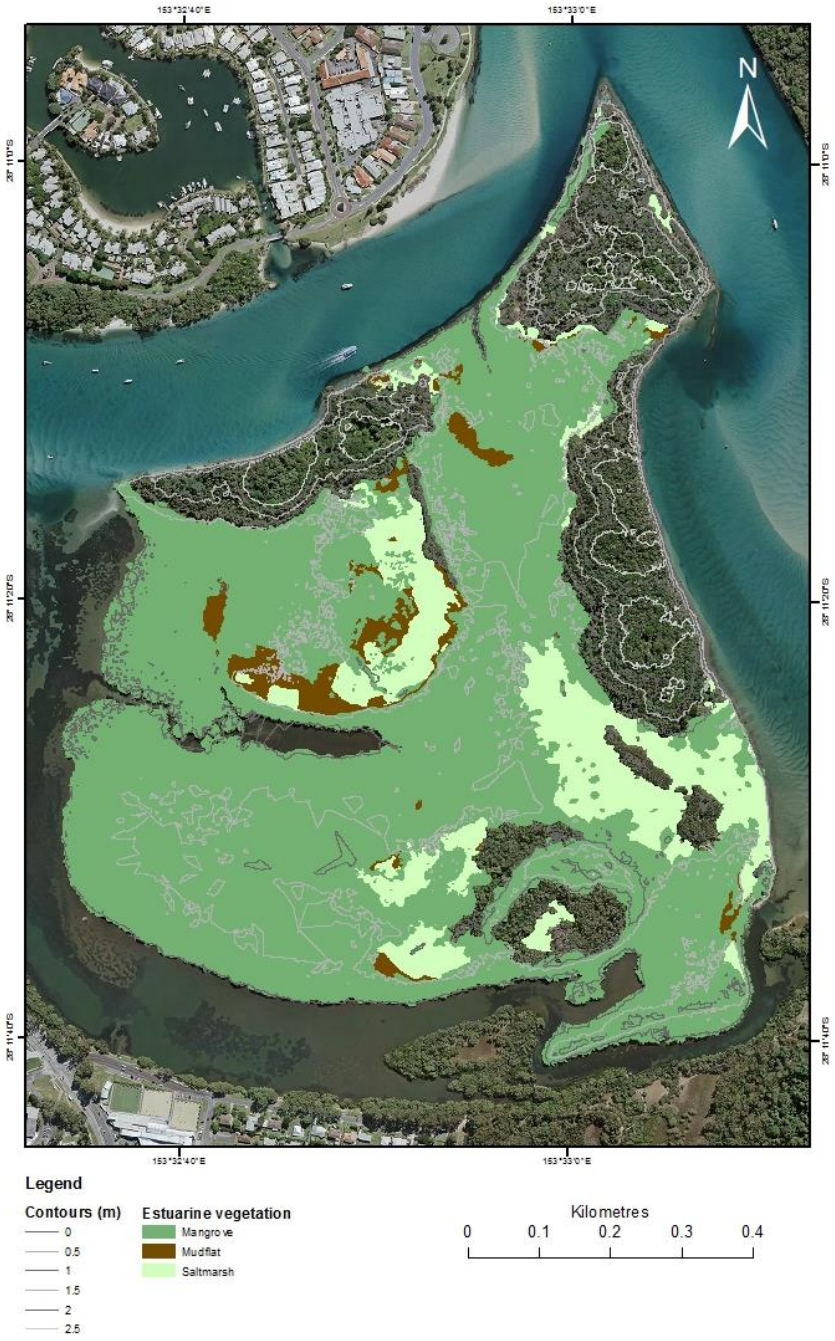

Figure 5.22: Mangrove, mudflat and saltmarsh extent at Ukerebagh Island, 22 April 2015.

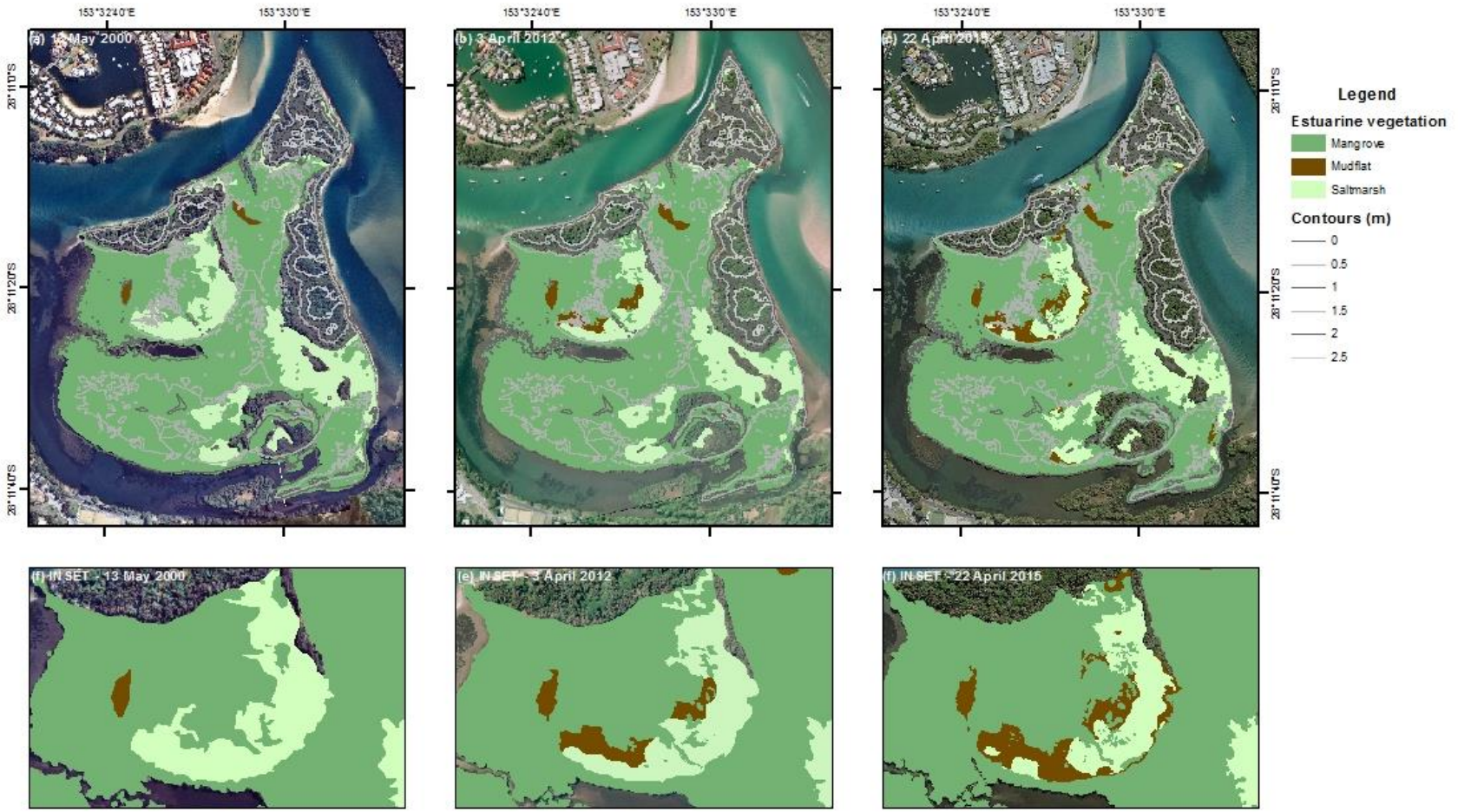

Figure 5.23: Saltmarsh, mangrove and mudflat extent at 13 May 2000, 3 April 2012 and 22 April 2015. Insets show changes in mudflat extent on main saltmarsh area.

Figure 5.24: Loss of saltmarsh extent and formation of extensive mudflats in lower section of saltmarsh flats, 23 March 2016. Extensive pneumatophore colonisation can be observed within mudflat area, indicating rapid colonisation of previous saltmarsh areas by adjacent mangroves.

Table 5.5: Change in total areal extent of saltmarsh, mangrove, mudflat and total intertidal area between 13 May 2000 - 22 April 2015 and 3 April 2012 - 22 April 2015.

Vegetation category	13 May 2000	3 April 2012	22 April 2015	Total areal change (2000-2015)	Total areal change (2012-2015)
Mangrove	47.06	47.16	49.34	2.28	2.19
Mudflat	0.41	1.31	2.19	1.78	0.88
Saltmarsh	11.37	9.28	8.40	-2.97	-0.88
Total intertidal area	*58.84*	*57.74*	*59.94*	*1.09*	*2.19*

Mudflat extent has increased extensively from 2000-2015, while saltmarsh extent has undergone decline (Table 5.5). Mudflat extent has increased by similar extents to saltmarsh decrease. Mangrove coverage has also increased, most notably in the 2012-2015 period. Apparent proliferation of mangrove pneumatophores within mudflat areas was also observed in several locations (Figure 5.23). A quarter of total saltmarsh loss across the monitoring period

(0.88 ha) occurred between 2012 and 2015. These changes have been predominantly within the central saltmarsh flat, especially in the southern portion (Figure 5.22, see insets). Conversely, saltmarsh flats on the east of the island have been barely affected by mudflat and mangrove expansion (Figure 5.22). Total intertidal area has varied throughout the monitoring period, with a slight increase evident on current mapping.

5.2.2. DEM ground truthing

Linear regression calculated for DEM elevations and RTK elevations returned an R^2 value of 0.9866 (n = 80), indicating a very high coefficient of determination between LiDAR derived points and total RTK points (Figure 5.24a). Clustering of elevation values was highly obvious between mangrove and saltmarsh points, providing an early indication of the difference in elevation between upper intertidal and lower intertidal vegetation communities. Linear fit correlation was then performed for saltmarsh points (R^2 = 0.8492, n = 54) and mangrove (R^2 = 0.212, n = 26). Coefficients of determination indicated a weak relationship between RTK and DEM values for mangrove, while demonstrating a much stronger relationship within saltmarsh (Figure 5.24b and c). Based on these correlations, DEM estimates of elevation were generally higher than RTK measurements for mangrove areas, while RTK and DEM measurements for saltmarsh were generally in agreement.

5.2.3. Flow length and accumulation

Flow length at the island generally decreased with proximity to the channel, with high flow lengths predominantly in the higher elevation terrestrial vegetation on the eastern side of the island, indicating that the majority of flow from the centre of the island is directed towards the central basin of the island where small pools are located (Figure 5.25). High flow lengths are also present within the saltmarsh on the east of the island, suggesting that these areas also drain towards the west. Flow accumulation networks support the drainage pattern suggested by flow length variations, with drainage networks from the higher elevation areas draining towards the central basin and the small channel south of the main saltmarsh and mudflat areas.

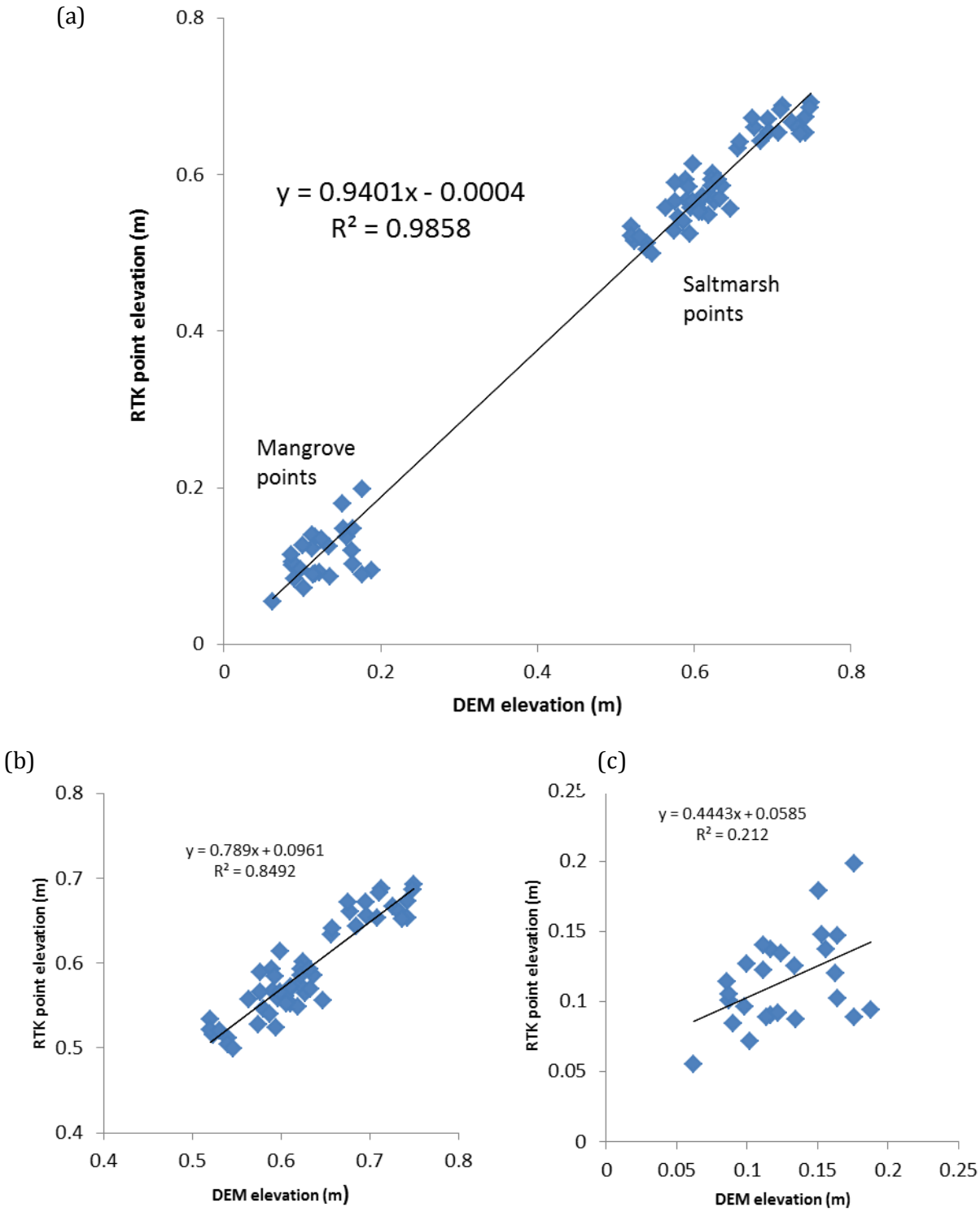

Figure 5.25: Linear correlation graphs for RTK point elevation vs. DEM elevation for (a) total points ($p < 0.0001$, RMSE = 0.027501, n = 80), (b) mangrove points ($p = 0.0017$, RMSE = 0.029406, n =26) and (c) saltmarsh points ($p < 0.0001$, RMSE = 0.022135, n = 54).

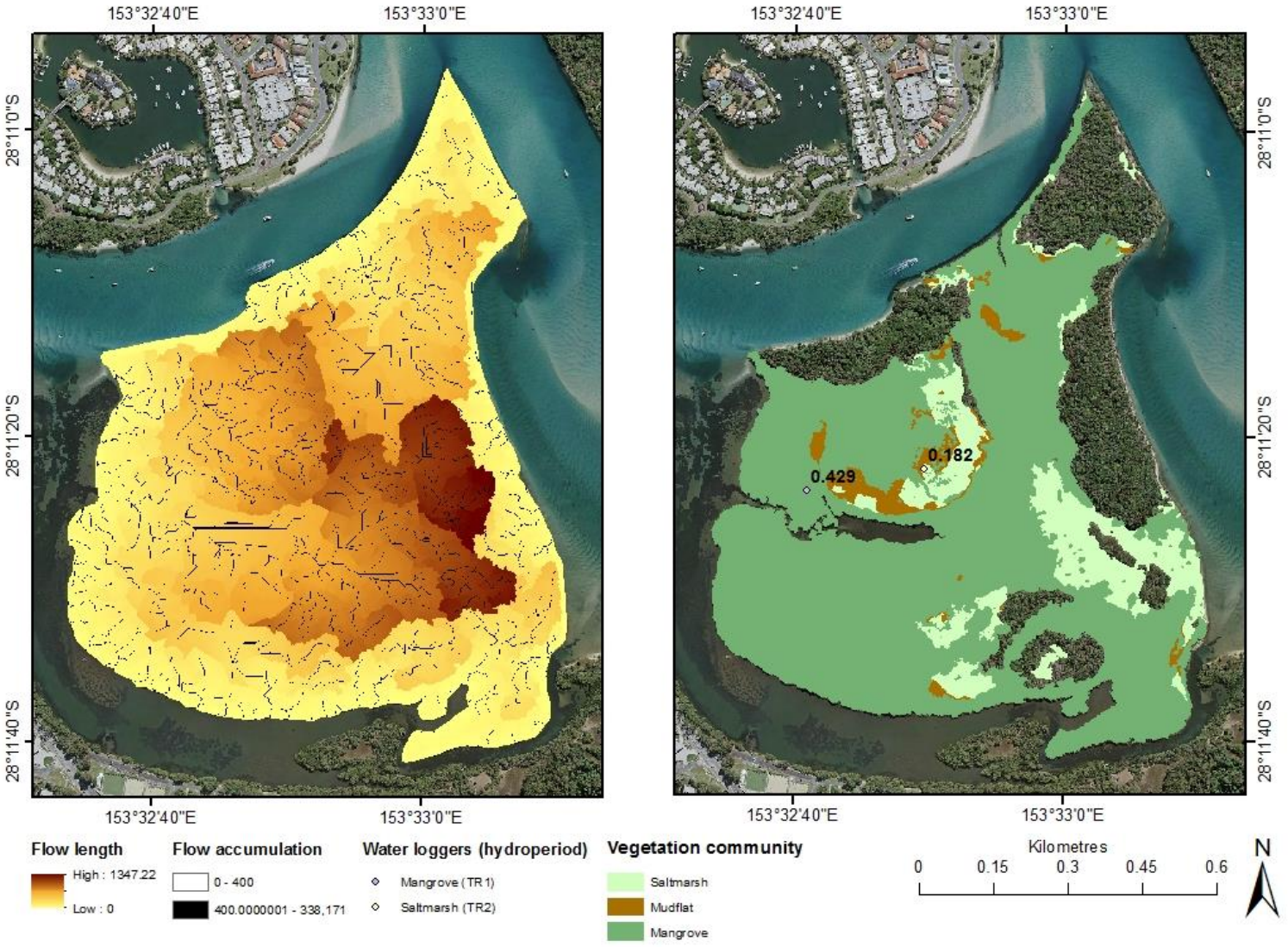

Figure 5.26: Flow length and accumulation, and hydroperiod value for TR1 (mangrove) and TR2 (saltmarsh) water level loggers for time period 5/05/2015-17/12/2015.

5.2.4. Inundation depth and hydroperiod

Mean mangrove inundation depth taken at mangrove SET 2 for the period 5/05/2015-17/12/15 was 0.235 m, while mean saltmarsh inundation depth (at saltmarsh SET1) was 0.045 m. This difference (0.19 m) is much smaller than the difference in RTK elevation between the two points (0.484 m). Subsequently, hydroperiod varied between water logger sites (Figure 5.25).

5.2.5. Relationship between vegetation community extent, elevation and hydrological characteristics

Oneway ANOVA analysis of the relationship between vegetation community and elevation, flow length and flow accumulation indicated a significant difference in means for all three characteristics by vegetation community type (Figure 5.27). Mean mudflat elevations occupy an intermediate position between mangrove and saltmarsh means. Standard errors for elevation values indicated a low variance between elevation means. Flow accumulation values were highest for mudflat areas, followed by mangrove and saltmarsh. Lastly, mudflat mean flow lengths also occupied an intermediate position in relation mangrove and saltmarsh. Post-hoc Tukeys HSD indicated that for elevation and flow length, all three vegetation communities were significantly different. However, Tukeys HSD for flow accumulation indicated that mangrove and mudflat were not significantly different, but both varied significantly from saltmarsh.

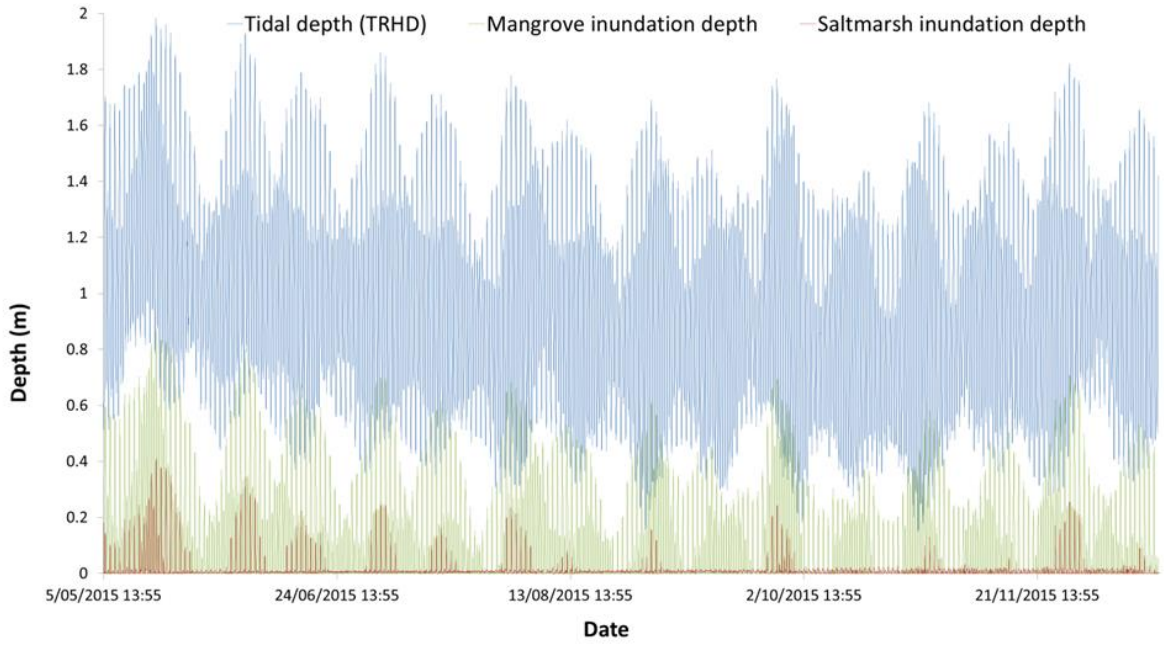

Figure 5.27: Tidal variation at Letitia 2A tidal gauge and variations in inundation depth for water loggers TR1 (mangrove) and TR2 (saltmarsh) for time period 5/05/2015-17/12/2015.

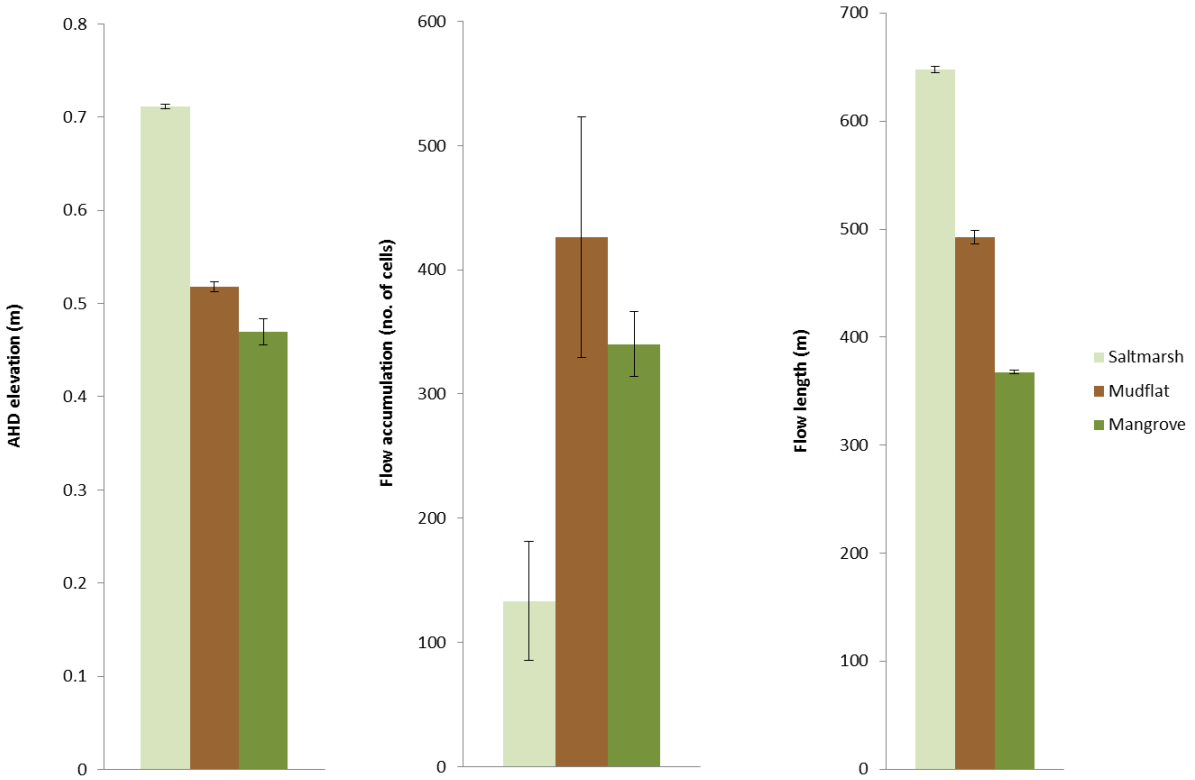

Figure 5.28: Differences in (a) mean elevation (DF = 42442, F = 3380.061, p < 0.0001), (b) mean flow accumulation (DF = 42442, F = 8.0475, p = 0.0003) and (c) flow length (DF = 42442, F = 3187.335, p < 0.0001).

Chapter 6. Discussion

Chapter 6 – Discussion presents further analysis of results and their implications for the management of the Tweed River estuary. More importantly, the value of $\delta^{13}C$ signatures from the study site as an indicator for vegetation change, and their implications for potential carbon sequestration will be explored. The effects of anthropogenic influences (e.g. the Tweed River Sand Bypass) on changing sedimentary and vegetation patterns within the estuary shall also be discussed.

6.1. Relationship between hydrological factors, vegetation community, and sediment accumulation rates

Sedimentation rates, and to a lesser extent, mass accumulation rates, have undergone acceleration throughout the analysis period covered by ^{210}Pb analysis. Although these time periods differ markedly as a result of discrepancies in the ^{210}Pb sample preparation method (A. Zawadzki, pers. comm.), the increases in both communities suggest that the vegetation communities have some capacity to build elevation in response to RSLR.

Although the use of only two cores for ^{210}Pb radiometric dating does not allow a robust statistical comparison of the sediment accretion rates between upper- and lower-intertidal vegetation communities, comparison between hydrological and elevation variables for the two cores suggest that these factors have considerable influence on mass accumulation and sedimentation rates (Table 6.1). Increased sedimentation and mass accumulation rates in the mangrove ^{210}Pb core correspond with increased hydroperiod and inundation depth, and decreased flow length and elevation, with the inverse relationship occurring in saltmarsh. The combined effect of these variables suggests that position within the tidal prism is the key determinant of sedimentation rates, which influences vegetation cover and position in tidal frame.

Table 6.1: Comparison of sedimentation rate variables from ^{210}Pb radiometric dating and local hydrological and elevation variables.

Core	Mean mass accumulation rate (g cm^{-2} yr^{-1}) (±SE)	Mean sedimentation rate (mm yr^{-1}) (±SE)	RTK AHD elevation (m)	Hydroperiod	Mean inundation depth (m)	Flow length (m)
^{210}Pb A (saltmarsh)	0.044 ± 0.004	1.11 ± 0.26	0.686	0.182	0.045	779.8
^{210}Pb B (Mangrove)	0.19 ± 0.004	4.32 ± 1.68	0.124	0.429	0.235	226.9

The differences in hydroperiod between mangrove and saltmarsh supports conclusions made by Cahoon & Reed (1995) that sediment accumulation rates vary spatially and temporally with hydroperiod. This also reflects conclusions made by Crase *et al.* (2013), where hydroperiod acted as the main driver of spatial distribution of mangroves within Darwin Harbour. Accordingly, gradual increases in inundation frequency and depth may then be a key factor in the acceleration in sedimentation.

As hydrological distance to channel (i.e. flow length) is a function of both elevation and tidal range, its importance as a driver of sedimentation rates has been recognised and has previously been incorporated in spatial and temporal sedimentation modelling (Temmerman *et al.* 2003). The correlation of flow length with differing sedimentation rates reflects the previous analysis undertaken at Ukerebagh Island by Rogers *et al.* (2014) where hydrological distance to channel was determined to be a significant contributor to variations in surface elevation change.

The distribution of grain size in recent sediments (Figure 5.9 and 5.10) in both mangrove and saltmarsh, and their comparison with deeper grain size distributions also reflects the contribution of elevated inundation depth and hydroperiod. The nature of sedimentation throughout the depth profile does not suggest that the nature of sediment supply to the estuary has significantly changed as a result of SLR or other disturbances. The only indication of deviations from the generally undisturbed deposition of mineralogenic material is the presence of increases in silt percentages between 20 and 30 cm in the mangrove cores on-site. The influx of finer-grained materials may be related to agricultural reclamation and development activities in the estuary throughout the 1960s (White *et al.* 2007), which resulted in seaward mangrove expansion within the tidal channel (Saintilan 1998). The high mass accumulation value for older mangrove sediments (^{210}Pb age = 1978 ± 8) suggests that increased sedimentation within the channel allowed mangroves to expand and accordingly influenced grain-size distribution in recent sediments.

Additionally, the nature of sediments at depth within the cores (i.e. approaching 100% sand) suggests that the wetland sediments overlie a pre-dominantly tide-deposited uniform sand layer where the majority of organic material has decomposed. Dry bulk density and moisture content values suggest that uniform dewatering and compaction of sediment occurs at depth.

Increased sedimentation rates comprised of similar material to historical accumulation are most likely the result of increased settling time, which in turn is a function of increased inundation depth and frequency (Cahoon & Guntenspergen 2010). Although the alterations to fluvial sediment supply appear to have influenced the nature of sedimentation in the later part of the 20th century, the nature of the sediment deposited at Ukerebagh Island and its position within

the tidal channel as defined by Saintilan (1998) indicate that the vast majority of sediment deposited on the island is derived from tidal deposition.

The comparison of sea level rise and sedimentation rate within the last three decades (Figure 6.1) reflects the differing ability of wetland vegetation types to respond sufficiently to RSLR (Cahoon *et al.* 2006; Saintilan *et al.* 2009; McKee *et al.* 2012) and also indicates that sedimentation responses to sea-level rise have not been instantaneous. Instead, it is apparent that both mangrove and saltmarsh sedimentation rates have experienced delays in their response to sea-level rise, which agrees with conclusions from the SET measurements from Rogers *et al.* (2014).

Although sedimentation rates appear to have accelerated in response to SLR, they have not been able to fully account for the increase in accommodation space within the estuary. As stated in Cahoon *et al.* (1995), vertical accretion rates cannot be used as a surrogate for elevation change. However, when ^{210}Pb sedimentation rates from Ukerebagh Island are compared to the surface elevation changes indicated by SET measurement (Rogers *et al.* 2014), they provide a reliable indication of the substantial influence of below-ground processes on surface elevation. As in other studies of eastern Australian coastal wetland systems (Woodroffe 1990, Rogers *et al.* 2006, Lovelock *et al.* 2011; Rogers *et al.* 2013) and internationally (Cahoon & Lynch 1997; Cahoon *et*

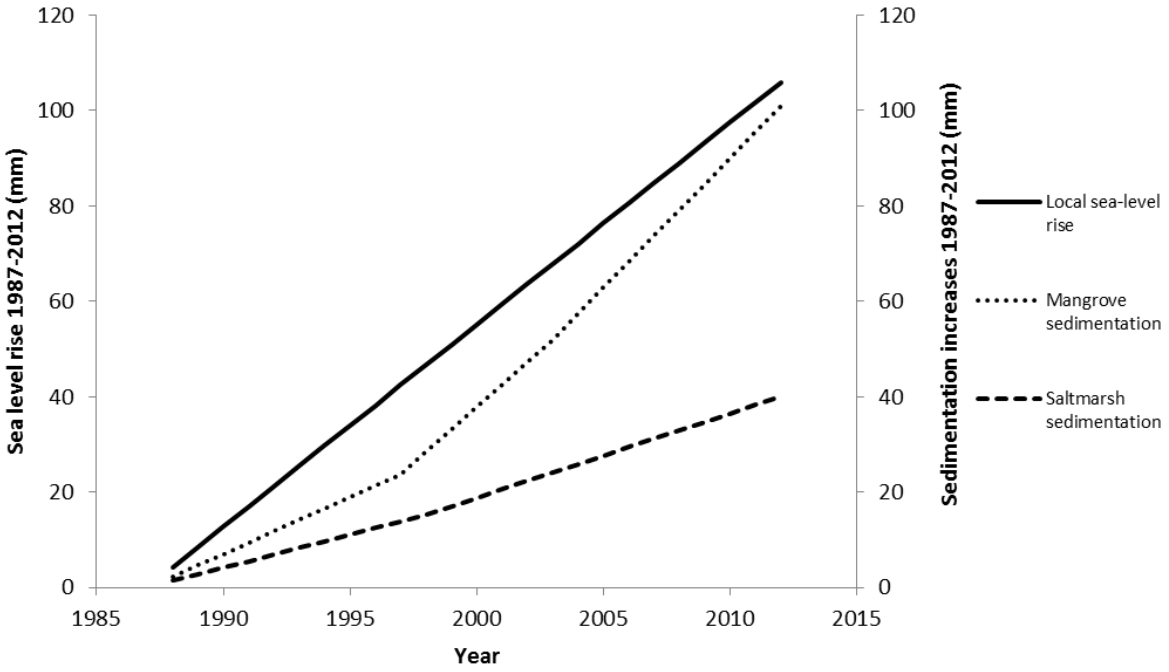

Figure 6.1: Comparison of sea-level rise within the estuary (from Rogers *et al.* 2014) and ^{210}Pb-derived vertical accretion for mangrove and saltmarsh for the period 1987-2012.

al. 1999, 2006; McKee *et al.* 2007), the imbalance between vertical accretion and surface elevation change can be contributed to a number of below-ground influences, such as compaction, root decomposition, and swelling/shrinkage effects (Rogers *et al.* 2013). In particular, Lovelock *et al.* (2011) highlighted the significant role of subsurface processes in determining surface elevation change on a similar subtropical intertidal environment in Moreton Bay, slightly to the north of the Tweed River. Conversely, the patterns observed in Lovelock's study and at this study site are contrary to surface elevation trends in Western Port Bay (Rogers *et al.* 2005), emphasising the varying effects of local factors on adjustment to RSLR. Another significant indicator of the level of sediment compaction that occurs on Ukerebagh Island may be the downward shift in mass accumulation rates at core surface in both saltmarsh and mangrove. This correlation may be due to the less compacted nature of sediment at the top of the core, and compared to older measurements at depth, suggests that a large degree of sediment autocompaction occurs over time.

The apparent increase of sedimentation rates in response to sea-level rise suggests that the saltmarsh at Ukerebagh Island does not possess a large level, if any, of what Cahoon and Guntenspergen (2010) refer to as 'elevation capital' – that is, an accumulation of contributions to surface elevation change that buffer the ecosystem from sea-level rise and increase wetland

Figure 6.2: Saltmarsh deterioration adjacent to encroaching mangroves and intermediate mudflat formation prior to mangrove colonisation.

resilience. The considerable difference between sea level rise and vertical accretion, even without accounting for subsurface processes, suggests that the saltmarsh will continue to deteriorate in response to continued SLR. The response reflects the feedback loop hypothesised by Pethick (1992) and expanded by Allen (2000) and Fagherazzi *et al.* (2012) in which the provision of accommodation space exceeds the relative supply of sediment to the marsh, and as a result, marsh drowning occurs. At Ukerebagh Island, this response to geomorphic change appears to manifest itself through mudflat formation in former saltmarsh areas, followed by mangrove colonisation (Figure 6.2).

Although mangroves have a greater ability to adjust to rising sea-levels (Alongi 2008; Duarte *et al.* 2013; Woodroffe *et al.* 2016), it appears that they too are experiencing a sediment supply deficit influenced by shallow subsidence. However, the lack of deterioration in mangrove extent at the channel boundaries of the island suggest that mangrove extent has not yet been affected by sea-level rise and the increased ability of mangroves to dissipate tidal energy (Duarte *et al.* 2013) and bind sediment (Woodroffe *et al.* 2016) are assisting the vegetation community to adjust to RSLR. Increased rates of sedimentation within mangroves may also reflect increased pneumatophore and aerial root density further inland on the island, with denser vegetation correlating with sedimentation rates (Hogarth, 1999). Extended inundation depth and frequency may enhance the ability of denser vegetation to accrete sediment.

^{210}Pb-derived sediment accretion rates are contrary to indications from marker horizons (MHs) laid down at Ukerebagh Island in 2000 (Rogers *et al.* 2014), Prior to MH deterioration, measurements that were collected were considerably higher than the mean ^{210}Pb accretion rates measured in this study. As the ^{210}Pb rates are averaged over a significant period of time, encompassing periods that are both prior to SET-MH installation and subsequent to the cessation of MH monitoring, the discrepancy could be affected by a number of factors. These include the impact of ENSO related variables (Rogers *et al.* 2005, 2006; Rogers & Saintilan 2009; Rogers *et al.* 2014) having significant effects on inter-annual sediment accretion variability. These higher MH vertical accretion measures also support the conclusion of this study that significant below-ground processes influence surface elevation change at Ukerebagh Island.

6.2. Soil carbon characteristics – sources, influences and storage

6.2.1. Origin of soil carbon – implications from δ^{13}C signatures

The unambiguous δ^{13}C signatures in saltmarsh and mangrove cores retrieved from Ukerebagh Island correlate strongly with reference δ^{13}C signatures from previous studies of estuarine wetland vegetation (Table 4.1). δ^{13}C signatures above partition points in all four saltmarsh cores

are similar to *Sporobolus* organic signatures from multiple sites throughout Australia and signify a C_4 plant origin for soil carbon. Mangrove cores also strongly suggest a C_3 origin for soil carbon, while the intermediate values found in the mixed cores, and the shifts towards more enriched values at shallow depth, suggest that a mixing effect between C_3 mangrove and C_4 saltmarsh contributions to soil carbon is affecting $\delta^{13}C$ signature. Overall, the $\delta^{13}C$ signatures indicate that autochthonously-derived soil carbon is the predominant contributor to carbon sequestration. The clear origin of the $\delta^{13}C$ signatures also allows the relatively reliable inference of historical vegetation type through the organic contribution of soil to below-ground carbon.

The down-core variation in mangrove cores strongly suggests the expected preferential microbial decomposition of carbon and resultant positive shift in $\delta^{13}C$ (Ehleringer *et al.* 2000; Garten *et al.* 2007). The down-core shift in values (not exceeding 3‰) may also reflect the contribution of decreasing $\delta^{13}C$ concentrations within the atmosphere as a result of the addition of $\delta^{13}C$-depleted carbon to the atmosphere via fossil fuel burning (Francey *et al.* 1999). This value also agrees with the commonly quoted value of 1-3‰ increases relative to litter layer in forest ecosystems (Bostrom *et al.* 2007) and is reflected in down-core mangrove profiles in the Amazon (Sanders *et al.* 2010), in southern China (Zhang *et al.* 2012) and in Australia (Saintilan *et al.* 2013). The Australian study, which encompassed a range of sites including Ukerebagh Island, also demonstrated that the significant enrichment of mangrove roots compared to mangrove leaves also makes a considerable contribution to less-depleted $\delta^{13}C$ at depth. The low enrichment down-core may indicate that root $\delta^{13}C$ enrichment relative to leaf values is the primary contributor to changes in $\delta^{13}C$ signature.

The saltmarsh cores (T1-1, T2-1, T2-2 and ^{210}Pb A) and the mixed vegetation cores (T1-2, T2-3) all gradually shift towards highly depleted $\delta^{13}C$ values at depth, converging with the signature of mangrove cores between 60 to 80 cm. The gradual down-core negative shift of mixed and saltmarsh cores suggest a range of possible scenarios with regards to former autochthonous sources of soil carbon:

1. Mangrove vegetation once extended throughout the estuary prior to infilling, and as elevation rose and the island centre transitioned from a lower- to upper-intertidal position, *Sporobolus* saltmarsh became established as mangrove extent deteriorated;
2. Mangroves proliferated throughout the estuary during the Holocene sea-level high-stand proposed by Sloss *et al.* (2007), and gradually transitioned to saltmarsh as sea levels fell to their current position;
3. C_3 saltmarshes such as those from the *Sarcocornia* genus, as found in other coastal wetland ecosystems along the east coast of Australia, were previously present on

Ukerebagh Island, but gradually declined as a result of *Sporobolus* expansion to the point where saltmarsh is a C_4 monoculture;

4. The $\delta^{13}C$ signature of C_4 sedimentary organic carbon in marsh areas experiences a considerable negative shift , similar to values reported from European and American mineral marshes, as a result of preferential decomposition of relatively labile and refractory components of soil organic carbon (after Middelburg *et al.* 1997).

There are a number of factors that support all four hypotheses, which both require several assumptions to be made.

For scenario (1), it must be assumed that significant sediment supply to the estuary has resulted in geomorphically-driven vegetation succession (Saintilan *et al.* 2009), burying previous mangrove root systems and allowing the establishment of saltmarsh at higher elevations. Physical evidence from the study site also supports this theory, with preserved mangrove roots being found at considerable depths within some cores (i.e. T1-2). A similar trend was also documented in bayhead deltas within the Hawkesbury River by Saintilan & Hashimoto (1999), where preserved mangrove root systems were found approximately 0.3 m below the current saltmarsh surface. Also, the presence of *Cerithium* shells at depth in mangrove sediments, an intertidal/sublittoral species which prefers silty sand habitats (Wilton *et al.* 1994), further supports the gradual geomorphic evolution of the island. Although the evidence from the Hawkesbury provides a precedent for this temporal pattern, a key limitation of this hypothesis is that there is currently no indication of the age of these preserved mangrove roots, which does not allow the placement of this vegetation in the sedimentary history of the island. However, radiocarbon dating of mangrove roots found at depth may provide a better indication of the viability of this hypothesis.

The Holocene sea-level curve proposed by Sloss *et al.* (2007), in which a sea-level high stand of approximately 1.5 m above present levels persisted from 7400 to 2000 cal. yr. BP, supports the larger extent of mangrove forest within the Tweed estuary and its decline at the expense of saltmarsh as sea level smoothly regressed to its current levels. Evidence that supports this hypothesis also supports scenario (1), such as the presence of preserved mangrove roots and shell presence at depth. More research into constraining the age of sediments at Ukerebagh Island may provide further indication of the increased plausibility of scenarios (1) or (2).

Scenario (3) is also plausible, if we assume that saltmarsh sedimentation has been established in the current location for a considerable period of time. Although saltmarsh diversity appears to have an inverse relationship to mean minimum temperature, with the highest saltmarsh diversity found at high latitudes in Tasmania and Victoria, the higher saltmarsh diversity as sites

to the north of the Tweed River such as Moreton Bay suggests that the C_4 saltmarsh monoculture at Ukerebagh Island is a regional anomaly. This difference may be explained by biological limits such as the level of inherent stress tolerance within saltmarsh species or factors such as nutrient supplies affecting competitive dynamics between species (Levine *et al.* 1998; Emery *et al.* 2001).

The conditions in scenario (4) were described by Middelburg *et al.* (1997) and attribute the down-core depletion of $\delta^{13}C$ signature in mineral saltmarshes to three possible processes. Firstly, the preferential decomposition of heavier labile soil carbon components (enriched $\delta^{13}C$) results in a depleted $\delta^{13}C$ signature down-core. Secondly, the contribution of allochthonous organic matter, in this case from fluvially-derived sediments, may skew $\delta^{13}C$ signature towards more negative values, and thirdly, the contribution of microbial carbon may have a slight depleting influence. Similar trends in *Spartina* marsh were found in the USA by Haines (1976), Ember *et al.* (1987), and Chmura *et al.* (1987), and in France by Creach (1995).

However, the lack of similar sites in Australia means that this down-core effect has not been previously observed, and findings by Saintilan *et al.* (2013) generally discount the contribution of allochthonously-derived material to soil carbon at depth. The evidence indicates that scenarios (1), (2) and (3) are more likely, but further investigation is required to determine the origin of $\delta^{13}C$ signatures at depth within saltmarsh and mixed cores, and sediment ages at depth within all cores.

6.2.2. 'Blue Carbon' – contribution of coastal wetland vegetation to carbon sequestration

Lower soil compaction at upper depths, especially within the mangrove cores, appears to affect soil carbon density. Low dry bulk densities, notwithstanding the effect of high soil carbon concentrations, generally appear to result in in low soil carbon density. The opposite effect was noted in the saltmarsh cores, where higher measures for dry bulk density in upper cores, combined with low % C, resulted in similar soil carbon density.

Although soil carbon concentration and density differed between vegetation types, and varied with depth (i.e. decomposition-related decreases), the total carbon store by core was highly variable, with no significant difference in carbon store between vegetation types on-site. Although the total carbon store values for mangroves were highly variable, the lower measurements (19 - 47 MgC ha^{-1}) may reflect their position closer to the tidal channel. As the island expanded into the tidal channel, shorter accumulation periods would be expected within more youthful sediments. Conversely, areas of the island that have persisted for longer periods of time (mixed and saltmarsh areas) may have higher total carbon stocks. Although estimates of

total carbon stocks vary widely both within and between vegetation communities (Howard *et al.* 2014), the high variability of carbon store within vegetation types at Ukerebagh Island may also be substantially affected by the incorporation of living material within the active root zone. Elevated soil carbon density values within the core, such as within mangrove core T2-4 at 12 cm, may have significant inflating effects on the method used to estimate total soil carbon. Similar effects can be observed in other cores. A soil carbon density value of 0.03 g cm^{-3} at 62 – 64 cm inflates estimated carbon values at higher and lower depths. Similar effects of varying magnitudes can be observed in the majority of cores, indicating that these results should be treated with a high level of caution.

It is possible that the expansion of mangroves may assist in boosting total carbon sequestration values within the estuary and add to 'blue carbon' storage (Kelleway *et al.* 2016). The lack of deterioration in the seaward edge of mangrove communities at Ukerebagh Island support their continued addition to below-ground carbon, while the higher carbon sequestration potential of mangroves proliferating within saltmarsh areas may contribute higher levels of carbon to below-ground stocks.

Because individual soil carbon densities vary significantly between vegetation types, it is probable that the inflating effect of outlier values has affected the accuracy of this analysis. Therefore, it is recommended that further investigations are undertaken into total carbon sequestration values at Ukerebagh Island.

Although there cannot be certainty about the total carbon storage values presented here, we have been able to unambiguously attribute the origin of recalcitrant soil carbon at Ukerebagh Island to in-situ vegetation via identification of $\delta^{13}C$ signatures. This supports the conclusions made by Saintilan *et al.* (2013) across multiple sites in south-eastern Australia.

6.3. Acceleration in vegetation community change rates – contributing factors

Although the patterns of vegetation change have been quantified previously at Ukerebagh Island by Rogers *et al.* (2014), the addition of new imagery and classification-based mapping to this dataset indicates that rates of saltmarsh decline and mudflat expansion have accelerated within the last three years. A conceptual model of the mechanisms behind vegetation community change is explained below (Figure 6.3).

The elevation and hydrological characteristics on the island appear to be substantial contributors to the variation in vegetation community across the island. Mudflat mean elevation and flow length occupy an intermediate position between mangrove (lower) and saltmarsh (higher). This relationship strongly reflects the position of each vegetation community in the

tidal prism and supports the formation of mudflats as an intermediate stage in wetland geomorphic response to sea-level rise. Interestingly, higher mean flow accumulation in mudflat may also contribute to the loss of vegetation. As the majority of mudflat distribution on the island is concentrated in the southern part of the main saltmarsh flat, this area may form a basin relative to the surrounding saltmarsh elevation. High flow accumulation values suggest that the mudflat areas form a basin where the flood tide pulse delivers water to the flat, but drainage from this area is less connected to tidal recession. Accordingly, drainage from the mudflat area may not be driven by the ebb tide, but more related to drawdown into the water table. As a consequence of SLR and longer drainage times for water drawdown rather than ebb tide drainage, the rate of saltmarsh drowning in these areas appears to be increasing, resulting in accelerated mudflat expansion.

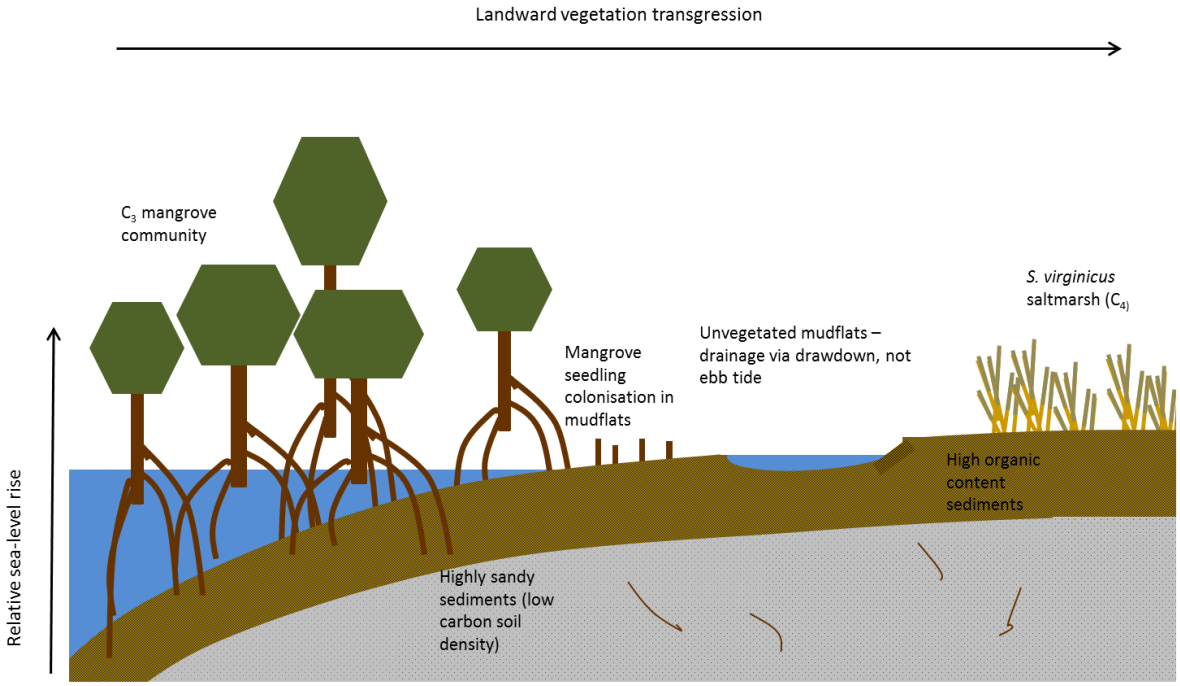

Figure 6.3: A conceptual diagram of vegetation response to SLR and factors affecting mudflat formation at Ukerebagh Island.

The conversion of saltmarsh to unvegetated mudflat results in the loss of ecosystem services (Craft *et al.* 2009) and has been documented throughout saltmarshes in the United States, with saltmarsh die-off converting marsh to open water or interior ponding (Gedan *et al.* 2011). Although sudden dieback of saltmarsh in peaty substrate may be related to physiological

variables and merely resemble marsh ponding (Kearney & Turner 2016), the high mineralogenic component of sediment at Ukerebagh Island, in addition to the high flow accumulation values, indicates that saltmarsh dieback is more likely to be related to increased inundation depth and frequency. Additionally, Gedan *et al.* (2009) characterises interior ponding and drowning as one of two main saltmarsh responses to SLR, alongside the landward migration of saltmarsh zones. At Ukerebagh Island, the presence of mangrove pneumatophores and seedlings on the edge of mudflat areas suggests that mangroves are already rapidly colonising these areas. This observation is in line with conclusions made by Rogers (2004), where RSLR and upslope mangrove migration are closely linked. Also, increased inundation frequencies and depths may be increasing soil moisture and reducing the high salinity typical of saltmarsh flats (Saintilan *et al.* 2009), improving the suitability of these intermediate areas for mangrove colonisation. While saltmarsh loss will potentially be extensive, the position of unvegetated mudflats as an intermediate geomorphic response may be a short-term state.

Some variation in mean elevation and hydrological variables may be due to inherent accuracies in the DEM used to derive these layers, specifically in the mangrove, where DEM estimates of elevation were generally higher than RTK measurements. Higher estimates of elevation would result in higher flow lengths and lower flow accumulation values. Accordingly, the estimates of flow length and accumulation for mangrove communities may be over-estimated and under-estimated respectively. Over-estimation of flow length would not have any impact on the conclusions made in this study. Also, the overestimation of flow accumulation in mangroves may affect the mean relationship between mangrove and mudflat flow accumulation. However, the key finding here is that there is a significant difference between flow accumulation in saltmarsh and mudflat areas, both of which reflect generally accurate DEM measurements due to the lack of overarching canopy vegetation.

The changes in vegetation community areal extent supports observations made by Saintilan and Rogers (2013) as part of a larger worldwide trend of woody plant encroachment on grassy vegetation. Regionally, the trends of saltmarsh decline and mangrove expansion at Ukerebagh Island concurs with early stages of the process proposed by Soares (2009) and reinforces the conclusions of Wilton (2002) of continued mangrove incursion into saltmarsh in south-eastern Australia, They also support local trends observed in long-term mapping of the Tweed River estuary undertaken by Saintilan (1998) and Wilton (2002), and short-term monitoring undertaken by Rogers *et al.* (2014) and the Tweed River Estuary vegetation monitoring program (Pacific Wetlands Environmental Consultants 2012).

If SLR trends continue at similar rates to the recorded levels for 1987-2012, the survival of saltmarsh within the central flat of Ukerebagh Island is highly unlikely. The presence of higher elevation dredge spoil on the northern fringes of the island and a levee bank where *Casuarina* vegetation dominates the vegetation distribution will likely exert a significant amount of coastal squeeze (Doody 2004; Chmura *et al.* 2013; Woodroffe *et al.* 2016) on the central saltmarsh flat. In addition to this, the topographic restriction of the saltmarsh flat (i.e. surrounded completely by mangrove vegetation) removes any ability to shift to higher elevations in response to SLR. This effect was expanded upon by Rogers *et al.* (2014) but in light of the recent accelerations in saltmarsh decline on site, the threat to continued saltmarsh persistence at Ukerebagh Island appears more severe. However, it is important to note that while sea-level trends may explain long-term patterns in wetland vegetation community and geomorphic change, short-term responses such as the ones described here may be confounded by climatic variables (Rogers *et al.* 2014).

Although the expansion of mangroves may assist in increasing carbon sequestration levels (Kelleway *et al.* 2016), it is important to consider the effects that saltmarsh loss may have for trophic relationships within the estuary. Numerous studies have emphasised the importance of saltmarsh communities in south-eastern Australia as nursery habitats for itinerant and resident fish species (Mazumder *et al.* 2006, 2011; Hollingsworth & Connolly 2006; Svensson *et al.* 2007; Mazumder 2009; Saintilan & Mazumder 2010) and the loss of saltmarsh as a feeding ground for these species may have follow-on effects for ecosystem health and potentially local fishery sustainability. The importance of these ecosystems for threatened microbats and migratory shorebirds has also been noted (Saintilan & Rogers 2013). Therefore, determining the importance of saltmarsh survival in these areas will require analysis of the potential costs and benefits of continued mangrove encroachment on saltmarshes.

6.4. Anthropogenic influences on sedimentation rates and vegetation change – the Tweed River Sand Bypass

As SET analyses appear to indicate that saltmarsh is either no longer building elevation or is continuing to do so at very low rates (Rogers *et al.* 2014), it was hypothesised that the impact of the Tweed River Sand Bypass may be influencing hydrodynamic and sediment deposition conditions within the estuary (K. Rogers, pers. comm.). Historical evidence for the consolidation of the islands within the Tweed River estuary behind the northern entrance training wall exists in aerial photography from the 1930s onward, and there is previous evidence for increased sedimentation within the estuary resulting in expansion of Ukerebagh Island into the channel (Saintilan 1998, Wilton 2002). Although sedimentation rates have increased substantially

throughout the last 30 years, there has been no corresponding seaward expansion at Ukerebagh Island in this period, suggesting that the increases in sedimentation have been primarily related to SLR rather than further anthropogenic disturbances to tidal and hydrodynamic conditions. The lack of recent mangrove expansion into the channel and its corresponding shift landwards also supports the influence of SLR rather than human inputs.

However, the impact of entrance breakwalls, dredging within the channel and river entrance as well as the presence of the Sand Bypass, may be influencing the capacity of vegetation to accrete sediment in response to SLR through decreased suspended sediment concentrations in tidal pulses and removal of sediment from the estuary (as per McKee *et al.* 2012). As ^{210}Pb sedimentation rates have shown a consistent pattern of acceleration, it is difficult to separate any detrimental effects of tidal sediment restriction from the impacts of relative sea level rise on the ability of vegetation to build sediment and maintain their position within the tidal prism.

Chapter 7. Conclusion

As stated in Section 1.4, the aims of this study were as follows:

- To reconstruct the long term vegetation trends on Ukerebagh Island by inferring historical vegetation type from soil $\delta^{13}C$ signatures;
- To calculate rates of sedimentation at the island throughout the 20th century via ^{210}Pb and ^{137}Cs analysis; and
- To determine if long-term vegetation community change and multi-decadal sedimentation trends are contrary to patterns previously observed.

Through the investigation of these aims, the following conclusions were met:

- $\delta^{13}C$ signatures from surface sediment samples reflected the $\delta^{13}C$ signature of the in-situ vegetation. Furthermore, down-core shifts in $\delta^{13}C$ signature in saltmarsh cores suggested that vegetation underwent a gradual shift from a C_4 monoculture to a C_3-dominated vegetation assemblage. Mangrove cores indicated long-term presence of C_3 species, while mixed vegetation cores exhibited an intermediate signature which suggests the influence of $\delta^{13}C$-depleted mangrove roots on saltmarsh C_4-derived soil carbon. Although there is evidence of preserved mangrove roots at depth in mixed vegetation cores, there is limited evidence to confirm that the C_3 signature at depth in saltmarsh cores is autochthonously derived from mangroves. Alternatively, the mix of saltmarsh species at wetland sites within the region suggests that this may have been the case at Ukerebagh Island. Further investigation (i.e. radiocarbon dating of preserved mangrove roots) may provide further indication of long-term vegetation community evolution.
- Soil carbon concentration and density did differ between saltmarsh and mangrove cores, but not between saltmarsh and mixed cores, and mangrove and mixed cores. Soil carbon density and concentration were also strongly controlled by depth, indicating significant decomposition of soil carbon over time. However, total carbon store did not differ significantly between vegetation types. This result may be highly influenced by methodological assumptions and as such should be treated with caution.
- ^{210}Pb analysis from both mangrove and saltmarsh cores indicated acceleration in sedimentation rates over the last 40 and 100 years respectively. This acceleration in sedimentation reflects relative sea-level rise within the estuary and also indicates the significant influence of below-ground processes on resultant surface elevation change. Issues with pre-processing methods in in mangrove sediments prevented full sample digestion and accordingly limited the ^{210}Pb dating range for this core.

- Notwithstanding the limitations of the radiometric dating method, the sedimentation record still provided considerable records pre- and post- Tweed River Sand Bypass installation. Although it was expected from previous studies that the island was no longer accreting sediment, ^{210}Pb rates for the corresponding period indicated that sediment accretion was still occurring.
- Changes in grain size may correspond to land-use disturbances within the estuary in the 1960s and 1970s. Additionally, accelerations in sedimentation, especially in the mangrove, do align with the commencement of Sand Bypass operation. However, the steady increase in sea-level rise and associated increases in sedimentation may be confounding attempts to determine the relative contributions of sea-level rise and anthropogenic modifications to variations in sedimentation rates.

The results from these investigations suggest that further studies at Ukerebagh Island may need to be conducted. Firstly, a more rigorous assessment of total soil carbon stock should be undertaken throughout the whole estuary, to add to the increasing body of research regarding 'blue carbon' stocks in Australian coastal wetlands (i.e. Kelleway *et al.* 2016; Owers *et al.* 2016). Secondly, further investigation of the long-term (i.e. beyond the scope of ^{210}Pb dating) sediment record of Ukerebagh Island is recommended, to fully encapsulate the depositional history of sediment within the island and obtain long-term indications of carbon sequestration rates. Possible methods for this analysis include radiocarbon dating of sediments (i.e. Brevik & Homburg 2004; Choi & Wang 2004; Kermode *et al.* 2016), and preserved organic material (i.e. Saintilan & Hashimoto, 1999). Additionally, microfossil and pollen marker analysis (Fletcher *et al.* 1993; Ellison 2008; Hayward *et al.* 2010) may provide indications of palaeoecological successions as a result of geomorphic change within the estuary, and dating of shell material via amino acid racemisation or radiocarbon dating (Murray-Wallace *et al.* 1993) may assist in constraining depositional periods. Further investigation into recent sedimentation rates is also required to ascertain why ^{210}Pb sedimentation rates provided different indications to vertical accretion rates indicated by Rogers *et al.* (2014).

The quantification of annual suspended sediment loads within the estuary similar to the approach undertaken by Eyre *et al.* (1998) in Moreton Bay and the application of tidal transport studies of sediment fluxes (Sternberg *et al.* 1986; Stevenson *et al.* 1988) may give an indication of the levels of suspended sediment retention within the estuary. Comparison of such studies with historical records of suspended sediment loads (Estuaries of NSW, Eyre *et al.* 2000) may provide clues as to the effect of Sand Bypass operation on the overall suspended sediment levels within the Tweed Estuary tidal channel.

Finally, spatial and temporal modelling approaches for the impact of sea-level rise and changes in hydrological conditions on coastal wetland survival (Temmerman *et al.* 2003, 2004; Oliver *et al.* 2012; Rogers *et al.* 2014) will assist in planning for the further management of the mangrove-saltmarsh communities on Ukerebagh Island. Accurate projections of future conditions within the estuary are essential for mitigating the future effects of SLR and 'coastal squeeze' on the survival of coastal wetland vegetation communities.

References

Abrantes, K., Sheaves, M. (2008). Incorporation of terrestrial wetland material into aquatic food webs in a tropical estuarine wetland. *Estuarine, Coastal and Shelf Science,*80, pp. 401-412.

Abril, J.M., & Brunskill, G.J. (2014) Evidence that 210Pb flux varies with sediment accumulation rate and implications for dating recent sediments. *Journal of Palaeolimnology,*

Acworth, C., & Lawson, S. (2012). The Tweed River Entrance Sand Bypassing Project – Ten Years of Managing Operations in a Highly Variable Coastal System. *Proceedings of the 20th NSW Coastal Conference,* 8-11 November 2011, Tweed Heads. 23pp.

Adam, P. (2002). Saltmarshes in a time of change. *Environmental Conservation,* 29(1), pp. 39-61.

Adam, P. (2009). Australian saltmarshes: global context. In: Australian Saltmarsh Ecology, ed. N Saintilan. pp. 1-22. CSIRO Publishing, Melbourne.

Alderson, B., Mazumder, D., Saintilan, N., Zimmerman, K., Mulry, P. (2013). Application of isotope mixing models to discriminate dietary sources over small-scale patches in saltmarsh. *Marine Ecology Progress Series,* 487(113-122).

Allen, J.R.L., (2000). Morphodynamics of Holocene saltmarshes: a review sketch from the Atlantic and Southern North Sea coasts of Europe. *Quaternary Science Reviews,* 19(12), pp. 1155-1231.

Alongi, D. M., Sasekumar, A., Tirendi, F., Dixon, P.(1998). The influence of stand age on benthic decomposition and recycling of organic matter in managed forests of Malaysia. *Journal of Experimental Biology and Ecology,* 225(2), pp. 197-218.

Alongi, D.M., Wattayakorn, G., Pfitzner, J., Tirendi, F., Zagorskis, I., Brunskill, G.J., Davidson, A., Clough, B.F. (2001). Organic carbon accumulation and metabolic pathways in sediments of mangrove forests in southern Thailand. *Marine Geology* ,179(1-2), pp. 85-103.

Alongi, D.M., Sasekumar, A., Chong, V.C., Pfitzner, J., Trott, L.A., Tirendi, F., Dixon, P., Brunskill, G.J. (2004). Sediment accumulation and organic material flux in a managed mangrove ecosystem: estimates of land-ocean-atmosphere exchange in peninsular Malaysia. *Marine geology,* 208(2-4), pp. 383-402.

Alongi, D.M. (2008). Mangrove forests: resilience, protection from tsunamis, and responses to global climate change. *Estuarine, Coastal and Shelf Sicence,* 76, pp. 1-13.

Alongi, D.M. (2009). The energetics of mangrove forests. Springer, Milton Keynes. ISBN 978-1-4020-4270-6.

Andersen, T.J., Svinth, S., Pejrup, M. (2011). Temporal variation of accumulation rates on a natural salt marsh in the 20th century — The impact of sea level rise and increased inundation frequency. *Marine Geology,* 279(1-4), pp. 178-187.

Appleby, P.G., Oldfield, F. (1978). The calculation of lead-210 dates assuming a constant rate of supply of unsupported ^{210}Pb to the sediment. *CATENA,* 5(1), pp. 1-8.

Appleby, P.G. (2001). Chronostratigraphic techniques in recent sediments. In: W.M. Last and J.P. Smol (eds). *Tracking environmental change using lake sediments, volume 1: Basin analysis, coring and chronological techniques,* pp. 171-203. Dordrecht. Kluwer Academic Publishers.

Australian Nuclear Science and Technology Organisation (2011). Environmental Radioactivity Measurement Centre (ERMC) Lead-210 dating sample preparation instruction.

Australian Nuclear Science and Technology Organisation (2011). Environmental Radioactivity Measurement Centre (ERMC) Polonium Chemical Isolation instruction.

Australian Nuclear Science and Technology Organisation (2011). Environmental Radioactivity Measurement Centre (ERMC) Radium chemical isolation instruction.

Baker, C., Thompson, J.R., Simpson, M. Hydrological Dynamics I: Surface Waters, Floods and Sediment Dynamics, in: Maltby, E, & Barker, T (eds). (2009). The Wetlands Handbook, Oxford, Wiley-Blackwell.

Bao, R., Alonso, A., Delgado, C., Pages, J.L. (2007). Identification of the main driving mechanisms in the evolution of a small coastal wetland (Traba, Galicia, NW Spain) since its origin 5700 cal yr BP. *Palaeogeography, Palaeoclimatology, Palaeoecology.* 247(3-4), pp. 296-312.

Barbier, E.B., Hacker, S.D., Kennedy, C., Koch, E.W., Stier, A.C., Silliman, B.R. (2011). The value of estuarine and coastal ecosystem services. *Ecological Monographs,* 81(2), pp. 169-193.

Bartholdy, A.T., Bartholdy, J., Kroon, A. (2010). Saltmarsh stability and patterns of sedimentation across a backbarrier platform. *Marine Geology,* 278(1-4), pp. 31-42.

Beaumont, N.J., Jones, L., Garbutt, A., Hansom, J.D., Toberman, M. (2014). The value of carbon sequestration and storage in coastal habitats. *Estuarine, Coastal and Shelf Science,* 137, pp. 32-40.

Begy, R., Timar-Gabor, A., Somlai, J., Cosma, C. (2011). A sedimentation study of St. Ana Lake (Romania) applying the Pb and Cs dating methods. *Geochronometria: Journal on Methods and Applications of Absolute Chronology,* 38(2), pp. 93-100.

Bellucci, L.G., Frignani, M., Cochran, J.K., Albertazzi, S., Zaggia, L., Cecconi, G., Hopkins, H. (2007). 210Pb and 137Cs as chronometers for salt marsh accretion in the Venice Lagoon – links to flooding frequency and climate change. *Journal of Environmental Radioactivity,* 97(2-3), pp. 85-102.

Bianchi, T.S., Allison, M.A., Zhao, J., Li, X, Comeaux, R.S., Feagin, R.A., Kularwardhana, R.W. (2013). Historical reconstruction of mangrove expansion in the Gulf of Mexico: Linking climate change with carbon sequestration in coastal wetlands. *Estuarine, Coastal and Shelf Science,* 119, pp. 7-16.

Bornman, T.G., Schmidt, J., Adams, J.B., Mfikili, A.N., Farre, R.E., Smit, A.J. (2016). Relative sea-level rise and the potential for subsidence of the Swartkops Estuary intertidal salt marshes, South Africa. *South African Journal of Botany,* in press.

Bostrom, B., Comstedt, D., Ekblad, A. (2007). Isotope fractionation and ^{13}C enrichment in soil profiles during the decomposition of soil organic matter. *Oecologia,* 153(1), pp. 89-98.

Bouillon, S., Connolly, R.M., Lee, S.Y. (2008). Organic matter exchange and cycling in mangrove ecosystems: recent insights from stable isotope studies. *Journal of Sea Research,* 59, pp. 44-58.

Bowie, C. (2015). Mangrove and saltmarsh dynamics in Homebush Bay: implications for management at Sydney Olympic Park. BEnviSci Hons, School of Earth and Environmental Sciences, University of Wollongong. http://ro.uow.edu.au/thsci/108.

Brain, M.J., Long, A.J., Woodroffe, S.A., Petley, D.N., Milledge, D.G., Parnell, A.C. (2012). Modelling the effects of sediment compaction of salt marsh reconstructions of recent sea-level rise. *Earth and Planetary Science Letters,* 345-348, pp. 180-193.

Brevik, E.C., & Homburg, J.A. (2004). A 5000 year record of carbon sequestration from a coastal lagoon and wetland complex, Southern California, USA. *Catena,* 57(3), pp. 221-232.

Breithaupt, J.L, Smoak, J.M., Smith, T.J., Sanders, C.J., Hoare, A. (2012). Organic carbon burial rates in mangrove sediments: strengthening the global budget. *Global Biogeochemical Cycles,* 26(3).

Bridgman, S.D., & Lamberti, G.A. (2009). Ecological Dynamics III: Decomposition in Wetlands, in: Maltby, E, & Barker, T (eds). (2009). The Wetlands Handbook, Oxford, Wiley-Blackwell.

Bureau of Meteorology (2016). Climate statistics for Coolangatta (station 04717). http://www.bom.gov.au/climate/averages/tables/cw_040717.shtml . Last accessed 18/04/2016.

Burrell, A. (2012). Mapping changes of saltmarsh and mangrove vegetation communities in Wagonga Inlet, NSW South Coast. Bachelor of Environmental Science (Honours), School of Earth and Environmental Science, University of Wollongong. http://ro.uow.edu.au/thsci/33.

Cahoon, D.R., & Reed, D.J. (1995). Relationships among marsh surface topography, hydroperiod and soil accretion in a deteriorating Louisiana salt marsh. *Journal of Coastal Research,* 11(2), pp. 357-369.

Cahoon, D.R, Reed, D.J., & Day, J.W. Jr. (1995). Estimating shallow subsidence in microtidal saltmarshes of the southeastern United States: Kaye and Barghoorn revisited. *Marine Geology,* 128, pp. 1-9.

Cahoon, D.R., & Lynch, J. (1997). Vertical accretion and shallow subsidence in a mangrove forest of southwestern Florida, U.S.A. *Mangroves and Salt Marshes,* 1 (3), pp. 173- 185.

Cahoon, D.R., Day, J.W. Jr, & Reed, D.J. (1999). The influence of surface and shallow subsurface soil processes on wetland elevation: a synthesis. *Current Topics in Wetland Biogeochemistry,* 3, pp. 72-88.

Cahoon, D.R., Lynch, J.C., Hensel, P., Boumans, R., Perez, B.C., Segura, B., Day, J.W. Jr (2002). High-precision measurements of wetland sediment elevation: 1. Recent improvements to the sedimentation-erosion table. *Journal of Sediment Resources,* 72, pp. 730-733.

Cahoon, D.R., & Guntenspergen, G.R. (2010). Climate change, sea-level rise, and coastal wetlands. *National Wetlands Newsletter,* 32(1), pp. 8-12.

Callaway, J.C., Cahoon, D.R., & Lynch, J.C. (2013). The surface elevation table-marker horizon method for measuring wetland accretion and elevation dynamics. In: *Methods in Biogeochemistry of Wetlands, SSSA Book Series, vol 10.,* ed R.D. DeLaune, K.R. Reddy, C.J. Richardson, J.P. Megonigal, 901-917. Madison: Soil Science Society of Australia.

Castelle, B., Turner, I.L., Bertin, X., Tomlinson, R. (2009). Beach nourishments at Coolangatta Bay over the period 1987-2005: Impacts and lessons. *Coastal engineering,* 56(9), pp. 940-950.

Cheng, X., Luo, Y., Chen, J., Lin, G., Chen, J., Li, B. (2006). Short-term C_4 plant *Spartina alterniflora* change the soil carbon in C3 plant-dominated tidal wetlands on a growing estuarine island. *Soil Biology and Biochemistry,* 38(12), pp. 3380-3386.

Cherry, J.A., McKee, K.L., Grace, J.B. (2009). Elevated CO_2 enhances biological contributions to elevation change in coastal wetlands by offsetting strssors associated with sea-level rise. *Journal of Ecology,* 97, pp. 67-77.

Chmura, G.L., Aharon, P., Socki, R.A., Abernethy, R. (1987). An inventory of ^{13}C abundances in coastal wetlands of Louisiana, USA: vegetation and sediments. *Oecologia,* 74, pp. 264-271.

Chmura, G.L., & Aharon, P. (1995). Stable carbon isotope signatures of sedimentary carbon in coastal wetlands as indicators of salinity regime. *Journal of Coastal Research,* 11(1), pp. 124-135.

Chmura, G.L. (2003). Global carbon sequestration in tidal, saline wetland soils. *Global biogeochemical cycles,* 17(4), pp. 1-12.

Choi, Y., Wang, Y., Hsieh, Y-P., Robinson, L. (2001). Vegetation succession and carbon sequestration in a coastal wetland in northwest Florida: Evidence from carbon isotopes. *Global Biogeochemical Cycles,* 15(2), pp. 311-319.

Choi, Y., & Wang, Y. (2004). Dynamics of carbon sequestration in a coastal wetland using radiocarbon measurements. *Global Biogeochemical Cycles,* 18(4).

Cifuentes, L.A., Coffin, R.B., Soloranzo, L., Cardenas, W., Espinoza, J., Twilley, R.R. (1996). Isotopic and elemental variations of carbon and nitrogen in a mangrove estuary. *Estuarine, Coastal and Shelf Science,* 43(6), pp. 781-800.

Cloern, J.E., Canuel, E.A., Harris, D. (2002). Stable carbon and nitrogen isotope composition of aquatic and terrestrial plants in the San Fransisco Bay estuarine system. *Limnology and Oceanography,* 47(3), pp. 713-729.

Coletti, J.Z., Hinz, C., Vogwill, R., Hipsey, M.R. (2013). Hydrological controls on carbon metabolism in wetlands. *Ecological Modelling,* 249, pp. 3-18.

Costanza, R., d'Arge, R., de Groot, R., Fraber, S., Grasso, M., Hannon, B., Limburg, K., Naeem, S., O'Neill, R.V., Paruelo, J., Raskin, R.G., Sutton, P., van den Belt, M. (1997). The value of the world's ecosystem services and natural capital. *Nature,* 387(6630), pp. 253-260.

Costanza, R., Perez-Maqueo, O., Martinez, M.L., Sutton, P., Anderson, S.J., Mulder, R (2008). The value of coastal wetlands for hurricane protection. *AMBIO: A Journal of the Human Environment,* 37(4), PP. 241-248.

Couto, T., Duarte, B., Cacador, I., Baeta, A., Marques, J.C. (2013). Salt marsh plants carbon storage in a temperate Atlantic estuary illustrated by a stable isotopic analysis-based approach. *Ecological Indicators,* 32, pp. 305-311.

Covelli, S., Fontolan, G., Faganeli, J., Ogrinc, N. (2006). Anthropogenic markers in the Holocene stratigraphic sequence of the Gulf of Trieste (northern Adriatic Sea). *Marine Geology,* 230 pp. 29-51.

Craft, C.B., Broome, S.W., Seneca, E.D., Showers, W.J. (1988). Estimating sources of soil organic matter in natural and transplanted estuarine marshes using stable isotopes of carbon and nitrogen. *Estuarine, Coastal and Shelf Science,* 26(6), pp. 633-641.

Craft, C.B., Clough, J., Ehman, J., Joye, S., Park, R., Pennings, S., Guo, H., Machmuller, M (2009). Forecasting the effects of accelerated sea-level rise on tidal marsh ecosystem services. *Frontiers in Ecology and the Environment,* 7(2), pp.73-78.

Cramer, W., Bondeau, A., Schaphoff, S., Lucht, W., Smith, B., Sitch, S. (2004). Tropical forests and the global carbon cycle: impacts of atmospheric carbon dioxide, climate change and rate of deforestation. *Philosophical transactions of the Royal Society: biological sciences,* 359(1443), pp. 331-343.

Crase, B., Liedloff, A., Vesk, P.A., Burgman, M.A., Wintle, B.A. (2013). Hydroperiod is the main driver of the spatial pattern of dominance in mangrove communities. *Global Ecology and Biogeography,* 22(7), pp. 806-817.

Creach, V. (1995). Origines et transferts de la matiere organique dans un marais littoral: utilisation des compositions isotopiques naturelles du carbone et de l'Azote. PhD thesis, Universite de Rennes.

Cundy, A.B., Kortekaas, S., Dewez, T., Stewart, I.S., Collins, P., Croudace, E.F., Maroukian, H., Papanastassiou, D., Gaki-Papanastassiou, P., Palvopoulos, K., Dawson, A. (2000). Coastal wetlands as recorders of earthquake subsidence in the Aegean: a case study of the 1894 Gulf of Atalanti earthquakes, central Greece. *Marine Geology,* 170, pp. 3-26.

Day, J.W. Jr, Scarton, F., Rismondo, A., Are, D. (1998). Rapid deterioration of a saltmarsh in Venice Lagoon, Italy. *Journal of Coastal Research,* 14(2), pp. 583-590.

Deegan, L.A., Johnson, D.S., Warren, R.S., Peterson, B.J., Fleeger, J.W., Fagherazzi, S., Wollheim, W.M. (2012). Coastal eutrophication as a driver of salt marsh loss. *Nature,* 490, pp. 388-392.

DeLaune, R.D. (1986). The use of $\delta^{13}C$ signature of C_3 and C_4 plants in determining past depositional environments in rapidly accreting marshes of the Mississippi River Delta Plain, Louisiana, USA. *Chemical Geology,* 59, pp. 315-320.

DeLaune, R.D., & White, J.R. (2011). Will coastal wetlands continue to sequester carbon in response to an increase in global sea level? A case study of the rapidly subsiding Mississippi River deltaic plain. *Climatic Change,* 110(1), pp. 297-314.

Di Nitto, D., Neukermans, G., Koedam, N., Defever, H., Pattyn, F., Kairo, J.G., Guebas-Dahdouh, F. (2014). Mangroves facing climate change: landward migration potential in response to projected scenarios of sea level rise. *Biogeosciences,* 11, pp. 857-871.

Dise, N.B. (2009). Biogeochemical Dynamics III: The critical role of carbon in wetlands, in: Maltby, E, & Barker, T (eds). (2009). The Wetlands Handbook, Oxford, Wiley-Blackwell.

Donato, D.C., Kauffman, J.B., Murdiyarso, D., Kurnianto, S., Stidham, M., Kanninen, M. (2011). Mangroves among the most carbon-rich forests in the tropics. *Nature Geoscience,* 4(5), pp. 293-297.

Doody, J.P. (2004). 'Coastal squeeze' – a historical perspective. *Journal of Coastal Conservation,* 10(1), pp. 129-138.

Doyle, T.W., Krauss, K.W., Conner, W.H., From, A.S. (2010). Predicting the retreat and migration of tidal forests along the northern Gulf of Mexico under sea-level rise. *Forest Ecology and Management,* 259(4), pp. 770-777.

Druery, B.E., Curedale, J.W., (1979). *Tweed River Dynamics Study.* Report No. 78009, NSW Public Works Department.

Duarte, C.M., Middleburg, J.J., Caraco, N. (2005). Major role of marine vegetation on the oceanic carbon cycle. *Biogeosciences,* 2(1), pp. 1-8.

Duarte, C.M., Losada, I.J. Hendriks, I.E., Mazarrasa, I., Marba, N. (2013). The role of coastal plant communities for climate change mitigation and adaptation. *Nature Climate Change,* 3(11), pp. 961-968.

Dubbert, M. (2012). Species-specific differences in temporal and spatial variation in $\delta^{13}C$ of plant carbon pools and dark-respired CO_2 under changing environmental conditions. *Photosynthesis Research,* 113(1-3), pp. 297-309.

Dyson, A., Victory, S., Connor, T. (2001). Sand Bypassing the Tweed River Entrance: An Overview. Proceedings of the 15th Australasian Coastal and Ocean Engineering Conference and the 8th Australasian Port and Harbour Conference, 25-28 September. QLD Australia. 6pp.

Ehleringer, J.R., Buchmann, N., Flanagan, L.B. (2000) Carbon isotope ratios in belowground carbon cycle processes. *Ecological Applications,* 10(2), pp. 412-422.

Ellison, J.C. & Stoddart, D.R. (1991). Mangrove ecosystem collapse during predicted sea-level rise: Holocene analogues and implications. *Journal of Coastal Research,* 7, pp. 151-165.

Ellison, J.C. (2008). Long-term retrospection on mangrove decelopment using sediment cores and pollen analysis: a review. *Aquatic Botany,* 89(2), pp. 93-104.

Ember, L.M., Williams, D.F., Morris, J.T. (1987). Processes that influence carbon isotopic variations in saltmarsh sediments. *Marine Ecology Progress Series,* 36, pp. 33-42.

Emery, N.C., Ewanchuk, P.J., Bertness, M.D. (2001). Competition and saltmarsh plant zonation: stress tolerators may be dominant competitors. *Ecology,* 82(9), pp. 2471-2485.

Eslami-Andargoli, L., Dale, P.E.R., Sipe, N., Chaseling, J. (2009). Mangrove expansion and rainfall patterns in Moreton Bay, Southeast Queensland, Australia. *Estuarine, Coastal and Shelf Science,* 85, pp. 292-298.

Eslami-Andargoli, L., Dale, P.E.R., Sipe, N., Chaseling, J. (2010). Local and landscape effects on spatial patterns of mangrove forest during wetter and drier periods, Moreton Bay, southeast Queensland, Australia. *Estuarine, Coastal and Shelf Science,* 85, pp. 53-61.

Eyre, B.D., Hossain, S., McKee, L. (1998). A suspended sediment budget for the modified subtropical Brisbane River estuary, Australia. *Estuarine, Coastal and Shelf Science,* 47(4), pp. 513-522.

Eyre, B.D (2000). Regional evaluation of nutrient transformation and phytoplankton growth in nine river-dominated sub-tropical east Australian estuaries. *Marine Ecology Progress Series,* 205, pp. 61-83.

Fagherazzi, S., Kirwan, M.L., Mudd, S.M., Guntenspergen, G.R., Temmerman, S., D'Alpaos, A., van de Koppel, J., Rybczyk, J.M., Reyes, E., Craft, C., Clough, J. (2012). Numerical models of saltmarsh evolution: ecological, geomorphic and climatic factors. *Reviews of Geophysics,* 50, pp. 1-28.

Farquhar, G.D., Ehleringer, J.R., & Hubick, K.T. (1989). Carbon isotope discrimination and photosynthesis. *Annual Review of Plant Biology,* 40(1), pp. 503-537.

Faure, G. & Mensing, T.M. (2005). Isotopes: Principles & Applications, 3rd edition. John Wiley & Sons, New Jersey. ISBN 0471384372.

Field, C.B., Raupach, M.R., Victoria, R. (2004). Ch 1: The Global Carbon Cycle: integrating humans, climate and the natural world, in: Global Carbon Cycle: integrating humans, climate and the natural world, Island Press, Washington USA.

Fletcher, C.H. III, van Pelt, J.E., Brush, G.S., Sherman, J. (1993). Tidal wetlands record of Holocene sea-level movements and climate history. *Palaeogeography, Palaeoclimatology, Palaeoecology,* 102(3-4), pp. 177-213.

Fourqurean, J. W., Duarte, C. M., Kennedy, H., Marbà, N., Holmer, M., Mateo, M. A., Apostolaki, E. T., Kendrick, G. A., Krause-Jensen, D., McGlathery, K. J., Serrano, O. (2012a). Seagrass systems as a globally significant carbon stock. *Nature Geoscience*, 5(7), pp.505-509.

Fourqurean, J.W., Kendrick, G.A., Collins, L.S., Chambers, R.M., Vanderklift, M.A. (2012b). Carbon, nitrogen and phosphorous storage in subtropical seagrass meadows: examples from Florida Bay and Shark Bay. *Marine and Freshwater Research,* 63(11), pp. 967-983.

Francey, R.J., Allison, C.E., Etheridge, D.M., Trudinger, C.M., Enting, I.G, Leuenberger, M., Langenfelds, R.L., Michel, E., Steele, L.P. (1999). A 1000-year high precision record of $\delta^{13}C$ in atmospheric CO_2. *Tellus,* 51B, pp.170-193.

French, J. (2006). Tidal marsh sedimentation and resilience to environmental change: exploratory modelling of tidal, sea-level and sediment supply forcing in predominantly allochthonous systems. *Marine Geology,* 235(1-4), pp. 119-136.

Furukawa, K., & Wolanski, E. (1996). Sedimentation in mangrove forests. *Mangroves and Salt Marshes,* 1(1), pp. 3-10.

Ganju, N.K., & Schoellhamer, D.H. (2010). Decadal-timescale estuarine geomorphic change under future scenarios of climate and sediment supply. *Estuaries and Coasts,* 33(1), pp. 15-29.

Garten, C.T., Hanson, P.J., Todd, D.E., Lu, B.B., Brice, D.J. (2007). Natural ^{15}N and ^{13}C abundance as indicators of forest nitrogen status and soil carbon dynamics. In: Michener, R., & Lajtha, K. (eds.) Stable isotopes in ecology and environmental science. Blackwell, Melbourne. ISBN 9781405126809.

Gedan, K.B., Silliman, B.R., Bertness, M.D. (2009). Centuries of human-driven change in salt marsh ecosystems. *Annual Review of Marine Science,* 1(1), pp. 117-141.

Gedan, K.B., Kirwan, M.L, Wolanski, E., Barbier, E.B., Silliman, B.R. (2011). The present and future role of coastal wetlands vegetation in protecting shorelines: answering recent challenges to the paradigm. *Climatic Change,* 106(1), pp. 7-29.

Gedan, K.B., Altieri, A.H., Bertness, M.D. (2011). Uncertain future of New England salt marshes. *Marine ecology progress series,* 434, pp. 229-237.

Gehrels, W.R. (2000). Using foraminiferal transfer functions to produce high-resolution sea-level records from saltmarsh deposits, Maine, USA. *The Holocene,* 10(3), pp. 367-376.

Gehrels, W.R., Roe, H.M., Charman, D.J. (2001). Foraminifera, testae amoebae and diatoms and sea level indicators in UK saltmarshes: a quantitative multiproxy approach. *Journal of Quaternary Science,* 16, pp. 201-220.

Goodman, J.E., Wood, M.E., Gehrels, W.R. (2007). A 17-yr record of sediment accretion in the saltmarshes of Maine(USA). *Marine Geology,* 242(1-3), pp. 109-121.

Grenfell, S.E., Callaway, R.M., Grenfell, M.C., Bertelli, C.M., Mendzil, A.F., Tew, I. (2016). Will a rising sea sink some estuarine wetland ecosystems? *Science of the Total Environment,* 554-555, pp. 276-292.

Guest, M.A., Connolly, R.M., and Loneragan, N.R., (2004). Within and among-site variability in $\delta^{13}C$ and $\delta^{15}N$ for three estuarine producers, *Sporobolus virginicus, Zostera capricorni,* and epiphytes of *Z. capricorni. Aquatic Botany,* 79, pp. 87-94.

Haines, E.B. (1976). Stable carbon isotope ratios in the biota, soils and tidal water of a Georgia salt marsh. *Estuarine, Coastal and Marine Science,* 4, pp. 609-616.

Hartig E.K., Gornitz, V., Kolker, A., Muschacke, F., Fallon, D. (2002). Anthropogenic and climate-change impacts on salt marshes of Jamaica Bay, New York City. *Wetlands,* 22(1), pp. 71-89.

Hatch, M.D., & Slack, C.R. (1970). Photosynthetic CO_2-fixation pathways. *Annual Reviews in Plant Physiology,* 21, pp. 141-162.

Hayward, B.W., Wilson, K., Morley, M.S., Cochran, U., Grenfell, H.R., Sabaa, A.T., Daymond-King, R. (2010). Microfossil record of the Holocene evolution of coastal wetlands in a tectonically active region of New Zealand. *The Holocene,* 20(3), pp. 405-421.

Heap, A., Bryce, S., Ryan, D., Radke, L., Smith, C., Harris, P., Heggie, D. (2001). *Australian Estuaries and Coastal Waterways: A geoscience perspective for improved and integrated resource management.* Australian Geological Survey Organisation. Record 2001/07. March 2001. Commonwealth of Australia, Canberra, 118p.

Hickey, D., & Bruce, E. (2010). Examining tidal inundation and salt marsh vegetation distribution patterns using spatial analysis (Botany Bay, Australia). *Journal of Coastal Research,* 26(1), pp. 94-102.

Hill, T.D., Anisfeld, S.C. (2015). Coastal wetland response to sea level rise in Conneticut and New York. *Estuarine, Coastal and Shelf Science,* 163(b), pp. 185-193.

Hollingsworth, A., & Connolly, R.M. (2006). Feeding by fish visiting inundated subtropical saltmarsh. *Journal of Experimental Marine Biology and Ecology,* 336, pp. 88-98.

Hogarth, P.J. (1999). The biology of mangroves. Oxford University Press, Oxford. ISBN 0-19-850223-0.

Hornibrook, E.R.C., Longstaffe, F.J., Fyfe, W.S. (2000). Evolution of stable carbon isotope compositions for methane and carbon dioxide in freshwater wetlands and other anaerobic environments. *Geochimica et Cosmochimica Acta,* 64(6), pp. 1013-1027.

Hossain, M.M.K. (2005). An examination of seagrass monitoring protocols as applied to two New South Wales estuarine settings. Australian Catholic University, School of Arts and Sciences.

Houston, W., Black, R., Elder, R., Black, L., Segal, R. (2012). Conservation value of solar salt ponds in coastal tropical eastern Australia to waterbirds and migratoy shorebirds.

Howard, J., Hoyt, S., Isensee, K., Telszewski, M, Pidgeon, E. (eds.) (2014). Coastal Blue Carbon: Methods for assessing carbon stocks and emissions factors in mangroves, tidal salt marshes and seagrasses. Conservation International, Intergovernmental Oceanographic Commission of UNESCO, International Union for Conservation of Nature. Arlington, Virginia, USA.

Howard, R.J., Krauss, K.W., Cormier, N., Day, R.H., Biagas, J., Allain, L. (2015). Plant-plant interactions in a subtropical mangrove-to-marsh transition zone: effects of environmental drivers. *Journal of Vegetation Science,* 26(6), pp. 1198-1211.

Hyder Consulting Pty Ltd, Patterson Britton & Partners Pty Ltd and WBM Oceanics Australia Joint Venture, "Tweed River Entrance Sand Bypassing Project, Permanent Bypassing System, Environmental Impact Statement – Impact Assessment Study. June 1997.

IPCC, 2013: Summary for Policymakers. In: Climate Change 2013: The Physical Science Basis. Contribution of Working Group I to the Fifth Assessment Report of the Intergovernmental Panel on Climate Change [Stocker, T.F., Qin, G-K., Plattner, M., Tignor, Allen , S.K., Boschung, J., Nauels, A., Xia, Y, Bex, V., Midgley, P.M. (eds.)]. Cambridge University Press, Cambridge, United Kingdom & New York, NY, USA.

Irving, A.D., Connell, S.D., Russell, B.D. (2011). Restoring coastal plants to improve global carbon storage: reaping what we sow. *PLoS ONE,* 6(3), pp. 1-6.

Johnson, B.J., Moore, K.A., Lehmann, C., Bohlen, C., Brown, T.A. (2007). Middle to late-Holocene fluctuations of C_3 and C_4 vegetation in a northern New England salt marsh, Sprague Marsh, Phippsburg Maine. *Organic Geochemistry,* 38(3), pp. 394-403.

Kathiresan, K. (2002). How do mangrove forests induce sedimentation? *Revista de Biologia Tropical,* 51(2), pp.

Kayranli, B., Scholz, M., Mustafa, A., Hedmark, A. (2009). Carbon storage and fluxes within freshwater wetlands: a critical review. *Wetlands,* 30(1), pp. 111-124.

Kearney, M.S., & Turner, R.E. (2016). Microtidal marshes: can these widespread and fragile marshes survive increasing climate-sea level variability and human action? *Journal of Coastal Research,* 32(3), pp. 686-699.

Keeling, C.D. (1979). The Suess effect: ^{13}carbon-^{14}carbon interrelations. *Environment International,* 2(4-6), pp.229-300.

Kelleway, J.J., Saintilan , N., Macreadie, P.I., Skilbeck, C.G., Zawadzki, A., Ralph, P.J. (2016). Seventy ears of continuous encroachment substantially increases 'blue carbon' capacity as mangroves replace intertidal salt marshes. *Global Change Biology,* 22(3), 1097-1109.

Kennish, M.J. (2001). Coastal saltmarsh systems in the US: a review of anthropogenic impacts. *Journal of Coastal Research,* 17(3), pp.731-748.

Kermode, S.J., Heijnis, H., Wong, H., Zawadzki, A., Gadd, P., & Permana, A. (2016). A Ramsar-wetland in suburbia: wetland management in an urbanised, industrialised area. *Marine and Freshwater Research,* 67, pp. 771-781.

Khan, N.S., Vane, C.H., Horton, B.P., Hillier, C., Riding, J.B., Kendrick, C.P. (2015). The application of δ^{13}C, TOC and C/N geochemistry to reconstruct Holocene relative sea levels and paleoenvironments in the Thames Estuary, UK. *Journal of Quaternary Science,* 30(5), pp. 417-433.

Kirchner, G., Ehlers, H. (1998). Sediment geochronology in changing coastal environments: potentials and limitations of the 137Cs and 210Pb methods. *Journal of Coastal Research,* 14(2), pp. 483-492.

Kirk, G. (2004). The Biogeochemistry of Submerged Soils. John Wiley & Sons, Chichester, England.

Kirwan, M.L., Guntenspergen, G.R., D'Alpaos, A., Morris, J.T., Mudd, S.M., Temmerman, S. (2010). Limits on the adaptability of coastal marshes to rising sea level. *Geophysical Research Letters,* 37(23), pp. 1-5.

Kirwan, M.L., & Blum, L.K. (2011). Enhanced decomposition offsets enhanced productivity and soil carbon accumulation in coastal wetlands responding to climate change. *Biogeosciences,* 8, pp. 987-993.

Kirwan, M.L., & Mudd, S.M. (2012). Response of salt-marsh carbon accumulation to climate change. *Nature,* 489(7417), pp. 550-553.

Kolker, A.S., Goodbred, S.L., Jr., Hameed, S., Cochran, J.K. (2009). High-resolution records of the response of coastal wetland systems to long-term and short-term variability. *Estuarine, Coastal and Shelf Science,* 84(4), pp. 493-508.

Krauss, K.W., McKee, K.L., Lovelock, C.E., Cahoon, D.R., Saintilan, N., Reef, R., Chen, Luzhen (2014). How mangrove forests adjust to rising sea level. *New Phytologist,* 202(1), p. 19-34.

Kubasek, J., Urban, O., Santrucek, J. (2013). C4 plants use fluctuating light less efficiently than do C3 plants: a study of growth, photosynthesis and carbon isotope discrimination. *Physiologia Plantarum,* 149(4), pp. 528-539.

Landry, J-S., Matthews, H.D., Ramankutty, N. (2015). A global assessment of the carbon cycle and temperature responses to major changes in future fire regime. *Climatic change,* 133, pp. 179-182.

Langley, J.A. McKee, K.L., Cahoon, D.R., Cherry, J.A., & Megonigal, J.P. (2009). Elevated CO_2 stimulates marsh elevation gain, counterbalancing sea-level rise. *Proceedings of the National Academy of Sciences of the United States of America,* 106(5), pp. 6182-6186.

Lawson, S. McMahon, J., Boswood, P. (2001). Environmental Management of the Construction and Operation of a Sand Bypassing System at the Tweed River Entrance. *Proceedings of the 15th Australasian Coastal and Ocean Engineering Conference and the 8th Australasian Port and Harbour Conference,* 25-28 September. QLD Australia. 8pp.

Levine, J.M., Brewer, J.S., Bertness, M.D. (1998). Nutrients, competition and plant zonation in a New England salt marsh. *Journal of Ecology,* 86(2), pp. 285-292.

Lim, J., Nahm, W-H., Kim, J-K., Yang, D-Y. (2010). Regional climate-driven C3 and C4 plant variation in the Cheollipo area, Korea, during the late Pleistocene. *Palaeogeography, palaeoclimatology, palaeoecology,* 298(3-4), pp. 370-377.

Limpens, J., Berendse, F., Blodau, C., Canadell, J.G., Freeman, C., Holden, J., Roulet, N., Rydin, H., Schaepman-Strub, G. (2008). Peatlands and the carbon cycle: from local processes to global implications – a synthesis. *Biogeosciences Discussions,* 5(2), pp. 1379-1419.

Liu, L., Chen, H., Zhu, Q., Yang, G., Zhu, E., Hu, J., Peng, C., Jiang, L., Zhan, W., Ma., T., He., Y., Zhu, D. (2016). Responses of peat carbon at different depths to simulated warming and oxidising. *Science of the Total Environment,* 548-549, pp. 429-440.

Loneragan, N.R., Bunn, S.E., Kellaway, D.M. (1997). Are mangroves and seagrasses sources of organic carbon for penaeid prawns in a tropical Australian estuary? A multiple stable-isotope study. *Marine Biology,* 130, pp. 289-300.

Lovelock, C.E., Bennion, V., Grinham, A., Cahoon, D.R. (2011). The role of surface and subsurface processes in keeping pace with sea level rise in intertidal wetlands of Moreton Bay, Queensland, Australia. *Ecosystems,* 14(5), pp. 745-757.

Lovelock, C., Adame, M., Bennion, V., Hayes, M., O'Mara, J., Reef, R., Santini, N. (2014). Contemporary rates of carbon sequestration through vertical accretion of sediments in mangrove forests and saltmarshes of south-east Queensland, Australia. *Estuaries and coasts,* 37(3), 763-771.

Lovelock, C.E., Adame, M.F., Bennion,V., Hayes, M., Reef, R., Santini, N., Cahoon, D.R. (2015). Sea level and turbidity controls on mangrove soil surface elevation change. *Estuarine, Coastal and Shelf Science,* 153, pp. 1-9.

Ma, Z., Ysebaert, T., van der Wal, D., de Jong, D.J, Li, X., Herman, P.M.J. (2014). Long-term salt marsh vertical accretion in a tidal bay with reduced sediment supply. *Estuarine, coastal and shelf science,* 143, pp. 14-23.

Marshall, J.D., Brooks, J.R., Lajtha, K. (2007). Sources of variation in the stable isotopic composition of plants, in: Michener, R., & Lajtha, K. (eds.) Stable isotopes in ecology and environmental science, Blackwell, Melbourne. ISBN 9781405126809.

Maynard, J.J., Dahlgren, R.A., O'Geen, A.T. (2014). Autochthonous and allochthonous carbon cycling in a eutrophic flow-through wetland. *Wetlands,* 34(2), pp. 285-296.

Mazumder, D., Saintilan, N., Williams, R.J. (2006). Trophic relationship between itinerant fish and crab larvae in a temperate Australian saltmarsh. *Marine and Freshwater Research,* 57, pp. 193-199.

Mazumder, D. (2009). Ecology of burrowing crabs in temperate saltmarsh of south-east Australia, in: Saintilan, N. (ed.) Australian Saltmarsh Ecology. CSIRO, Melbourne.

Mazumder, D., Iles, J., Kelleway, J., Kobayashi, T., Knowles, L., Saintilan, N., Hollins, S. (2010). Effect of acidification on elemental and isotopic compositions of sediment organic matter and macro-invertebrate muscle tissues in food web research. *Rapid communications in mass spectrometry,* 24, pp. 2938-2942.

Mazumder, D., Saintilan, N., Williams, J., & Szymczak, R. (2011). Trophic importane of a temperate intertidal wetland to resident and itinerant taxa: evidence from multiple stable isotope analyses. *Marine and Freshwater Research* 62, pp. 11-19.

McKee, K.L., Cahoon, D.R., Feller, I.C. (2007). Caribbean mangroves adjust to rising sea level through biotic controls on change in soil elevation. *Global Ecology and Biogeography,* 13, pp. 65-73.

McKee, K.L., & Rooth, J.E. (2008). Where temperate meets tropical: multi-factorial effects of elevated CO_2, nitrogen enrichment, and competition on a mangrove-saltmarsh community. *Global Change Biology,* 14, pp. 971-984.

McKee, K.L., Rogers, K., and Saintilan, N. (2012). Response of salt marsh and mangrove wetlands to changes in atmospheric CO_2, climate and sea level. In: Middleton, B. (ed.) *Global change and the function of wetlands,* pp. 63-96. Springer, Dordrecht, NL.

McLeod, E., Chmura, G.L., Bouillon, S., Salm, R., Bjork, M., Duarte, C.M., Lovelock, C.E., Schlesinger, W.H., Silliman, B.R. (2011). A blueprint for blue carbon: toward an improved understanding of the role of vegetated coastal habitats in sequestering CO_2. *Frontiers in ecology and the environment,* 10, pp. 552-650.

Medvedeff, C.A., Inglett, K.S., Inglett, P.W. (2015). Patterns and controls of anaerobic soil respiration and methanogenesis following extreme restoration of calcareous subtropical wetlands. *Geoderma,* 245-246, pp. 74-82.

Mesnage, V., Bonneville, S., Laignel, B., Lefebvre, D., Dupont, J-P., Mikes, D. (2002). Filling of a wetland (Seine estuary, France): natural eutrophication or anthropogenic process? A sedimentological and geochemical study of wetland organic sediments. *Hydrobiologia,* 475-476, pp. 423-435.

Middelburg, J.J., Nieuwenhuize, J., Lubberts, R.K., van de Plassche, O. (1997). Organic carbon isotope systematics of coastal marshes. *Estuarine, Coastal and Shelf Science,* 45, pp. 681-687.

Mitra, S., Wassmann, R., & Vlek, P.L.G. (2005). An appraisal of global wetland area and its organic carbon stock. *Current Science,* 88(1), pp. 25-35.

Moorhead, K.K., Brinson, M.M, (1995). Response of wetlands to rising sea level in the lower coastal plain of North Carolina. *Ecological Application,* 5(1), pp. 261-271.

Mudd, S.M. (2011). The life and death of salt marshes in response to anthropogenic disturbance of sediment supply. *Geology,* 39(5), pp. 511-512.

Murray-Wallace, C.V., Belperio, A.P., Gostin, V.A., Cann, J.H. (1993). Amino acid racemization and radiocarbon dating of interstadial marine strata (oxygen isotope stage3), Gulf of St Vincent, South Australia. *Marine Geology,* 110(1-2), pp. 83-92.

Nellemann, C., Corcoran, E., Duarte, C.M., Valdes, L., DeYoung, C., Fonseca, L., and Grimsditch, G.E. (2009). Blue Carbon: A Rapid Response Assessment. United Nations Environment Programme, GRID-Arendal, Norway.

Nittrouer, C.A., Sternberg, R.W., Carpenter, R., Bennett, J.T., (1979). The use of Pb-210 geochronology as a sedimentological tool: application to the Washington continental shelf. *Marine Geology,* 31(3), pp. 297-316.

NSW Department of Public Works (1991). Lower Tweed Estuary River Management Plan, September 1991. ISBN 0 7305 8635 0, PWD 91052.

NSW Office of Environment & Heritage (2012). Estuaries of NSW – Tweed River. http://www.environment.nsw.gov.au/estuaries/stats/TweedRiver.htm. Accessed 18/04/2016.

Oczkowski, A., Hanson, A., Wigand, C., Markham, E. (2014). Carbon stable isotopes as indicators of coastal eutrophication. *Ecological Applications,* 24(3), pp. 457-466.

O'Laughlin, C., & Proosdij, D. (2013). Influence of varying tidal prism on hydrodynamics and sedimentary processes in a hypertidal salt marsh creek. *Earth Surface Processes and Landforms,* 38(5), pp. 534-546.

O'Leary, M.H. (1988). Carbon isotopes in photosynthesis. *BioScience,* 38(5), pp. 328-336.

Oliver, T.S.N., Rogers, K., Chafer, C.J., Woodroffe, C.D. (2012). Measuring, mapping and modelling: an integrated approach to the management of mangrove and saltmarsh in the Minnamurra River estuary, southeast Australia. *Wetlands Ecology and Management,* 20(4), pp. 353-371.

Olsen, Y.S., Dausse, A., Garbutt, A., Ford, H., Thomas, D.N., Jones, D.L. (2011). Cattle grazing drives nitrogen and carbon cycling in a temperate salt marsh. *Soil Biology and Biogeochemistry,* 43(3), pp. 531-541.

Olsson, L., Ye, S., Yu, X., Wei, M., Krauss, K.W., & Brix, H. (2015). Factors influencing CO_2 and CH_4 emissions from coastal wetlands in the Liaohe delta, northeast China. *Biogeosciences,* 12, pp. 4965-4977.

Orson, R.A., & Howes, B.L. (1992). Salt marsh development studies at Waquoit Bay, Massachusetts: influence of geomorphology on long-term plant community structure. *Estuarine, Coastal and Shelf Science,* 35(5), pp. 453-471.

Osland, M.J., Enwright, N., Day, R.H., Doyle, T.W. (2013). Winter climate change and coastal wetland foundation species: salt marshes vs. mangrove forests in the southeastern United States. *Global Change Biology,* 19, pp. 1492-1494.

Owers, C., Rogers, K., Mazumder, D., & Woodroffe, C.D. (2016). Spatial variation in carbon storage: a case study for Currambene Creek, NSW, Australia. *Journal of Coastal Research,* 75, pp. 1297-1301.

Pacific Wetlands Environmental Consultants (2012). Tweed River Estuary – Estuarine Vegetation Monitoring Program - Final Report, December 2012.

Patterson, C.S., & Mendelssohn, I.A. (1991). A comparsion of physicochemical variables across plant zones in a mangal/salt marsh community in Louisiana. *Wetlands,* 11, pp. 139-161.

Patterson, D., Boswood, P. & Elias, G. (2012). Tweed River Sand Bypassing Long Term average sand transport rate. 20th NSW Coastal Conference, Tweed Heads, November 2012.

Payne, M., Chenhall, B.E., Murrie, M., Jones, B.G. (1997). Spatial variation of sediment-bound zinc, lead, copper and rubidium in Lake Illawarra, a coastal lagoon in eastern Australia. *Journal of Coastal Research,* 13, pp. 1181-1191.

Pendleton, L., Donato, D.C., Murray, B.C., Crooks, S., Jenkins, W.A., Sifleet, S., Craft, C., Fourqurean, J.W., Kauffman, J.B., Marba, N., Megonigal, P., Pidgeon, E., Herr, D., Gordon, D., Baldera, A., Thrush, S. (2012). Estimating global 'blue carbon' emissions from conversion and degradation of vegetated coastal ecosystems. *PLoS ONE,* 7(9), pp. 1-7.

Pethick, J.S. (1992). Saltmarsh geomorphology. In: Allen, J.R.L., Pye, K., (Eds). Saltmarshes, Morphodynamics, Conservation and Engineering Significance. Cambridge University Press, Cambridge, pp. 41-62.

Petrokofsky, G., Kanamaru, H., Achard, F., Goetz, S.J., Joosten, H., Holmgren, P., Lehtonen, A., Menton, M.C.S., Pullin, A.S., Wattenbach, M. (2012). Comparsion of methods for measuring and assessing carbon stocks and carbon stock changes in terrestrial carbon pools. How do the accuracy and precision of current methods compare? A systematic review protocol. *Enviornmental Evidence,* 1(1), pp. 1-21.

Phan L.K., van Thiel de Vries ,J.S.M., Stive, M.J.F. (2015). Coastal mangrove squeeze in the Mekong Delta. *Journal of Coastal Resources,* 31, pp. 233-43.

Pidgeon, E. (2009). Carbon sequestration by coastal marine habitats: important missing sinks. In: Laffoley, DdA., Grimsditch D. (eds). The Management of Natural Coastal Carbon Sinks, Gland, Switzerland, IUCN, pp. 47-51.

Pigati, J.S., Rech, J.A., Nekola, J.C. (2010). Radiocarbon dating of small terrestrial gastropod shells in North America. *Quaternary Geochronology,* 5, pp. 519-532.

Pressey, R.L., Griffith, S.J. (1987). *Coastal Wetlands And Associated Communities in Tweed Shire, Northern NSW.* NSW National Parks and Wildlife Service.

Proudfoot, M., Singh Peterson, L. (2011). Positive SOI, negative PDO and spring tides as simple indicators of the potential for extreme coastal erosion in northern NSW. *Australasian Journal of Environmental Management,* 18(3), pp. 170-181.

Ray, R., Ganguly, D., Chowdhury, C., Dey, M., Das, S., Dutta, M.K., Mandel, S.K., Majumder, N., De, T.K., Mukhopadhyay, S.K., Jana, T.K. (2011). Carbon sequestration and annual increase of carbon stock in a mangrove rainforest. *Atmospheric environment,* 45(28), pp. 5016-5024.

Robbins, J.A., & Edgington, D.N,. (1975). Determination of recent sedimentation rates in Lake Michigan using 210Pb and 137Cs. *Geochimica et Cosmochimica Acta,* 39(5), pp. 285-304.

Rogers, K., Saintilan N., *et al.* (2003). Tweed River Estuary: Estuarine Vegetation Monitoring Program p.a.n.r NSW Department of Infrastructure and W.E.P. Agency.

Rogers, K. (2004). Mangrove and saltmarsh surface elevation dynamics in relation to environmental variables in south-eastern Australia. PhD thesis. University of Wollongong.

Rogers, K., Saintilan, N., & Heijnis, H. (2005). Mangrove encroachment of salt marsh in Western Port Bay, Victoria: the role of sedimentation, subsidence and sea level rise. *Estuaries,* 28(4), pp. 551-559.

Rogers, K., Wilton, K.M., Saintilan, N. (2006). Vegetation change and surface elevation dynamics in estuarine wetlands of south-east Australia. *Estuarine, Coastal and Shelf Science,* 66(3-4), pp. 559-569.

Rogers, K., & Saintilan, N. (2008). Relationships between surface elevation and groundwater in mangrove forests of southeast Australia. *Journal of Coastal Research,* 24(1A), pp. 63-69.

Rogers, K., Saintilan, N., Woodroffe, C.D. (2014). Surface elevation change and vegetation distribution dynamics in a subtropical coastal wetland: implications for coastal wetland response to climate change.

Roman, C.T., Peck, J.T., Allen, J.R., King, J.W., Appleby, P.G. (1997). Accretion of a New England (U.S.A.) saltmarsh in response to inlet migration, storms and sea-level rise. *Estuarine, Coastal and Shelf Science,* 45, pp. 717-727.

Ross, P., Minchinton, T., Ponder, W. (2009). The ecology of molluscs in Australian saltmarshes, in: Saintilan, N. (ed.) Australian Saltmarsh Ecology. CSIRO, Melbourne.

Roy, P.S., Williams, R.J., Jones, A.R., Yassini, I., Gibbs, P.J., Coates, B.P., West, R.J., Scanes, P.R., Hudson, J.P., and Nichol, S. (2001). Structure and function of south-east Australian estuaries. *Estuarine, Coastal and Shelf Science,* 53, pp. 351-384.

Saintilan, N. (1998). Photogrammetric survey of the Tweed River wetlands. *Wetlands,* 17(2), pp. 74-82.

Saintilan, N., & Hashimoto, T.R. (1999). Mangrove-saltmarsh dynamics on a bay-head delta in the Hawkesbury River estuary, New South Wales, Australia. *Hydrobiologia,* 413, pp. 95-102.

Saintilan, N., & Williams, R.J. (1999). Mangrove transgression into saltmarsh environments in south-east Australia. *Global Ecology and Biogeography,* 8, pp. 117-124.

Saintilan, N., & Williams, R.J. (2000) Short note: the decline of saltmarsh in southeast Australia: results of recent surveys. *Wetlands (Australia)* 18(2), pp. 49-54.

Saintilan, N., & Mazumder, D. (2010). Fine-scale variability in the dietary sources of grazing invertebrates in a temperate Australian saltmarsh. *Marine and Freshwater Research,* 61, pp. 615-620.

Saintilan, N., Rogers, K., Mazumder, D., Woodroffe, C. (2013). Allochthonous and autochthonous contributions to carbon accumulation and carbon store in southeastern Australian coastal wetlands. *Estuarine, Coastal and Shelf science,* 128, pp.84-92.

Saintilan, N., & Rogers, K. (2013). The significance and vulnerability of Australian saltmarshes: implications for management in a changing climate. *Marine and Freshwater Research,* 64, pp. 66-79.

Saintilan, N., & Rogers, K. (2015). Woody plant encroachment of grasslands: a comparison of terrestrial and wetland settings. *New Phytologist,* 205(3), pp. 1062-1070.

Sanders,C.J., Smoak, J.M., Sathy Naidu, A., Sanders, L.M., Patchineelam, S.R. (2010). Organic carbon burial in a mangrove forest, margin and intertidal mud flat. *Estuarine, Coastal and Shelf Science,* 90, pp. 168-172.

Sanders, C.J., Smoak, J.M., Waters, M.N., Sanders, L.M., Brandini, N., Patchineelam, S.R. (2012). Organic matter content and particle size modifications in mangrove sediments as responses to sea level rise. *Marine Environmental Research,* 77, pp. 150-155.

Sedjo, R., & Sohngen, B. (2012). Carbon sequestration in forests and soils. *Annual Review of Resource Economics,* 4(1), pp. 127-144.

Sharp, Z. (2007). Priniciples of stable isotope geochemistry. Pearson Education, Sydney. ISBN 9780130091390.

Silliman, B.R., Bertness, M.D., Edwin, D., Grosholz, E.D. (Eds). (2009). Human impacts on salt marshes, a Global Perspective. Uniersity of California Press, Berkeley, 329 pp.

Sloss, C.R., Murray-Wallace, C.V., Jones, B.G. (2006). Aminostratigrahy of two Holocene wave-dominated barrier estuaries in southeastern Australia.

Sloss, C.R., Murray-Wallace, C.V., & Jones, B.G. (2007). Holocene sea-level change on the southeast coast of Australia: a review. *The Holocene,* 17(7), pp. 999-1014.

Smoak, J.M., Breithaupt, J.L., Smith, T.J., III, Sanders, C.J. (2013). Sediment accretion and organic carbon burial relative to sea-level rise and storm events in two mangrove forests in Everglades National Park. *CATENA,* 104, pp. 58-66.

Soares, M.L.G. (2009). A conceptual model for the responses of mangrove forests to sea level rise. *Journal of Coastal Research*, SI 56, pp. 267-271.

Spencer, J., Monamy, V., Breitfuss, M. (2009). Saltmarsh as habitat for birds and other vertebrates, in: Saintilan, N. (ed.) Australian Saltmarsh Ecology. CSIRO, Melbourne.

Staddon, P.L. (2004). Carbon isotopes in functional soil ecology. *Trends in Ecology and Evolution,* 19(3), pp. 148-154.,

Stern, H., de Hoedt, G., Ernst, J. (2000). Objective classification of Australian climates. *Australian Meterological Magazine,* 49, pp. 87-96.

Sternberg, R.W. Cacchione, D.A., Drake, D.E., Kranck, K. (1986). Suspended sediment transport in an estuarine tidal channel within San Fransisco Bay, California. *Marine Geology,* 71(3-4), pp. 237-258.

Stevenson, J.C., Ward, L.G., Kearney, M.S. (1988). Sediment transport and trapping in marsh systems: implications of tidal flux studies. *Marine Geology,* 80(1-2), pp. 37-59.

Still, C.J., Berry, J.A., Collatz, G.J., DeFries, R.S. (2003). Global distribution of C3 and C4 vegetation: carbon cycle implications. *Global Biogeochemical Cycles,* 17(1), pp. 1-14.

Stumpf, R.P. (1983). The process of sedimentation on the surface of a salt marsh. *Estuarine, Coastal and Shelf Science,* 17, pp. 495-598.

Sun, L., Liu, W., Liu, G., Chen, T., Wu, X., Zhang, W., Wu, X., Zhang, G., Zhang, Y., Li, L., Zhang, B., Zhang, B., Wang, B., Yang, R. (2016). Temporal and spatial variations in the stable carbon isotope composition and carbon and nitrogen contents in current-season twigs of *Tamarix chinensis* Lour. and their relationships to environmental factors in the Laizhou Bay wetland in China. *Ecological Engineering,* 90, pp. 417-426.

Svensson, C.J., Hyndes, G.A., & Lavery, P.S. (2007). Food web analysis in two permanently open temperate estuaries: Consequences of saltmarsh loss? *Marine Environmental Research,* 64(3), pp. 286-304.

Swales, A., Bentley, S.J. Sr., Lovelock, C.E. (2015). Mangrove-forest evolution in a sediment-rich estuarine system: Opportunists or agents of geomorphic change? *Earth surface processes and landforms,* 40(12), pp. 1672-1687.

Syvitski, J.P.M., Kettner, A.J., Overeem, I., Hutton, E.W.H., Hannon, M.T., Brakenridge, G.R., Day, J., Vorosmarty, C., Saito, Y., Giosan, L., Nicholls, R.J. (2009). Sinking deltas due to human activities. *Nature Geoscience,* 2, pp. 681-686.

Tanner, B.R., Uhle, M.E., Kelley, J.T., Mora, C.I. (2007). C3/C4 variations in salt-marsh sediments: An application of compound specific isotopic analysis of lipid biomarkers to late Holocene paleoenvironmental research. *Organic Geochemistry,* 38(3), pp. 474-484.

Temmerman, S., Govers, G., Wartel, S., Meire, P. (2003). Spatial and temporal factors controlling short-term sedimentation in a salt and freshwater tidal marsh, Scheldt estuary, Belgium, SW Netherlands. *Earth Surface Processes and Landforms,* 28(7), pp. 739-755.

Temmerman, S., Govers, G., Wartel, S., Meire, P. (2004). Modelling estuarine variations in tidal marsh sedimentation: response to changing sea level and suspended sediment concentrations. *Marine Geology,* 212(1-4), pp. 1-19.

Tereshin, A.G, Klimenko, A.V., Klimenko, V.V. (2015). Golden age of gas and its impact on world energy, the global carbon cycle and climate. *Thermal engineering,* 62(5), 311-321.

Trimble (2014). Trimble R8 GNSS System Datasheet. http://www.rizopoulos.gr/documents/TrimbleR8GNSS_DS.pdf. Accessed 17/08/2016.

Tweed River Sand Bypassing Project (2014) – Project Background. http://www.tweedsandbypass.nsw.gov.au/why-tweed-sand-bypassing/project-background. Accessed 11/04/2016.

Valiela, I., Bowen, J.K., York, J.K. (2001). Mangrove forests - one of the world's threatened major tropical environments. *Bioscience,* 51, pp. 807-815.

Van Santen, P., Augustinus, P.G.E.F., Janssen-Stelder, B.M., Quartel, S., Tri, N.H. (2007). Sedimentation in an estuarine mangrove system. *Journal of Asian Earth Sciences,* 29(4), pp. 566-575.

van Wijnen, H.J., & Bakker, J.P. (2001). Long-term surface elevation change in salt marshes: a prediction of marsh response to future sea-level rise. *Estuarine, Coastal and Shelf Science,* 52(3), pp. 381-390.

Verburg, P. (2007). The need to correct for the Suess effect in the application of $\delta^{13}C$ in sediment of autotrophic Lake Tanganyika, as a productivity proxy in the Anthropocene. *Journal of Palaeolimnology,* 37(4), pp. 591-602.

Verhoeven, J.T.A. (2009). Wetland Biogeochemical Cycles and their Interactions, in: Maltby, E, & Barker, T (eds). (2009). The Wetlands Handbook, Oxford, Wiley-Blackwell.

Wang, X-C., Altabet, M.A., Callahan, J., Chen, R.F. (2004). Stable carbon and nitrogen isotopic compositions of high molecular weight dissolved organic matter from four U.S. estuaries. *Geochimica et Cosmochimica Acta.,* 68(12), pp. 2681-2691.

Wang, H., Ge, Z., Yuan, L., Zhang, L. (2014). Evaluation of the combined threat from sea-level rise and sedimentation reduction to the coastal wetlands in the Yangtze Estuary, China. *Ecological Engineering,* 71, pp. 346-354.

Wang, F., Zong, Y-Q., Li, J-F., Tian, L-Z., Shang, Z-W., Chen, Y-S., Jiang, X-Y., Yang,J-L., Yang, B., Wang, H (2016). Recent sedimentation dynamics indicated by $^{210}Pb_{exc}$ and ^{137}Cs records from the subtidal area of Bohai Bay, China. *Journal of Coastal Research,* 32(2), pp. 416-423.

Warren, R.S., Niering, W.A. (1993). Vegetation change on a north-east tidal marsh: interaction of sea-level rise and marsh accretion. *Ecology,* 74(1), pp. 96-103.

Watson, E.B., Szura, K., Wigand, C., Raposa, K.B., Blount, K., Cencer, M. (2016). Sea level rise, drought and the decline of *Spartina patens* in New England marshes. *Biological Conservation,* 196, pp. 173-181.

Webb, E.L., Friess, D.A., Krauss, K., Cahoon, D.R., Guntenspergen, G.R., Phelps, J. (2013). A global standard for monitoring coastal wetland vulnerability to accelerated sea-level rise. *Nature Climate Change,* 3, pp. 458-465.

Whitaker, K., Rogers, K., Saintilan, N., Mazumder, D., Wen, L. (2015). Vegetation persistence and carbon storage: implications for environmental water management for *Phragmites australis. Water Resources Research,* 51(7), pp. 5284-5300.

White, I., Melville, M., Macdonald, B., Quirk, R., Hawken, R., Tunks, M., Buckley, D., Beattie, R., Williams, J., Heath, L. (2007). From conflicts to wise practice agreement and national strategy: cooperative learning and coastal stewardship in estuarine floodplain management, Tweed River, eastern Australia. *Journal of Cleaner Production,* 15(16) pp. 1545-1558.

Whiting, G.J., & Chanton, J.P. (2001). Greenhouse carbon balance of wetlands: methane emissions versus carbon sequestration. *Tellus B.,* 53(5), pp. 521-528.

Williams, E.K., Rosenheim, B.E. (2015). What happens to soil organic carbon as coastal marsh ecosystems change in response to increasing salinity? An exploration using ramped pyrolysis. *Geochemistry, Geophysics, Geosystems,* 16(7), pp. 2322-2335.

Wilsey, B.J., Parent, G., Roulet, N.T., Moore, T.R., Potvin. C. (2002). Tropical pasture carbon cycling: relationships between C source/sink strength, above-ground biomass and grazing. *Ecology Letters,* 5(3), pp. 367-376.

Wilson, B., Wilson, C, & Baker, P. (1994). Australian Marine Shells. Odyssey Publishing, Leederville W.A.

Wilton, K. (2002). Coastal Wetland Habitat Dynamics in Selected New South Wales Estuaries. PhD thesis, Australian Catholic University.

Woodroffe, C.D (1990). The impact of sea-level rise on mangrove shorelines. *Progress in Physical Geography,* 14, pp. 483-520.

Woodroffe, C.D. (1992). 2. Mangrove sediments and geomorphology. In: A.I. Robertson and D.M. Alongi (eds.) Tropical Mangrove Ecosystems.

Woodroffe, C.D., Rogers, K., McKee, K.L., Lovelock, C.E., Mendelssohn, I.A., Saintilan, N. (2016). Mangrove sedimentation and response to relative sea-level rise. *Annual Review of Marine Science,* 8, 243-266.

Woolnough, S.J., Allen, J.R.L., Wood, W.L. (1995). An exploratory numerical model of sediment deposition over tidal salt marshes. *Estuarine, Coastal and Shelf Science,* 41(5), pp. 515-543.

Yang, J., Gao, J., Cheung, A., Liu, B., Schwendenmann, L., Costello, M.J. (2013). Vegetation and sediment characteristics in an expanding mangrove forest in New Zealand. *Estuarine, Coastal and Shelf Science,* 134, pp. 11-18.

Yang, J., Gao, J., Liu, B., Zhang, W. (2014). Sediment deposits and organic carbon sequestration along mangrove coasts of the Leizhou Peninsula, southern China. *Estuarine, Coastal and Shelf Science,* 136, pp. 3-10.

Yu, O.T., & Chmura, G.L. (2009). Soil carbon may be maintained under grazing in a St Lawrence Estuary tidal marsh. *Environmental Conservation,* 36(4), pp. 312-320.

Zawadzki, A. CIC and CRS ^{210}Pb dating applications. ANSTO Institute for Environmental Research, Environmental Radioactivity Measurement Centre. August 2015.

Zedler, J.B., & Kircher, S. (2005). Wetland resources: status, trends, ecosystem services and restorability. *Annual Reviews in Environmental Resources,* 30, pp. 39-74.

Zhang, Y., Ding, W., Luo, J., Donnison, A. (2010). Changes in soil organic carbon dynamics in an eastern Chinese coastal wetlands following invasion by a C_4 plant *Spartina alterniflora. Soil Biology and Biochemistry,* 42(10), pp. 1712-1720.

Zhang, J.P., Shen, C.D., Wang, J., Han, W.D. (2012). Estimating change in sedimentary organic carbon content during mangrove restoration in southern China using carbon isotopic measurements. *Pedosphere,* 22(1), pp. 58-66.

Zhao, Q., Bai, J., Liu, P., Gao, H., Wang, J. (2015). Decomposition and carbon and nitrogen dynamics of *Phragmites australis* litter as affected by flooding periods in coastal wetlands. *CLEAN: Soil, Air, Water,* 43(3), pp.441-445.

Zhou, J., Wu, J., Zhang, J., Kang, Q., Liu, Z. (2006). Carbon and nitrogen composition and stable isotope as potential indicators of source and fate of organic matter in the salt marsh of the Changjiang Estuary, China. *Chemosphere,* 65(2), pp. 310-317.

Appendix 1: Elemental analysis results

Australian Government | ansto
Nuclear-based science benefiting all Australians

Institute for Environmental Research

Stable Isotope Analysis Report

Client Details

Company Name: University of Wollongong
Address: Northfields Avenue, Wollongong
Contact Name: Campbell Young
Tel: 0413 160 805
Email: cly611@uowmail.edu.au
Purchase Order No. AINSE

Sample Details

Number: 119
Material: Sediment

Sample Tracking

LIMS Batch Number: 2016/0170J
Registration Date: 24/06/2016

Analysis Details

Isotope(s) : $\delta^{13}C$

Method(s): $\delta^{13}C$ by combustion

Report Date: 21/09/2016

Name: Jennifer van Holst

Signature: Jennifer van Holst.

Date: 21/09/2016

Australian Government | ansto Nuclear-based science benefiting all Australians

Analysis of $\delta^{13}C$ and $\delta^{15}N$

This report contains determinations of relative difference of isotope ratios, δ, of ($^{13}C/^{12}C$) and ($^{15}N/^{14}N$), elsewhere referred to as $\delta^{13}C$ and $\delta^{15}N$ respectively . The values will be reported as parts per thousand (‰ or per mil).

Samples were run using an established on-line combustion, continuous-flow IRMS method.

In brief, the crushed and dried samples are weighed into tin capsules and introduced sequentially into an elemental analyser (Thermo Fisher Flash 2000 HT EA) using an autosampler. Each sample is then combusted into CO_2 and N_2 in a combustion furnace (silvered cobaltous/ic oxide, chromium oxide, quartz chips and quartz wool) at 1020ºC before being transferred with a helium carrier gas (100 mL/min) into a reduction furnace (copper) at 600ºC, where any excess nitrous oxides are converted into N_2 and excess O_2 is removed. The analyte gases are then passed through a water trap before the CO_2 and N_2 are separated by a GC column at 40ºC. The gases are then transferred to a Thermo Fisher Conflo IV and into a Thermo Fisher Delta V Plus isotope ratio mass spectrometer for $\delta^{13}C$ and $\delta^{15}N$ measurements.

The data reported relative to IAEA secondary standards that have been certified relative to VPDB for carbon and air for nitrogen. A two point calibration is employed to normalise the data, utilising standards that bracket the samples being analysed. Two quality control references were also included in each run; see page 5 for details of the standards used.

Results are accurate to 1% for both N % and C % and +/- 0.3 permil for $\delta^{15}N$ and $\delta^{13}C$.

$$\delta^{13}C = \delta(^{13}C/^{12}C)_{P/reference} = \frac{R(^{13}C/^{12}C)_P - R(^{13}C/^{12}C)_{reference}}{R(^{13}C/^{12}C)_{reference}}$$

$$\delta^{15}N = \delta(^{15}N/^{14}N)_{P/reference} = \frac{R(^{15}N/^{14}N)_P - R(^{15}N/^{14}N)_{reference}}{R(^{15}N/^{14}N)_{reference}}$$

Reference: Ohlsson K, Wallmark P. 1999. Novel calibration with correction for drift and non-linear response for continuous flow isotope ratio mass spectrometry applied to the determination of delta N-15, total nitrogen, delta C-13 and total carbon in biological material. Analyst 124: 571–577.

AUSTRALIAN NUCLEAR SCIENCE AND TECHNOLOGY ORGANISATION
New Illawarra Road, Lucas Heights (Locked Bag 2001, Kirrawee DC NSW 2232) T +61 2 9717 3111 F +61 2 9543 5097
www.ansto.gov.au

Australian Government | ansto
Nuclear-based science benefiting all Australians

					Carbon Data		
LIMS Number	Client Identification			Sample No.	C %	$\delta^{13/12}C_{VPDB}$ ‰	Sample Comments
2016/0170J-1	T1-1	0	-2	1	1.3		SM16Aug15
2016/0170J-1	T1-1	0	-2	1 (2)	1.1	-15.7	Sm16sep08
2016/0170J-2	T1-1	5	-7	2	1.7	-15.2	SM16Aug15
2016/0170J-2	T1-1	5	-7	2 (2)	1.4	-15.1	Sm16sep08
2016/0170J-3	T1-1	10	-12	3	2.5	-19.4	SM16Aug15
2016/0170J-3	T1-1	10	-12	3 (3)	2.0	-19.5	Sm16sep08
2016/0170J-4	T1-1	15	-17	4	1.3	-16.6	SM16Aug15
2016/0170J-4	T1-1	15	-17	4 (2)	1.1	-16.4	Sm16sep08
2016/0170J-5	T1-1	20	-22	5	0.7	-17.5	SM16Aug15
2016/0170J-5	T1-1	20	-22	5 (2)	0.5	-17.7	Sm16sep08
2016/0170J-6	T1-1	25	-27	6	0.9		SM16Aug15
2016/0170J-6	T1-1	25	-27	6 (2)	0.7	-19.9	Sm16sep08
2016/0170J-7	T1-1	30	-32	7	0.3		SM16Aug15
2016/0170J-7	T1-1	30	-32	7 (2)	0.3	-19.6	Sm16sep08
2016/0170J-8	T1-1	40	-42	8	1.1	-19.0	SM16Aug15
2016/0170J-9	T1-1	50	-52	9	1.5	-18.8	SM16Aug15
2016/0170J-9	T1-1	50	-52	9 (2)	1.3	-18.5	Sm16sep08
2016/0170J-10	T1-1	60	-62	10	0.8	-22.9	SM16Aug15
2016/0170J-10	T1-1	60	-62	10 (2)	0.7	-22.8	Sm16sep08
2016/0170J-11	T1-1	70	-72	11	0.2	-23.1	SM16Jul12
2016/0170J-12	T1-1	80	-82	12	0.2	-23.8	SM16Aug15
2016/0170J-12	T1-1	80	-82	12 (2)	0.2	-23.7	Sm16sep08
2016/0170J-13	T1-1	90	-92	13	0.1		SM16Aug15
2016/0170J-13	T1-1	90	-92	13 (2)	0.1	-24.4	Sm16sep08
2016/0170J-14	T1-1	100	-102	14	1.1	-19.3	SM16Aug15
2016/0170J-14	T1-1	100	-102	14 (2)	0.9	-19.3	Sm16sep08
2016/0170J-15	T1-2	0	-2	15	1.4	-25.4	SM16Aug15
2016/0170J-15	T1-2	0	-2	15 (2)	1.2	-25.4	Sm16sep08
2016/0170J-16	T1-2	5	-7	16	1.5	-24.4	SM16Aug15
2016/0170J-16	T1-2	5	-7	16 (2)	1.2	-24.8	Sm16sep08
2016/0170J-17	T1-2	10	-12	17	0.6	-22.7	SM16Jul12
2016/0170J-18	T1-2	15	-17	18	1.0	-21.4	SM16Aug15
2016/0170J-18	T1-2	15	-17	18 (2)	0.8	-21.4	Sm16sep08
2016/0170J-19	T1-2	20	-22	19	3.1		SM16Aug15
2016/0170J-19	T1-2	20	-22	19 (2)	2.2	-23.8	Sm16sep08
2016/0170J-20	T1-2	25	-27	20	1.5	-22.6	SM16Aug15
2016/0170J-20	T1-2	25	-27	20 (2)	1.2	-22.1	Sm16sep08
2016/0170J-21	T1-2	30	-32	21	0.7	-22.2	SM16Aug15
2016/0170J-21	T1-2	30	-32	21 (2)	0.8	-22.0	Sm16sep08
2016/0170J-22	T1-2	40	-42	22	1.6	-23.9	SM16Aug15
2016/0170J-22	T1-2	40	-42	22 (2)	1.7	-23.9	Sm16sep08
2016/0170J-23	T1-2	50	-52	23	1.6	-24.6	SM16Aug15
2016/0170J-23	T1-2	50	-52	23 (2)	1.6	-25.0	Sm16sep08
2016/0170J-24	T1-2	60	-62	24	0.5	-24.3	SM16Aug15
2016/0170J-24	T1-2	60	-62	24 (2)	0.5	-24.2	Sm16sep08
2016/0170J-25	T1-2	70	-72	25	0.6	-23.1	SM16Aug15
2016/0170J-25	T1-2	70	-72	25 (2)	0.6	-23.2	Sm16sep08
2016/0170J-26	T1-2	80	-82	26	0.4	-23.2	SM16Jul12
2016/0170J-27	T1-2	90	-92	27	0.2	-23.5	SM16Aug15
2016/0170J-27	T1-2	90	-92	27 (2)	0.3	-23.5	Sm16sep08
2016/0170J-28	T1-2	100	-102	28	0.1	-24.5	SM16Aug15
2016/0170J-29	T1-3	0	-2	29	10.4	-26.9	SM16SEP19
2016/0170J-30	T1-3	5	-7	30	12.3	-26.0	SM16SEP19
2016/0170J-31	T1-3	10	-12	31	9.3	-26.0	SM16SEP19
2016/0170J-32	T1-3	15	-17	32	8.8	-26.1	SM16SEP19
2016/0170J-33	T1-3	20	-22	33	4.4	-25.7	SM16SEP19
2016/0170J-34	T1-3	25	-27	34	6.5	-25.2	SM16SEP19
2016/0170J-35	T1-3	30	-32	35	1.5	-23.6	SM16Aug15
2016/0170J-35	T1-3	30	-32	35 (2)	1.6	-23.8	SM16SEP19
2016/0170J-36	T1-3	40	-42	36	0.4	-24.5	SM16Aug15
2016/0170J-36	T1-3	40	-42	36 (2)	0.5	-24.3	SM16SEP19
2016/0170J-37	T1-3	50	-52	37	0.5	-23.4	SM16Aug15
2016/0170J-37	T1-3	50	-52	37 (2)	0.6	-23.4	SM16SEP19
2016/0170J-38	T1-3	60	-62	38	0.4	-23.2	SM16Jul12
2016/0170J-39	T1-3	70	-72	39	0.4	-24.4	SM16Aug15
2016/0170J-39	T1-3	70	-72	39 (2)	0.4	-24.2	SM16SEP19
2016/0170J-40	T1-3	80	-82	40	0.3	-24.0	SM16Aug15
2016/0170J-40	T1-3	80	-82	40 (2)	0.3	-24.0	SM16SEP19

Australian Government | ansto
Nuclear-based science benefiting all Australians

					Carbon Data		
LIMS Number	Client Identification			Sample No.	C %	$\delta^{13/12}C_{V-PDB}$ ‰	Sample Comments
2016/0170J-41	T2-1	0	-2	41	0.9	-15.5	SM16Aug15
2016/0170J-41	T2-1	0	-2	41 (2)	1.0	-15.7	SM16SEP19
2016/0170J-42	T2-1	5	-7	42	0.9	-14.8	SM16Aug15
2016/0170J-42	T2-1	5	-7	42 (2)	1.1	-14.8	SM16SEP19
2016/0170J-43	T2-1	10	-12	43	1.3	-15.6	SM16Aug15
2016/0170J-43	T2-1	10	-12	43 (2)	1.2	-16.0	SM16SEP19
2016/0170J-44	T2-1	15	-17	44	0.6	-16.8	SM16Aug15
2016/0170J-44	T2-1	15	-17	44 (2)	0.9	-17.0	SM16SEP19
2016/0170J-45	T2-1	20	-22	45	0.5	-18.8	SM16Aug16
2016/0170J-46	T2-1	25	-27	46	0.7	-19.2	SM16Aug16
2016/0170J-47	T2-1	30	-32	47	0.4	-21.8	SM16Aug16
2016/0170J-48	T2-1	40	-42	48	1.6	-23.2	SM16Aug16
2016/0170J-48	T2-1	40	-42	48 (2)	1.5	-23.3	SM16SEP19
2016/0170J-49	T2-1	50	-52	49	1.1	-25.4	SM16Aug16
2016/0170J-50	T2-1	60	-62	50	0.3	-24.3	SM16Aug16
2016/0170J-51	T2-1	70	-72	51	0.2	-24.8	SM16Aug16
2016/0170J-52	T2-1	80	-82	52	0.1	-24.8	SM16Aug15
2016/0170J-52	T2-1	80	-82	52 (2)	0.1	-24.8	SM16SEP19
2016/0170J-53	T2-1	90	-92	53	0.2	-23.8	SM16Aug16
2016/0170J-54	T2-1	100	-102	54	0.2	-24.0	SM16Aug16
2016/0170J-55	T2-2	0	-2	55	0.7	-18.2	SM16Aug16
2016/0170J-56	T2-2	5	-7	56	0.7	-16.3	SM16Aug16
2016/0170J-57	T2-2	10	-12	57	0.9	-16.7	SM16Jul12
2016/0170J-58	T2-2	15	-17	58	0.5	-19.6	SM16Aug16
2016/0170J-59	T2-2	20	-22	59	0.5	-22.1	SM16Aug16
2016/0170J-60	T2-2	25	-27	60	0.7	-19.3	SM16Aug16
2016/0170J-61	T2-2	30	-32	61	0.8	-24.7	SM16Aug16
2016/0170J-62	T2-2	40	-42	62	1.4	-23.6	SM16Aug16
2016/0170J-63	T2-2	50	-52	63	4.8		SM16Aug16
2016/0170J-63	T2-2	50	-52	63 (2)	5.1	-25.5	SM16SEP19
2016/0170J-64	T2-2	60	-62	64	1.3	-23.5	SM16Aug16
2016/0170J-65	T2-2	70	-72	65	0.3	-25.4	SM16Aug16
2016/0170J-66	T2-2	80	-82	66	0.2	-25.2	SM16Jul12
2016/0170J-67	T2-2	90	-92	67	0.2	-24.6	SM16Aug16
2016/0170J-68	T2-2	100	-102	68	0.1	-24.9	SM16Aug16
2016/0170J-69	T2-3	0	-2	69	0.5	-23.1	SM16Aug16
2016/0170J-70	T2-3	5	-7	70	0.8	-22.9	SM16Aug16
2016/0170J-71	T2-3	10	-12	71	0.6	-21.7	SM16Jul12
2016/0170J-72	T2-3	15	-17	72	0.9	-19.7	SM16Aug16
2016/0170J-73	T2-3	20	-22	73	1.4	-24.2	SM16Aug16
2016/0170J-74	T2-3	25	-27	74	0.5	-22.8	SM16Aug16
2016/0170J-75	T2-3	30	-32	75	0.9	-22.9	SM16Aug16
2016/0170J-76	T2-3	40	-42	76	2.0	-23.6	SM16SEP19
2016/0170J-77	T2-3	50	-52	77	2.8	-24.4	SM16SEP19
2016/0170J-78	T2-3	60	-62	78	1.7	-25.4	SM16SEP19
2016/0170J-79	T2-3	70	-72	79	0.6	-25.7	SM16Aug16
2016/0170J-80	T2-3	80	-82	80	1.7	-26.5	SM16SEP19
2016/0170J-81	T2-3	90	-92	81	0.3	-24.6	SM16Aug16
2016/0170J-82	T2-3	100	-102	82	0.3	-24.4	SM16Aug16
2016/0170J-83	T2-3	110	-112	83 (2)	0.3	-25.1	SM16SEP19 small sample size - Use

Australian Government | ansto Nuclear-based science benefiting all Australians

LIMS Number	Client Identification			Sample No.	Carbon Data		Sample Comments
					C %	$\delta^{13/12}C_{VPDB}$ ‰	
2016/0170J-84	T2-4	0	-2	84	6.6	-26.2	SM16SEP19
2016/0170J-85	T2-4	5	-7	85	7.0	-26.1	SM16SEP19
2016/0170J-86	T2-4	10	-12	86	5.0	-26.0	SM16SEP19
2016/0170J-87	T2-4	15	-17	87	6.7	-26.0	SM16SEP19
2016/0170J-88	T2-4	20	-22	88	9.1	-25.8	SM16SEP19
2016/0170J-89	T2-4	25	-27	89	2.3	-30.4	SM16Aug16
2016/0170J-90	T2-4	30	-32	90	0.6	-26.5	JvH16Aug22
2016/0170J-91	T2-4	40	-42	91	0.3	-24.3	JvH16Aug22
2016/0170J-91	T2-4	40	-42	91 (2)	0.3	-24.4	SM16SEP19
2016/0170J-92	T2-4	50	-52	92	0.4	-23.6	JvH16Aug22
2016/0170J-92	T2-4	50	-52	92 (2)	0.4	-23.8	SM16SEP19
2016/0170J-93	T2-4	60	-62	93	0.2	-23.6	JvH16Aug22
2016/0170J-93	T2-4	60	-62	93 (2)	0.2	-23.8	SM16SEP19
2016/0170J-94	T2-4	70	-72	94	0.2	-24.2	JvH16Aug22
2016/0170J-94	T2-4	70	-72	94 (2)	0.2	-24.2	SM16SEP19
2016/0170J-95	T2-4	80	-82	95	0.2	-24.1	SM16Jul12
2016/0170J-96	SM A	0	-2	96	1.4	-14.7	JvH16Aug22
2016/0170J-96	SM A	0	-2	96 (2)	1.4	-15.0	SM16SEP19
2016/0170J-97	SM A	5	-7	97	1.4		JvH16Aug22
2016/0170J-97	SM A	5	-7	97 (2)	1.4	-15.3	SM16SEP19
2016/0170J-98	SM A	10	-12	98	0.9	-15.5	SM16Jul12
2016/0170J-99	SM A	15	-17	99	0.7	-16.4	JvH16Aug22
2016/0170J-99	SM A	15	-17	99 (2)	0.7	-16.7	SM16SEP19
2016/0170J-100	SM A	20	-22	100	1.4	-16.7	JvH16Aug22
2016/0170J-100	SM A	20	-22	100 (2)	1.3	-17.0	SM16SEP19
2016/0170J-101	SM A	25	-27	101	0.6		JvH16Aug22
2016/0170J-101	SM A	25	-27	101 (2)	0.5	-17.2	SM16SEP19
2016/0170J-102	SM A	30	-32	102	0.3		JvH16Aug22
2016/0170J-102	SM A	30	-32	102 (2)	0.4	-18.2	SM16SEP19
2016/0170J-103	SM A	40	-42	103	0.8		JvH16Aug22
2016/0170J-103	SM A	40	-42	103 (2)	0.6	-21.5	SM16SEP19
2016/0170J-104	SM A	50	-52	104	0.6		JvH16Aug22
2016/0170J-104	SM A	50	-52	104 (2)	0.7	-21.3	SM16SEP19
2016/0170J-105	SM A	60	-62	105	0.1	-22.9	JvH16Aug22
2016/0170J-105	SM A	60	-62	105 (2)	0.1	-23.2	SM16SEP19
2016/0170J-106	SM A	70	-72	106	0.1		JvH16Aug22
2016/0170J-106	SM A	70	-72	106 (2)	0.1	-22.8	SM16SEP19
2016/0170J-107	SM A	80	-82	107	0.2	-23.0	SM16Jul12
2016/0170J-108	SM A	90	-92	108	0.3		JvH16Aug22
2016/0170J-108	SM A	90	-92	108 (2)	0.4	-27.3	SM16SEP19
2016/0170J-109	MAN B	0	-2	109	5.4		JvH16Aug22
2016/0170J-109	MAN B	0	-2	109 (2)	5.6	-26.2	SM16SEP19
2016/0170J-110	MAN B	5	-7	110	6.6	-25.7	JvH16Aug22
2016/0170J-110	MAN B	5	-7	110 (2)	6.1	-26.0	SM16SEP19
2016/0170J-111	MAN B	10	-12	111	5.5		JvH16Aug22
2016/0170J-111	MAN B	10	-12	111 (2)	5.5	-25.6	SM16SEP19
2016/0170J-112	MAN B	15	-17	112	4.3	-25.3	JvH16Aug22
2016/0170J-112	MAN B	15	-17	112 (2)	3.8	-25.6	SM16SEP19
2016/0170J-113	MAN B	20	-22	113 (2)	2.0	-25.3	SM16SEP19
2016/0170J-114	MAN B	25	-27	114 (2)	1.4	-25.2	SM16SEP19
2016/0170J-115	MAN B	30	-32	115	1.4		JvH16Aug22
2016/0170J-115	MAN B	30	-32	115 (2)	1.4	-25.3	SM16SEP19
2016/0170J-116	MAN B	40	-42	116	0.6		JvH16Aug22
2016/0170J-116	MAN B	40	-42	116 (2)	0.6	-24.7	SM16SEP19
2016/0170J-117	MAN B	50	-52	117	0.5		JvH16Aug22
2016/0170J-113	MAN B	20	-22	113	1.7	-24.6	JvH16Aug22
2016/0170J-118	MAN B	60	-62	118	0.3		JvH16Aug22
2016/0170J-118	MAN B	60	-62	118 (2)	0.3	-24.0	SM16SEP19
2016/0170J-119	MAN B	70	-72	119	0.3	-24.9	SM16Jul12

Australian Government | ansto Nuclear-based science benefiting all Australians

QC CHECKS

RUN NO.	ID	C%	$\delta^{13/12}C_{V\text{-}PDB}$‰
CERTIFIED VALUES for QC1	**SC0419**	**40.3 ± 0.3**	**-30.3 ± 0.1**
		n=4	n=5
SM16Jul12	SC0419	40.8	-30.4
			n=3
SM16Aug15	SC0419		-30.4
			n=2
SM16Aug16	SC0419		-30.6
		n=4	n=4
JvH16Aug22	SC0419	40.1	-30.0
		n=2	n=4
Sm16sep08	SC0419	40.7	-30.1
AVERAGE		**40.5**	**-29.4**
S.D.		**0.4**	**2.2**
Diff from Actual		**0.2**	**0.9**

CERTIFIED VALUES for QC1	**SC0419***	**40.4 ± 0.2**	**-26.9 ± 0.1**
		n=2	n=4
Sm16sep19	SC0419	40.5	-27.0
*new std batch B/N 265504			
AVERAGE		**40.5**	**-27.0**
S.D.			
Diff from Actual		**0.1**	**-0.1**

QC CHECKS

RUN NO.	ID	C%	$\delta^{13/12}C_{V\text{-}PDB}$‰
CERTIFIED VALUES for QC2	**USGS 40**	**40.9 ± 0.5**	**-26.4 ± 0.04**
		n=3	
SM16Jul12	USGS 40	40.7	
			n=1
SM16Aug15	USGS 40		-26.4
		n=1	
SM16Aug16	USGS 40	40.3	
		n=2	
JvH16Aug22	USGS 40	40.9	
		n=4	n=1
Sm16sep08	USGS 40	41.7	-26.4
		n=3	n=1
Sm16sep19	USGS 40	40.5	-26.4
AVERAGE		**40.8**	**-26.4**
S.D.		**0.5**	**0.0**
Diff from Actual		**-0.1**	**0.0**

QC CHECKS

RUN NO.	ID	C%	$\delta^{13/12}C_{V\text{-}PDB}$‰
CERTIFIED VALUES for QC3	USGS 41	42 ± 0.6	37.6 ± 0.05
		n=4	
SM16Jul12	USGS 41	42.3	
		n=4	
JvH16Aug22	USGS 41	41.7	
			n=1
Sm16sep08	USGS 41		38.4
		n=4	n=1
Sm16sep19	USGS 41	41.9	37.6
AVERAGE		42.0	38.0
S.D.		0.3	0.5
Diff from Actual		0.0	0.4

QC CHECKS

RUN NO.	ID	C%	$\delta^{13/12}C_{V\text{-}PDB}$‰
CERTIFIED VALUES for QC4	B2151	9.15 ± 0.12	-26.27 ± 0.15
		n=3	n=3
SM16Jul12	B2151	9.3	-26.9
		n=1	n=2
SM16Aug15	B2151	9.3	-26.8
		n=3	n=3
SM16Aug16	B2151	9.0	-26.6
		n=3	n=3
Sm16sep08	B2151	9.3	-26.4
		n=3	n=3
Sm16sep19	B2151	9.0	-26.6
AVERAGE		9.2	-26.6
S.D.		0.2	0.2
Diff from Actual		0.0	-0.4

QC CHECKS

RUN NO.	ID	C%	$\delta^{13/12}C_{V\text{-}PDB}$‰
CERTIFIED VALUES for QC5	B2153	1.52 ± 0.02	-27.46 ± 0.11
		n=3	n=3
SM16Jul12	B2153	1.5	-28.0
		n=3	n=3
SM16Aug15	B2153	1.8	-27.4
		n=3	n=2
SM16Aug16	B2153	1.7	-27.8
		n=1	
Sm16sep08	B2153	1.7	
		n=3	n=2
Sm16sep19	B2153	1.7	-27.8
AVERAGE		1.7	-27.7
S.D.		0.1	0.2
Diff from Actual		0.2	-0.3

Appendix 2: ^{210}Pb and ^{137}Cs analysis results

a) Mangrove core

Client Name:	Campbell Young
Client Institution:	UoW
Project Title:	2016rc0051a
Core Description:	Ukerebagh Island Tweed Heads (Mangrove)

CIC model
Mass Accumulation Rate 0.162 ± 0.034 g/cm2/y
r2 = 0.8522

ANSTO ID	Uncorrected Depth (cm)	Dry Bulk Density (g/cm^3)	Cumulative Dry Mass (g/cm^2)	Count Date	Total ^{210}Pb (Bq/kg)	Supported ^{210}Pb (Bq/kg)	Unsupported ^{210}Pb Decay corrected to 26-Apr-16 (Bq/kg)	Calculated CIC Ages (years)	Calculated CRS Ages (years)	CRS model Mass Accumulation Rates (g/cm^2/year)
S373	0 - 1	0.27	0.2 ± 0.2	28-Apr-16	134 ± 6	3.1 ± 0.3	131 ± 6	0.81 ± 1	0.7363 ± 0.8581	0.206 ± 0.011
S374	2 - 3	0.36	0.9 ± 0.2	28-Apr-16	114 ± 5	4.3 ± 0.5	110 ± 5	4.68 ± 1	4.1275 ± 2.0316	0.221 ± 0.011
S375	7 - 8	0.34	2.5 ± 0.2	28-Apr-16	119 ± 5	3.0 ± 0.3	116 ± 5	13.27 ± 3	12.6282 ± 3.5536	0.161 ± 0.009
S608	9 - 10	0.36	3.3 ± 0.2	27-Jul-16	100 ± 4	3.7 ± 0.4	97 ± 4	17.56 ± 4	17.5409 ± 4.1882	0.166 ± 0.009
S609	12 - 13	0.99	4.8 ± 0.2	27-Jul-16	80 ± 3	3.8 ± 0.4	77 ± 4	25.88 ± 6	27.2312 ± 5.2184	0.154 ± 0.009
S376	14 - 15	0.65	6.7 ± 0.3	28-Apr-16	42 ± 2	2.9 ± 0.4	39 ± 2	35.99 ± 8	37.6232 ± 6.1338	0.221 ± 0.013
S377	23 - 24	0.85	13.6 ± 0.3	28-Apr-16	33 ± 2	3.8 ± 0.4	30 ± 2			
S378	32 - 34	0.60	20.3 ± 0.4	28-Apr-16	40 ± 2	2.6 ± 0.4	38 ± 2			
S610	40 - 42	0.81	26.0 ± 0.4	27-Jul-16	53 ± 2	3.9 ± 0.4	50 ± 2			
S611	50 - 51	0.87	33.8 ± 0.4	27-Jul-16	29 ± 2	5.2 ± 0.5	24 ± 2			

Extra samples were analysed from the Ukerebagh Mangrove core (see Table above in red fonts)
Unsupported 210Pb activities in this core are decreasing with depth between 0 and 13 cm depth.
Below 13 cm the activities fluctate between 24 and 50 Bq/kg. At 43 cm the activity is still relatively high.
Using unsupported 210Pb data in the top 13 cm depth only the CIC and CRS ages were calculated (see Table above).
The calculated ages are in close agreements.

There are 2 reasons why unsupported 210Pb activity is still high (>10 Bq/kg) at the bottom of the core:

1 The digestion method we use has not completely extracted 226Ra (supported 210Pb) from the sample matrix.
Thus we are underestimating the activity of supported 210Pb.

2 Unsupported 210Pb has not reached background at 43 cm thus extra samples need to be analysed below 43 cm depth.

Before we process extra samples below 44 cm, we can check the 226Ra activities using gamma spectrometry which does not require sample digestion.
Also at the same time we can analyse for 137Cs.

I suggest we analyse samples from the following depths for 226Ra (at 186 kev) and 137Cs (at 661 keV) by gamma spectrometry:

5 - 6 cm
10 - 11 cm
15 - 16 cm
20 - 21 cm

Samples were sieved and dried by Campbell Young.
Dried and sieved samples were processed for alpha spectrometry analysis by Campbell and Brodie Cutmore.
Data entries checked by Daniela Fierro.
Report prepared by Atun Zawadzki 9 August 2016

Gamma spectrometry analysis results:

	Depth (cm)	226Ra (186 keV) Bq/kg	±	137Cs (661 keV) Bq/kg	±
S716	4.0 - 5.0	38.0	7.8	6.8	1.3
S717	14.0 - 15.0	67.6	5.6	4.9	0.8
S718	18.0 - 19.0	16.6	13.4	8.5	1.9

226Ra (supported 210Pb) results from gamma spectrometry analysis are much higher than from alpha spectrometry (see columns shaded in blue)
These indicate that the sample digestion for alpha spectrometry analyses had not extracted all of the 226Ra in the sample matrix.
Therefore, if supported 210Pb is about 40 Bq/kg, as estimated from gamma spectrometry for sample S716 (see dotted line on Figure 3), this core is only able to be dated down to 12 cm.
Below 12 cm total 210Pb is almost equal to supported 210Pb, thus negligible unsupported 210Pb activities.

137Cs activities were detected down to 19 cm. However we cannot use these data to validate the 210Pb chronology without analysing extra samples.

Gamma spectrometry analysis was performed by Daniela Fierro
Report prepared by Atun Zawadzki 19 August 2016

Figure 1

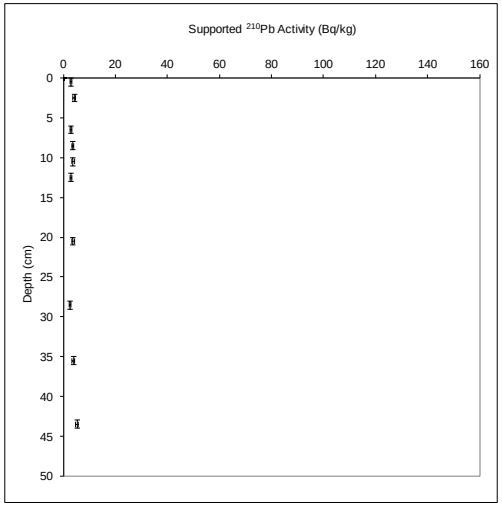

Figure 2

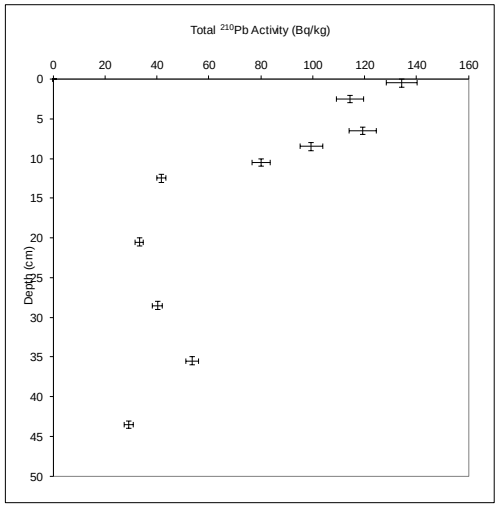

Figure 3

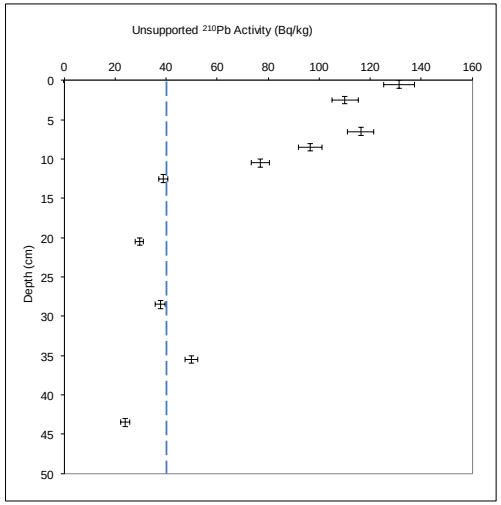

Figure 4

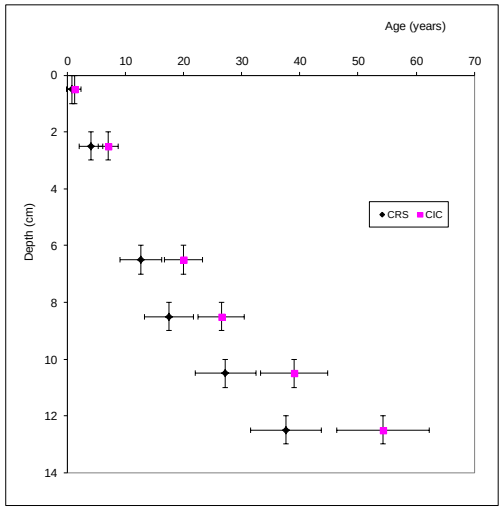

b) Saltmarsh core

Client Name:	Campbell Young
Client Institution:	UoW
Project Title:	2016rc0052a
Core Description:	Ukerebagh Island Tweed Heads (SM)

CIC model
Mass Accumulation Rate 0.062 ± 0.008 g/cm2/y
r2 = 0.9512

Table 1

ANSTO ID	ncorrected Dep (cm)	Dry Bulk Density (g/cm^3)	Cumulative Dry Mass (g/cm^2)	Count Date	Total ^{210}Pb (Bq/kg)	Supported ^{210}Pb (Bq/kg)	Unsupported ^{210}Pb Decay corrected to 26-Apr-16 (Bq/kg)	Calculated CIC Ages (years)	Calculated CRS Ages (years)	CRS model Mass Accumulation Rates (g/cm^2/year)
S379	0 - 1	0.49	0.3 ± 0.3	28-Apr-16	140 ± 7	3 ± 0	137 ± 7	5 ± 5	3.726 ± 1.930	0.079 ± 0.004
S380	3 - 4	0.44	1.5 ± 0.3	28-Apr-16	82 ± 3	4 ± 0	79 ± 3	24 ± 6	17.888 ± 4.229	0.088 ± 0.006
S381	6 - 8	0.52	3.3 ± 0.3	28-Apr-16	64 ± 3	2 ± 0	63 ± 3	53 ± 8	45.112 ± 6.717	0.047 ± 0.005
S382	10 - 11	0.63	5.5 ± 0.3	28-Apr-16	20 ± 1	4 ± 0	16 ± 1	88 ± 13	94.166 ± 9.704	0.040 ± 0.009
S383	14 - 15	0.64	7.9 ± 0.3	28-Apr-16	7 ± 0	4 ± 0	3 ± 1	126 ± 17	165.521 ± 21.354	0.025 ± 0.016
S384	18 - 19	0.79	10.5 ± 0.4	28-Apr-16	7 ± 0	3 ± 0	4 ± 1	170 ± 23		

Table 2

ANSTO ID	Count Date	Depth (cm)	^{137}Cs Corrected to reference date 26-Apr-16 (mBq/g) or (Bq/kg)
S612	28-Jul-16	1.5 ± 0.5	2.62 ± 0.18
S584	28-Jun-16	3.5 ± 0.5	5.85 ± 0.47
S585	05-Jul-16	4.5 ± 0.5	5.22 ± 0.42
S586	07-Jul-16	5.5 ± 0.5	5.64 ± 0.31
S587	11-Jul-16	6.5 ± 0.5	3.96 ± 0.32
S588	13-Jul-16	7.5 ± 0.5	1.85 ± 0.25
S613	04-Aug-16	10.5 ± 0.5	0.87 ± 0.15

Samples between 3 and 8 cm were analysed for 137Cs to validate the 210Pb chronology.
A peak in 137Cs activity in a sediment core should mark the year 1963 (as a result of atomic bomb testing undertaken in 1950s and 60s).
According to the 210Pb chronology, the 137Cs peak should be found at 5-6 cm depth for this core, where the sediment age is about 50 years old (2016-1963 = 53 years).
137Cs activities are shown in Table 2 above. The activities are higher in the top 6 cm of the core and lower below 6 cm depth.
Although the 137Cs profile does not clearly exhibit a peak at 5-6 cm, the higher activity of 137Cs in the top 6 cm could be an indication the sediment above 6 cm had accumulated post 1963 (see Figure 4).
The interpretation of the 137Cs profile for this core should be discussed further. Perhaps more samples should be analysed above 3 cm and below 8 cm.

137Cs was determined by gamma spectrometry in a Well Detector by Daniela Fierro.
Report prepared by Atun Zawadzki 22/7/2016

---

2 extra samples were analysed for 137Cs activity (S612 and S613) to see if a clear peak of 137Cs can be observed, see Table 2.
Figure 4 shows the 137Cs profile between 1 and 11 cm depth. There is clearly a broad peak of 137Cs activity between 3 and 6 cm.
According to the 210Pb profile we should find the 137Cs peak, which marks sediment from 1963, between 5 and 6 cm depth (shaded area on Figure 4).
Although the 137Cs peak from this core is relatively broad, it is in a greement with the 210Pb dating profile where the sediment from 1963 should be found.

Note: samples for 137Cs analysis were not sieved through a 63 µm sieve, due to the limitaion on the sample available for analysis.

137Cs was determined by gamma spectrometry in a Well Detector by Daniela Fierro.
Report prepared by Atun Zawadzki 8/8/2016

Figure 1

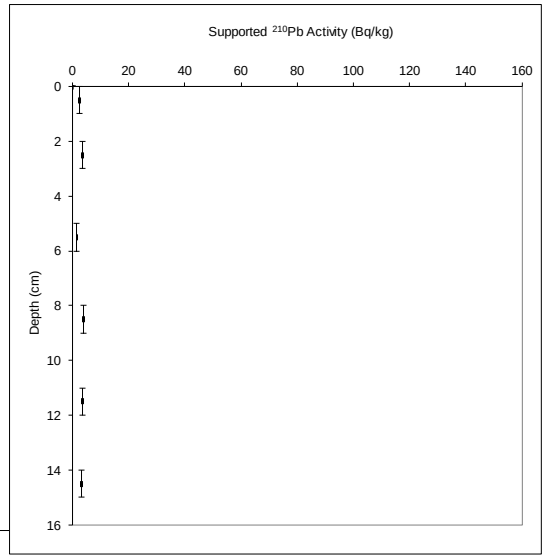

Figure 2

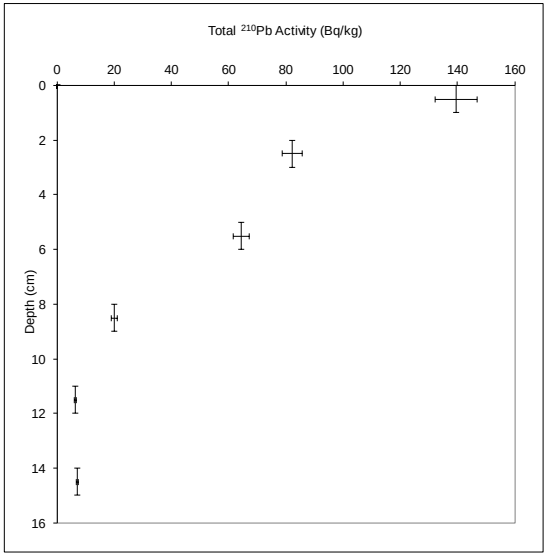

Figure 5

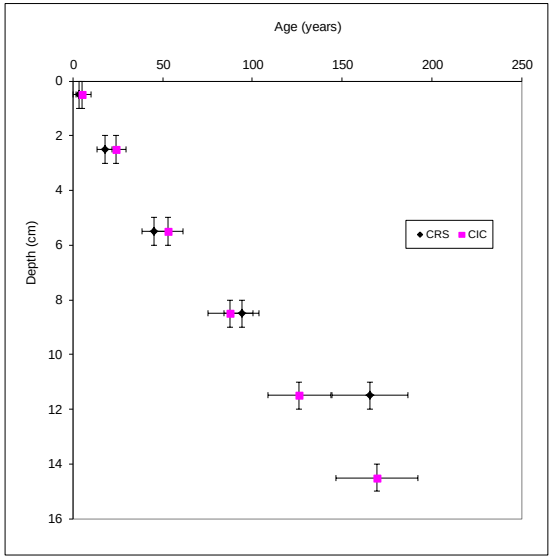

Figure 3

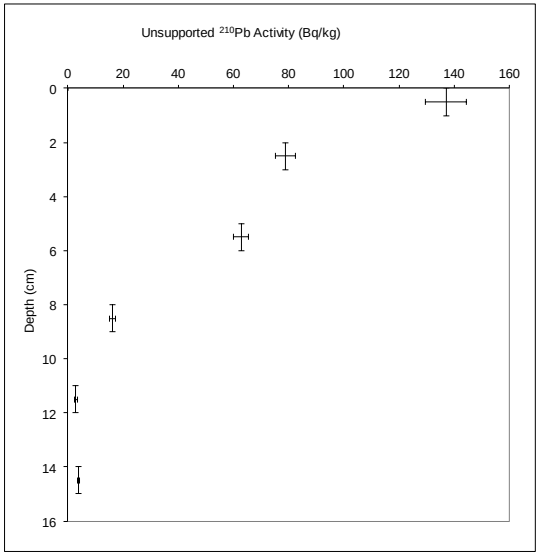

Figure 4

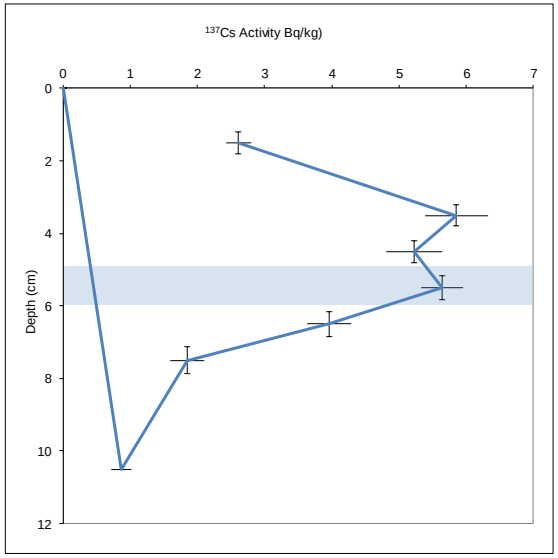

137Cs peak indicates 1963 between 3 and 6 cm depth

210 Pb chronology indicates 1963 should be found between 5 and 6 cm